Topology optimization of continuum structures: A review*

Hans A Eschenauer

Research Center for Multidisciplinary Analyses and Applied Structural Optimization, FOMAAS, University of Siegen, D-57068 Siegen, Germany; esch@fb5.uni-siegen.de

Niels Olhoff

Institute of Mechanical Engineering, Aalborg University, DK-9220 Aalborg East, Denmark; no@ime.auc.dk

It is of great importance for the development of new products to find the best possible topology or layout for given design objectives and constraints at a very early stage of the design process (the conceptual and project definition phase). Thus, over the last decade, substantial efforts of fundamental research have been devoted to the development of efficient and reliable procedures for solution of such problems. During this period, the researchers have been mainly occupied with two different kinds of topology design processes; the Material or Microstructure Technique and the Geometrical or Macrostructure Technique. It is the objective of this review paper to present an overview of the developments within these two types of techniques with special emphasis on optimum topology and layout design of linearly elastic 2D and 3D continuum structures. Starting from the mathematical-physical concepts of topology and layout optimization, several methods are presented and the applicability is illustrated by a number of examples. New areas of application of topology optimization are discussed at the end of the article. This review article includes 425 references. [DOI: 10.1115/1.1388075]

Keywords: Mathematical-Physical Fundamentals, Definitions, Formulations, Material Models—Microstructure Techniques, Homogenization, Perimeter, and Filtering Techniques—Macrostructure Techniques, Approach by Growing and Degenerating a Structure (Material Removal), Approach by Inserting Holes—New Applications of Topology Optimization

CONTENTS

Transmitted by Associate Editor FG Pfeiffer

* Dedicated to our friend and colleague, Professor Ernest Hinton, PhD (1946–1999), in fond memory

1 INTRODUCTION

1.1 Structures, materials, optimization: A multidisciplinary task

Two scientists established not only the classical theory of elasticity, but they also laid the foundation for the increasingly important field of structural optimization. The first concepts of seeking the optimal shapes of structural elements are contained in the works of Galilei [37]. Thus, in his book, *Discorsi, Galileo Galilei* (1564–1642) was the first to perform systematic investigations into the fracture process of brittle bodies. In this context, he described the influence of the shape of a body (hollow bodies, bones, blades of grass) on its strength, thus posing and answering questions addressing the ''Theory of bodies with equal strength.'' On the other hand, *Robert Hooke* (1653–1703) formulated the fundamental law of linear theory of elasticity: Strain (change of length) and stress (load) are proportional to each other. Based on these considerations one could assume the theory of elasticity and to a wider extent continuum mechanics to be a field of science whose problems might be considered as being solved to a large extent. This, however, would be a fundamental error. The previous years have witnessed increasing challenges in terms of the design of ever more complex mechanical systems and components as well as of extremely lightweight constructions, a fact that has led, among others, to the development of advanced materials and hence to the demand for increasingly precise calculation methods. The substantial and still undiminished importance of structural mechanics is due to the fact that questions toward finding an optimal design in terms of load bearing capacity, reliability, accuracy, costs, etc, have to be answered already in an early stage of the design process (concept phase). In this context, research into the fields of material laws, advanced materials, contact mechanics, damage mechanics, etc, proved to be of particular importance for solving various problems. This development naturally includes computer science and technology, the enormously fast development of which has facilitated, over the previous decades, the programming and thus the availability of more sophisticated software systems for treating large-scale, highly nonlinear systems.

The development and construction of products, especially in industrial practice frequently raises the question of which measures must be taken to improve the quality and reliability in a well-aimed manner without exceeding a certain cost limit. In this respect, a new area in the scope of Computer Aided Engineering has emerged, namely the optimization of structures, commonly called *Structural Optimization*. It offers to the engineers of the development, calculation, and design departments a tool which, by means of mathematical algorithms, allows to determine better, possibly optimal, designs in terms of admissible structural responses (deformations, stresses, eigenfrequencies, etc), manufacturing, and the interaction of all structural components. Hence, structural optimization has become a multidisciplinary field of research. Its foundations, however, date back to one of the last universal scholars of modern times, *Gottfried Wilhelm Leibniz* (1646–1716), whose works in the fields of mathematics and natural sciences can be seen as the basis of any analytic procedure and highlight the tremendous importance of coherent scientific thinking (the latter being an important precondition of structural optimization). He laid the foundation of differential calculus, and he also built the first mechanical computer. Without these achievements, modern optimization calculations would not be possible to a larger extent. In this respect, it is of utmost importance to mention *Leonard Euler* (1707–1783) who has played a most significant scientific role. One of his many achievements is his development of the theory of extremals which provided the basis for the development of the calculus of variations. With this method *Jakob Bernoulli* (1655–1705) determined the ''curve of the shortest falling time'' (Brachistochrone) and *Sir Isaac Newton* (1643–1727) the body of revolution with the smallest resistance. By formulating the principle of the smallest effect, and by developing an integral principle *Lagrange* (1736–1813) and *Hamilton* (1805–1865) contributed toward the completion of variational calculus as one of the fundamentals for several types of optimization problems. *Euler*, Lagrange [60], Clausen [186], and *de Saint Venant* performed initial investigations into the determination of the optimum shape of one-dimensional load bearing structures under arbitrary loads. Typical examples for these pursuits are the problems of optimal design of columns, torsion bars and cantilever beams for which optimum cross-sections were determined by means of variational calculus. To achieve this, optimality criteria are derived as necessary conditions; in the case of unconstrained problems *Euler* equations are used. Constraints are considered by applying the Lagrangian multiplier method. As regards the optimum design of arches and trusses, an important place is held by the works of Lévy [64]. For the history of mechanical principles, see Szabo [106].

Thus we can state that structural mechanics in the widest sense is hardly a subject for specialists any more. Living as well as artificial structures appear in overwhelming variety; research into them must be supported by broad knowledge and by establishing analogies. Scientific progress usually can be only achieved today by experts of different disciplines working together. Although there still exist tendencies of isolation today, the interdisciplinary exchange of information meanwhile has considerably improved. One very important reason is the development of advanced materials (ceramics, plastics, composites etc) which have great impact on the development of new, highly complex constructions and structures.

In order to account for the manifold phenomena of materials several theories of finite elasticity, plasticity, viscoelasticity, and viscoplasticity have developed independent of each other. In this context, the works of Truesdell and Noll set a milestone within the theory of material behavior (see, among others, Truesdell [110,111], Truesdell and Noll [406], Noll [324], Prager [82], Krawietz [56]).

Owing to the increasing demands on the efficiency, reliability, and shortened development cycle of a product, it has become inevitable to solve problems by computer-aided procedures. Substantial progress has been achieved in computational analysis of structures and components, especially by

means of the versatile finite element method (FEM). In many applications, an algorithm-based optimization of the component dimensions has already become general use, however, the development of applicable methods and strategies is still in progress for generating best-possible initial layouts for components. An overview of the different procedures is given in [13,28,31,38,390].

In recent years, substantial efforts have been made in the development of topology optimization procedures, and there are several different strategies whose use is in most cases highly problem dependent. Topology strategies are to determine an optimal topology according to the defined optimization problem independently of the designer. They shall support the interactive work in the design process, since an isolated optimization calculation often does not yield an optimal result. Thus, it is important to include the designer's creativity especially in those cases where essential demands cannot be modelled sufficiently in the optimization process. Creativity should not be underestimated particularly in complex design processes, and it is also important in topology optimization.

Michell [305] developed a design theory for the topology of thin-bar structures that are optimal with regard to weight. The bars in these structures are all perpendicular to each other and form an optimal arrangement in terms of either maximum tensile or compressive stresses. Very important subsequent generalizations were made by Prager [83,348], and Rozvany and Prager [368], who solved a range of different topology optimization problems by analytical procedures based on optimality criteria. For an overview, see also Rozvany *et al* [370,371].

1.2 Survey of topology optimization of continuum structures

Topology Optimization is often referred to as *layout optimization* (or *generalized shape optimization*) in the literature (cf, Olhoff and Taylor [332], Kirsch [264], Bedsøe *et al* [146], Rozvany *et al* [90], Bendsøe and Mota Soares [10], Cherkaev [21], Rozvany and Olhoff [91]) and these labels will be used interchangeably in this review. The importance of this type of optimization lies in the fact that the choice of the appropriate topology of a structure in the conceptual phase is generally the most decisive factor for the efficiency of a novel product. Moreover, usual sizing and shape optimization cannot change the structural topology during the solution process, so a solution obtained by one of these methods will have the same topology as that of the initial design. Topology or layout optimization is therefore most valuable as preprocessing tools for sizing and shape optimization (Fleury [218], Bremicker [158], Olhoff *et al* [327]).

Two types of topology optimization exist (discrete or continuous), depending on the type of a structure. For inherently discrete structures, the optimum topology or layout design problem consists in determining the optimum number, positions, and mutual connectivity of the structural members. This area of research has been active for several decades and has been largely developed by Prager and Rozvany. For an up-to-date account of the area of layout optimization of discrete structures, the reader is referred to eg, the comprehensive review paper by Rozvany *et al* [92,367], the monograph by Bendsøe [9] and the proceedings by Eschenauer and Olhoff [28], Olhoff and Rozvany [75], Gutkowski and Mroz [44], Rozvany [89], Bloebaum [16], the annual Proceedings of the ASME Design Automation Conferences, among others, Gilmore *et al* [41], and Topping and Papadrakis [109].

The present review paper is dedicated to topology optimization of continuum structures. This research has been extremely active since the publication of the papers by Bendsøe and Kikuchi [150] and Bendsøe [142]. Examples of more recent publications that provide an overview of the subject are: Atrek [130], Kirsch [264], Eschenauer and Schumacher [210,211], Duysinx [24], Olhoff [325], Cherkaev and Kohn [22], Haber and Bendsøe [236], Bendsøe [143,144], Hassani and Hinton [252], Maute *et al* [303], and Olhoff and Eschenauer [328]. In topology optimization of continuum structures, the shape of external as well as internal boundaries and the number of inner holes are optimized simultaneously with respect to a predefined design objective. It is assumed that the loading is prescribed and that a given amount of structural material is specified within a given 2D or 3D design domain with given boundary conditions. There are several research activities going on throughout the world concentrating on these problems, and different solution procedures have been developed. Very roughly, one can distinguish between two classes of approaches, the so-called Material- or Micro-approaches *vs*, the Geometrical or Macro-approaches.

Section 2 of this paper briefly outlines the basic concepts and mathematical-physical fundamentals of the problem. Firstly, the term *topology* is discussed and defined mathematically. Then the conceptual processes of topology optimization are presented for the two main types of solution techniques just mentioned, the Microstructure (Material) approaches and the Macrostructure (Geometrical) approaches. Subsequently, a brief overview is presented of the basic equations of elasticity and the variational and energy principles that constitute the mathematical-physical foundation for topology optimization, and two typical formulations for such a problem are outlined, a variational formulation and a mathematical programming formulation. Finally, we present some periodic, perforated microstructured material models of variable material density which constitute the basis for the so-called Microstructure (Material) approaches of topology optimization.

Now, as was originally pointed out by Lurie (see Ref. [66] for references) a topology optimization problem is not well-posed if the design space is not closed in an appropriate sense, and a regularization of the formulation of the problem is then needed [180,181,290,266,267]. Mathematical indications of the need for regularization are generation of anisotropy in the design and the impossibility of satisfying second order necessary conditions for optimality in certain subregions of the structural domain (Olhoff *et al* [329], Lurie *et al* [290], Cheng [176]). Numerically, the need manifests itself by lack of convergence or by dependence of the topol-

ogy on the size of the applied finite element mesh (Cheng and Olhoff [180,181], Olhoff *et al* [329], and Cheng [176]).

There are two paths out of this dilemma: one can either extend the design space to include solutions with microstructure in the problem formulation, or restrict the space of admissible solutions in the formulation (Niordson [320,321], Bendsøe [141]).

Section 3 deals with the former path which encounters an approach termed *relaxation* in which materials with periodic, perforated microstructure of continuously varying volume density and orientation are included as admissible designs (see Olhoff *et al* [329], Cheng and Olhoff [181], Kohn and Strang [266,267], Avellaneda [134], Mlejnek [312], Lipton [280,281]), and where their effective mechanical properties are determined via some sort of homogenization technique, eg, mathematically based homogenization (Bourgat [157], Bensoussan *et al* [12], Sanchez-Palencia [93]), a *smear-out* method (Olhoff *et al* [329], Cheng and Olhoff [181], Thomsen [108]) or by quasiconvexification (Gibiansky and Cherkaev [40], Cherkaev and Palais [185], Buttazzo and Del Maso [165], Allaire [122]).

Section 4 is devoted to the path out of the above mentioned dilemma which implies introduction of an appropriate restriction in the problem formulation that renders the topology optimization problem well-posed (Haber *et al* [237–239], Ambrosio and Buttazzo [128], Fernandes *et al* [34], Petersson [80], Petersson and Sigmund [345]). The approaches of this kind generally provide a means to control the complexity of the topology design and include the *Perimeter method* (Haber *et al* [237–239]) by which a bound constraint on the perimeter or surface area of the solid domain (of 2D or 3D designs, respectively) restricts solutions to be entirely composed of purely solid and void domains. The same can be achieved in a much simpler way by use of filtering techniques known from image processing (Sigmund [97,377,378]), and this approach is also discussed in Section 4.

Section 5 deals with so-called Geometrical or Macro-approaches to topology optimization of continuum structures, and these approaches are all based on constitutive laws for usual solid, isotropic materials. Among these techniques, the *variable thickness sheet model* for prediction of topology was first suggested by Rossow and Taylor, 1973 [365]. Here, the admissible domain for topology optimization is divided into a large number of smaller sub-areas, the thicknesses of which are defined as design variables and are then optimized subject to minimum compliance. The *Shape-method* developed by Atrek and Kodali [133] and Atrek [4,131] is based on precisely the same idea and combined with a technique of cutting away elements (sub-areas of the structure) with thicknesses that end up being equal to the prescribed lower limit value. The same idea is again found in Mattheck [69] and Mattheck *et al* [298] and implemented in the CAO (Computer Aided Optimization)-/SKO (Soft Kill Option-) Method where Young's Modulus of the material plays the role as variable thickness and understressed elements are cut away such that a *fully stressed design* may result. Evolutionary Structural Optimization (ESO) is a further numerical method of topology optimization which is developed by Xie and Steven [412] and Querin *et al* [350–352], and integrated with finite element analysis. Bidirectional ESO (BESO) is an extension to this method and can begin with a minimum amount of material in contrast to ESO, which uses an initially oversized structure, see Young [120,417], Young *et al* [418]. The same is valid for the Material Density Functions method by Yang and Chuang [416]. A novel topology optimization method, called *Metamorphic Development* (MD), for both trusses and continuum structures and also for combined truss/continuum structures has been developed by Liu *et al* [285–287] at the Engineering Design Centre of the University of Cambridge.

In the last part of Section 5, a further important macrostructure approach is presented which uses an iterative positioning and hierarchically structured shape optimization of new holes, so-called *bubbles*. This means that the boundaries of the structure are considered to be variable, and that the shape optimization of new bubbles and of the other variable boundaries of the component is carried out as a parameter optimization problem (Eschenauer *et al* [208,209], Eschenauer and Wahl [214], Eschenauer and Schumacher [212], Rosen and Grosse [364], Schumacher [95], Thierauf [404]). Following this idea, Garreau *et al* [230] recently proposed a similar yet modified approach by using so-called topological gradients, which provides information on the possible advantage of the occurrence of a small hole in the body. Cea *et al* [172] developed a topological optimization algorithm based on a fixed point method using the topological gradient. Sokolowski and Zochowski [99] gave some mathematical justifications to the topological gradient in the case of free boundary conditions on the hole and generalized it to various cost functions. Using domain truncation and an adaptation of Lagrange's method, Garreau *et al* [230] exhibit the topological gradient for a large class of problems, boundary conditions for the hole, and cost functions.

Section 6 presents an overview of different kinds of problems, design objectives, and constraints that can be currently handled in the area of topological optimization of structures. While the problems dealt with in initial papers on topology optimization concerned stiffness maximization (minimization of compliance) for a single case of loading, subsequent extensions include, eg, handling of multiple load cases; bimaterial structures; plate and shell bending problems; eigenfrequency optimization; buckling eigenvalue optimization problems; and stress minimization problems. In Section 6, we also demonstrate by way of examples that in very recent years, new avenues have been opened for the application of topology optimization in Biomechanics (Reiter and Rammerstorfer [359], Reiter [358], Tanaka *et al* [399], Pettermann *et al* [346], Folgado and Rodrigues [222], Pedersen and Bendsøe [78]), as well as in areas of design of materials for prescribed mechanical properties (Sigmund [377,378]) and design of compliant mechanisms (Sigmund [379,380]).

Section 7, finally, presents the conclusions of this article.

2 MATHEMATICAL-PHYSICAL FUNDAMENTALS

2.1 Definition and terms of topology

Prior to the treatment of the actual topic of the present review article, topology optimization, the term *topology* as a subfield of geometry shall be explained and defined. Etymologically, the word is derived from the Greek noun *topos* which means location, place, space or domain. Mathematically speaking, topology is concerned with objects that are deformable in a so-called *rubber-like manner*, ie, it can be shown that Euler's Polyhedron Rule maintains its validity in the three-dimensional space if objects like tetrahedrons, cubes, octahedrons etc. are deformed in an arbitrary manner. In the 1950s and 1960s, important papers on topology were contributed by Alexandroff [1], Bourbaki [19], Franz [36], Hilton and Wylie [48], Hocking and Young [49], Kelley [53], Koethe [55], Pontryagin [81], and Schubert [94]. All subsets of $\mathfrak{R}^3$ (including straight lines, sets of points etc) are called topological domains. From a mathematical point of view, all *distortions* are transformations or reversibly unique mappings. As topological transformations or topological mappings we define those transformations of one topological domain into another that neither destroy existing nor generate new neighborhood relations. Two topological domains are termed *topologically equivalent* if there exists a topological mapping of one of the domains into the other one (Fig. 1). Hence, a topological property of a domain is a characteristic maintained at all topological mappings ie, it is invariant.

Topology is therefore considered as the invariants theory of topology domains. The term topological mapping can be reduced to the term continuous mapping, where mapping in a topology domain is called continuous if it does not violate any existing neighborhood relations. In a general manner, topological transformations can be formulated as a continuous transformations whose reverse transformation is also continuous. The latter case is also called *homomorphism*, ie, the transformations are reversibly unique (bijective) and continuous (for further information see [304]).

Based on the above-given terms and definitions of topology, a link shall now be established between topology and optimization. For that purpose, the term topology class is to be introduced that describes certain objects to be topologically equivalent. A topology class is generally defined by the degree of connection of domains. Domains that belong to one topology class are topologically equivalent (Fig. 2*a*). A second topology class is defined by the degree to which the domains are connected (Fig. 2*b*). A further topology class is termed n-fold connected, if $(n-1)$ cuts from one boundary to another are required to transform a given, multiply connected domain into a simply connected domain (Fig. 2*c*).

Up to this point, topology has only been considered as a mathematical definition. In the following, the definitions of structural or design optimization as presented in the subsequent sections shall be adapted to topology optimization.

As indicated in Fig. 2*a*, the neighborhood relations of the single elements that establish a domain remain unviolated in the classical shape optimization of a component; the mapping rules of homomorphisms are valid. Topology optimization, however, changes the neighborhood relation, ie, a transformation into a different topology class is performed. From a mathematical point of view the position and shape of the new domain is of no importance (Fig. 2*b*). At any rate, both positioning and shape influence the structural mechanical behavior of a component, and it is therefore usually intended to improve the component by both topology and shape optimization.

The *set-oriented topology* [23,51,52] describes those properties of geometrical shapes that remain unchanged even if the domain is subjected to distortions that are large enough to eliminate all metric and projective properties. The *topological properties* are the most general qualities of a domain.

In the classical shape optimization of structural components, interrelations between the elements that constitute a domain are maintained, and the isomorphous mapping laws are valid. Topology optimization, ie, improving transformations into other topology classes, modifies these interrelations.

2.2 Classification of topology optimization

2.2.1 Conceptual processes

The topology of a structure, ie, the arrangement of material or the positioning of structural elements in the structure, is crucial for its optimality. Traditionally, the topology of a design is in most cases chosen either intuitively or inspired by already existing designs (*Current-Design-World-State*) [204]. However, there is a significant necessity of and interest in improving the quality of products by finding their best possible topology in a very early stage of the design process.

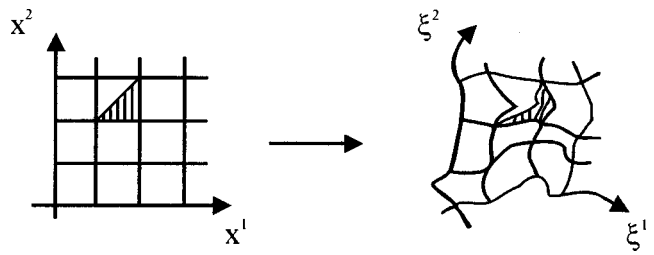

Fig. 1 Topological mapping/transformation

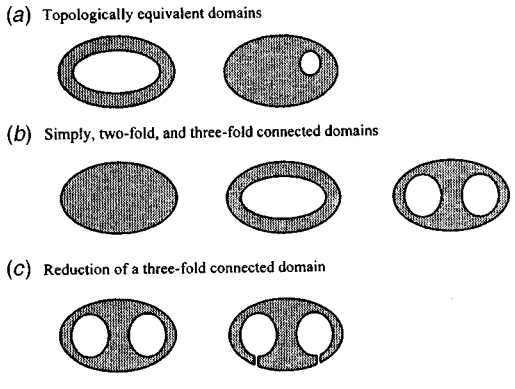

Fig. 2 Topological properties of two-dimensional domains

Very roughly one can distinguish between two classes of approaches, the so-called material or *Micro-approaches*, and the geometrical or *Macro-approaches*.

As was briefly mentioned in Section 1.2, there are essential conceptual differences between these two types of approaches. These can be presented in the following abbreviated manner, and illustrated in Fig. 3:

• *Microstructure-approaches (Material)*

It is our design objective to find that structural topology which renders a given design objective an optimum value subject to a prescribed amount of structural material. It is assumed that in solid form the amount of material is less than the amount that would be needed to cover the entire admissible domain for the continuum. Hence, for the initial design it is normally chosen to distribute the material evenly in some porous, microstructural form over the admissible design domain (see left-hand column of Fig. 3). In the Microstructure-approach to topology optimization, it is customary to use a fixed finite element mesh to describe the geometry and the mechanical response fields within the entire admissible design domain. Typically, the mesh is a uniform, rectangular partition of space, and the design variables are assumed to attain constant values within each finite element. For the analysis, we apply finite elements with constitutive properties that reflect relationships between stiffness components and material density based on physical modeling of the porous microstructures whose orientation and density are described by continuous variables over the admissible domain. The optimization consists in determining whether each element in the continuum should contain material or not. To this end, the density of material within each finite element is used as a design variable defined between limits 1 (solid material, shown in black in the left-hand column of Fig. 3) and 0 (void or very weak material indicated by white), see, eg [10,21,66,67,91,176,180,181,266,267,290,329,367]. In the optimization process, the design variables tend to attain one of their limiting values, thereby forming a design with aggregations of points (finite elements) with solid material or void, respectively. The result is a rough description of outer as well as inner boundaries of the continuous structure that represents the overall optimum topology design. Based on this topology, subsequent shape optimization is usually carried out such as to yield a design that is optimal with regard to both topology and shape [158,218,327].

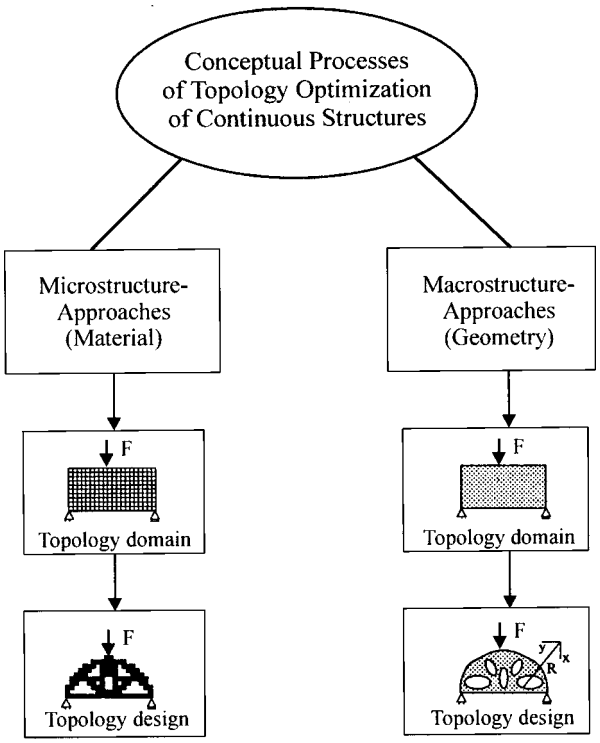

Fig. 3 Conceptual processes of topology optimization

• *Macrostructure-approaches (Geometry)*

In this class, solid isotropic materials are considered as opposed to porous, microstructured ones, and as the topology optimization is performed in conjunction with a shape optimization, the finite element mesh cannot be a fixed one, but must change with the changes of the boundaries of the design. Within the Macrostructure-approach, the topology of a solid body can be changed by growing or degenerating material or by inserting holes. The first method recognizes that an optimal design is simply a subset of the admissible design domain and that it can be obtained by appropriately adding or removing material from the admissible design domain, see [4,132,133,363].

The second method mentioned consists of an iterative positioning of new holes (''bubbles'') at specific points in the topology domain. In each iteration, the holes and the existing variable boundaries of the continuous body are simultaneously subjected to a shape optimization procedure (see [138,209,210,211,230,298]).

2.3 Energy principles

The variational or energy principles represent the basis of shape and topology optimization of discrete and continuum structures; therefore, we will first compile some of the fundamental laws and formulations and their assumptions. Further details like the Fundamental Principles of Thermodynamics, the Principle of Energy Conservation with their state or potential functions internal energy $\bar{E}$ and free energy $\bar{F}$, the constitutive equations etc, can be found in the publications by Freudenthal and Geiringer [228], Truesdell and Toupin [407], Truesdell and Noll [406], Green and Zerna [43], Naghdi [317], Sedov [96], Eschenauer [26], Atkin and Craine [129], Washizu [115], Ben-Tal and Taylor [154], Taylor [400], Eschenauer *et al* [29,32,212,213], Milton and Cherkaev [309], and Krawietz [56].

2.3.1 Assumptions: Basic equations of linear elasticity theory

Our considerations of continua are based on the following assumptions [26,29,61,98]:

a) The processes produced in a stressed body are reversible, ie, no dissipative effects (eg, plastic deformations) occur. We limit our considerations to the scope of the classical *Linear Theory of Elasticity*. Hence, the specific deforma-

tion energy U and the specific complementary energy $\overline{U}^*$ are used as the governing potential functions.

b) The deformation process takes an *isothermal* course, ie, there is no interaction between deformation and temperature.

c) The load process is quasi-static, ie, the kinetic energy or the forces of inertia can be neglected.

d) The state of displacement of a solid body is described according to a Lagrangian approach.

e) The theorem of mass conservation ($d\hat{V}=dV$) holds and the volume forces in the deformed and undeformed bodies ($\dot{f}\equiv f$) are equal.

Expressed in terms of general tensors with Latin indices taking values 1,2,3 unless otherwise stated and assuming summation over dummy indices (Einstein's summation convention), the system of basic equations of linear elasticity theory consists of

three conditions of equilibrium

$$\sigma^{ij}|_j+f^i=0 \quad \leftrightarrow \quad \mathbf{Div}\,\boldsymbol{\sigma}+\boldsymbol{f}=0, \tag{2.1a}$$

six strain-displacement relations

$$\varepsilon_{ij}=\frac{1}{2}(u_i|_j+u_j|_i) \quad \leftrightarrow \quad \boldsymbol{\varepsilon}=\boldsymbol{L}^*\boldsymbol{u}, \tag{2.1b}$$

six constitutive equations (material law)

$$\sigma^{ij}=E^{ijkl}\varepsilon_{kl} \quad \leftrightarrow \quad \boldsymbol{\sigma}=\boldsymbol{E}\boldsymbol{\varepsilon} \tag{2.1c}$$

or

$$\varepsilon_{ij}=C_{ijkl}\sigma^{kl} \quad \leftrightarrow \quad \boldsymbol{\varepsilon}=\boldsymbol{C}\boldsymbol{\sigma} \tag{2.1d}$$

with $\boldsymbol{\varepsilon}$ the strain matrix, $\boldsymbol{L}^*$ a differential operator, $\boldsymbol{\sigma}$ the stress matrix, and the corresponding tensors denoted by ε_{ij} and σ^{ij} $(i,j=1,2,3)$, and $\boldsymbol{u}$ and u_i denote the displacement vector. The components of the elasticity tensor E^{ijkl} yield the elasticity matrix $\boldsymbol{E}$, and the components of the compliance tensor C_{ijkl} the compliance matrix $\boldsymbol{C}$.

Altogether there are 15 equations for 15 unknown field quantities (6 stresses σ^{ij}, 6 strains ε_{ij}, 3 displacements u_i). For more details on the derivation of these equations and the tensor calculus see eg, Green and Zerna [43], Naghdi [317], Sokolnikoff [98], and Eschenauer [29]. For solving (2.1a,b,c), one has to deal with a boundary-value problem, in most cases a mixed boundary value problem (see Fig. 4) with given surface tractions at S_t

$$p^i_{(S_t)}=(\sigma^{ij}n_j)_{S_t} \tag{2.2}$$

and given displacements at S_d

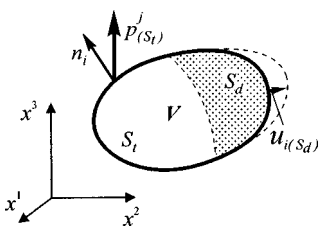

Fig. 4 Illustration of a mixed boundary value problem

$$u_{i(S_d)}=(u_i)_{S_d} \tag{2.3}$$

as boundary conditions.

2.3.2 Material law and energy expressions

The material law for *Hookean* bodies (1c,d) follows from the constitutive equations $\sigma^{ij}=\partial\overline{U}/\partial\varepsilon_{ij}$.

The generalized material law of an anisotropic, linearly elastic body can be written in index notation according to (2.1*c*) as

$$\sigma^{ij}=E^{*ijkl}\varepsilon_{kl} \tag{2.4}$$

This yields $3^4=81$ components for the fourth order elasticity tensor E^{*ijkl} which reduce to 21 owing to the symmetry of the stress tensor ($\sigma^{ij}=\sigma^{ji}$) and to the symmetry of the tensor of elasticity $E^{*ijkl}=E^{*klij}$ due to energy considerations. Hence, 21 different material quantities are required for calculation of deformations of a generally anisotropic body [43,26] and Eschenauer *et al* [29,32].

Given the special case of an isotropic material the components of the elasticity tensor can be calculated from the following relation:

$$E^{*ijkl}=E^{ijkl}=\lambda g^{ij}g^{kl}+\mu(g^{ik}g^{jl}+g^{il}g^{jk}) \tag{2.5a}$$

with the Lamé constants μ and λ defined in terms of Young's modulus E, Poisson's ratio ν, and the shear modulus G as follows:

$$\mu=\frac{E}{2(1+\nu)}\hat{=}G, \quad \lambda=\frac{E\nu}{(1+\nu)(1-2\nu)}=G\frac{2\nu}{1-2\nu}. \tag{2.5b}$$

The energy expressions for the specific deformation energy $\overline{U}$ and the specific complementary energy $\overline{U}^*$ read as follows:

$$\overline{U}\hat{=}\overline{U}^*=\frac{1}{2}\sigma^{ij}\varepsilon_{ij}$$

or

$$=\frac{1}{2}\boldsymbol{\sigma}^T\boldsymbol{\varepsilon}=\frac{1}{2}\boldsymbol{\varepsilon}^T\boldsymbol{\sigma} \tag{2.6}$$

with the vectors of the strains $\boldsymbol{\varepsilon}$ and of the stresses $\boldsymbol{\sigma}$.

Introducing (2.3a,b) into (2.6), we obtain the following quadratic functions which are positive definite because of $\overline{U}>0$ and $\overline{U}^*>0$:

$$\overline{U}=\frac{1}{2}E^{ijkl}\varepsilon_{ij}\varepsilon_{kl}=\frac{1}{2}\boldsymbol{\varepsilon}^T\boldsymbol{E}\boldsymbol{\varepsilon} \tag{2.7a}$$

$$\hat{=}\overline{U}^*=\frac{1}{2}C_{ijkl}\sigma^{ij}\sigma^{kl}=\frac{1}{2}\boldsymbol{\sigma}^T\boldsymbol{C}\boldsymbol{\sigma}. \tag{2.7b}$$

According to *Hamilton's Principle* (see [43,115]) the variation

$$\delta\int_{t_0}^{t_1}(K-U+W)dt=0 \tag{2.8}$$

is valid over the time period $t_0 < t < t_1$ for displacements u, which fulfil the equations of motion and the geometrical boundary conditions prescribed at the surface section $S = S_d$ with

$$K = \frac{1}{2}\int_V \rho \frac{\partial u^i}{\partial t}\frac{\partial u_i}{\partial t} dV \qquad \text{kinetic energy,} \quad (2.9a)$$

$$U = \frac{1}{2}\int_V \sigma^{ij}\varepsilon_{ij} dV \qquad \text{deformation energy,} \quad (2.9b)$$

$$W = \int_V f^i u_i dV + \int_{S_t} \sigma^{ij} n_j u_i dV$$

work of the applied loads, (2.9*c*)

S_t = section of the surface subjected to prescribed surface tractions.

For the static case ($K = 0$), Hamilton's Principle comprises the *Principle of Virtual Displacements* in form of

$$\delta W = \delta U. \quad (2.10)$$

It states that for virtual displacements δu_i of the equilibrium state u_i, the virtual work δW of external forces acting on a body equals the increase of the virtual deformation energy $\delta U = \delta \int_V \overline{U} dV$ of the body.

The *Principle of Virtual Work* or *Virtual Displacements* is one of the fundamental axioms of mechanics from which basic differential equations and boundary conditions of mechanics are derived. In addition, the principle forms the basis of numerous approximation procedures for variational formulations as well as for shape and topology optimization problems. In the scope of this review paper we will only outline this principle; for further details on energy principles the reader is referred to Langhaar [61], Lanzcos [62], Michlin [72], Levinson [276], Reissner [356], Eschenauer *et al* [29], and Washizu [115].

The virtual external work of an elastic body B consists of three contributions from volume forces, surface traction, and concentrated forces (Fig. 5) and can be written as

$$\delta W = \int_V f^i \delta u_i dV + \int_S p^i \delta u_i dS + F^i \delta u_i^0 \quad (2.11a)$$

or in vector notation

$$\delta W = \int_V \boldsymbol{f}^T \delta \boldsymbol{u} dV + \int_S \boldsymbol{p}^T \delta \boldsymbol{u} dS + \boldsymbol{F}^T \delta \boldsymbol{u}^0 \quad (2.11b)$$

with

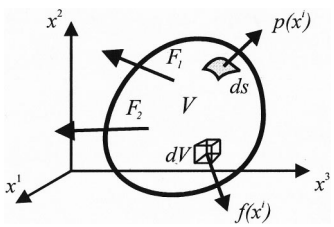

Fig. 5 Elastic body subjected to external forces

$\boldsymbol{f}^T = (f_x, f_y, f_z)$ vector of volume forces,
$\boldsymbol{p}^T = (p_x, p_y, p_z)$ vector of surface tractions,
$\boldsymbol{u}^T = [u, v, w]$ displacement vector of an elastic body,
$\boldsymbol{F}^T = (\boldsymbol{F}_1^T, \boldsymbol{F}_2^T, \ldots, \boldsymbol{F}_i^T)$ vector of concentrated forces, $\boldsymbol{F}_i^T = (F_x, F_y, F_z)_i$,
$(\boldsymbol{u}^0)^T = [\boldsymbol{u}_1^0, \boldsymbol{u}_2^0, \ldots, \boldsymbol{u}_n^0]$ vector of displacement vectors for points of action of concentrated forces; $(\boldsymbol{u}_1^0)^T = (u^0, v^0, w^0)_i$

The external forces remain constant during application of the virtual displacements, ie, they are independent of the displacements and are therefore not varied. We can thus write for a conservative system (here without concentrated loads)

$$\delta\left[\int_V \overline{U} dV - \int_V \boldsymbol{f}^T \boldsymbol{u} dV - \int_S \boldsymbol{p}^T \boldsymbol{u} dS\right] = 0. \quad (2.12)$$

If the deformation energy is defined as internal potential Π_i

$$U = \int_V \overline{U} dV \hat{=} \Pi_i, \quad (2.13a)$$

and if the work of the conservative external forces is substituted by the external potential Π_e

$$W = \int_V \boldsymbol{f}^T \boldsymbol{u} dV + \int_S \boldsymbol{p}^T \boldsymbol{u} dS = -\Pi_e, \quad (2.13b)$$

we obtain the total potential as

$$\Pi = \Pi_i + \Pi_e \quad (2.13c)$$

and the principle of the virtual total potential as

$$\delta\Pi = \delta(\Pi_i + \Pi_e) = 0, \quad (2.13d)$$

ie, with a virtual displacement relative to the state of equilibrium, the first variation of the total potential vanishes. This leads directly to the principle of the stationary value of the total potential

$$\Pi = \Pi_i + \Pi_e = \text{Extremum.} \quad (2.14a)$$

Assuming linearly elastic material behavior, Eq. (2.14*a*) yields Green-Dirichlet's principle of a minimum

$$\Pi = \Pi_i + \Pi_e = \text{Minimum} \quad (2.14b)$$

which by (2.13*a*,*b*) may be alternatively stated as

$$\Pi = U - W = \text{Minimum.} \quad (2.14c)$$

In the further course of the structural optimization this classical principle will be used for finding continuum structures with maximum stiffness and minimum compliance.

2.4 Problem formulations of shape and topology optimization

2.4.1 Variational formulation

For the mixed boundary value problem (2.1*a*,*b*,*c*) with (2.2),(2.3), a typical optimization problem can be defined as a variational problem. As an example, let us assume that the objective shall be to minimize the material volume of the body:

$$F=\int_V \rho dV \rightarrow \text{Minimum}, \tag{2.15a}$$

where ρ is a variable volume density of material on the structural domain ($\rho=1$ for solid material).

In addition, the problem is assumed to have the following additional integral expressions as inequality constraints

$$G_\nu=\int_V g_\nu(\sigma^{ij},u_i)dV<G_\nu^0, \quad \nu=1,2,\ldots,N, \tag{2.15b}$$

which may be transformed to equality constraints by using slack variables μ_ν^2

$$G_\nu=\int_V g_\nu(\sigma^{ij},u_i)dV=G_\nu^0-\mu_\nu^2. \tag{2.15c}$$

Using (2.1) and (2.2) one can formulate a Lagrangean functional L for solving the optimization problem

$$L=\int_V f_L(\sigma^{ij},u_i)d\boldsymbol{V}+\sum_{\nu=1}^{N}\lambda_\nu(G_\nu^0-\mu_\nu^2), \tag{2.16a}$$

with

$$f_L=\rho+\sum_{\nu=1}^{N}\lambda_\nu g_\nu(\sigma^{ij},u_i)+\psi_i[\sigma^{ij}|_j+f^i] + \chi_{ij}[\sigma^{ij}-E^{ijkl}\varepsilon_{kl}]+\kappa^{ij}\left[\varepsilon_{ij}-\frac{1}{2}(u_i|_j+u_j|_i)\right]. \tag{2.16b}$$

In (2.16*b*) ψ_i, χ_{ij} and κ^{ij} are adjoint functions as special Lagrangean multipliers of the mechanical problem, while the Lagrangean multipliers λ_ν are employed to consider the constraints of the optimization problem.

The adjoint functions ψ_i, χ_{ij} and κ^{ij} can be interpreted as the *pseudo* initial displacements, *pseudo* initial stresses, and *pseudo* initial strains of a corresponding body due to the self-adjointness of the elliptical operator of elasticity [190,191,208,209,212,268]. If the stresses in this body (which is also called *adjoint body*) equal zero, there are already initial displacements, and vice versa. This corresponding body possesses the same dimensions as the original body. The calculation of the adjoint functions, ie, of the suitable *pseudo* initial states, depends on the constraints G_ν, and may require a large analytical effort. In the case of so-called *self-adjoint* problems, the corresponding body does not have to be calculated explicitly since the adjoint functions can be determined directly from the state of the original body. This formulation is used for topology optimization problems by inserting holes (see Section 5).

2.4.2 Mathematical formulation for topology optimization

To discuss a mathematical formulation for topology optimization of a continuum structure, we consider the classical problem of topology design for maximum stiffness of statically loaded linearly elastic structures under a single loading condition. This problem is equivalent to design for minimum compliance defined as the work done by the set of given loads against the displacements at equilibrium, which, in turn, is equivalent to minimizing the total elastic energy at the equilibrium state of the structure. This can be verified by considering the work W in (2.13*b*) done by given external forces

$$W[\boldsymbol{u}(x)]=\int_V[\boldsymbol{f}(x)]^T\boldsymbol{u}(x)dV+\int_S[\boldsymbol{p}(x)]^T\boldsymbol{u}(x)dS. \tag{2.17}$$

Here, x denotes a structural point, and $\boldsymbol{u}(x)$ is the displacement field at equilibrium. In order to use (2.17) the structure must be in equilibrium which requires that the equilibrium problem is solved in advance by finite element analysis. In order to express the problem in finite element terms the well-known equation for the total potential energy Π is used as this is the basis for static analysis. The total potential energy according to (2.13*c*), using (2.7*a*), can be expressed as

$$\Pi=U-W=\int_V[\varepsilon(x)]^T\boldsymbol{E}(x)\varepsilon(x)dV - \int_V[\boldsymbol{f}(x)]^T\boldsymbol{u}(x)dV-\int_S[\boldsymbol{p}(x)]^T\boldsymbol{u}(x)dS, \tag{2.18}$$

where $\varepsilon(x)$ is the strain field and $\boldsymbol{E}(x)$ is the elasticity matrix due to (2.1*c*). By applying standard finite element procedures of discretizing the structure into N finite elements and interpolating displacements from the nodal degrees of freedom, (2.18) can be transformed into the well known finite element form

$$\Pi=U-W=\frac{1}{2}\boldsymbol{d}^T\boldsymbol{K}\boldsymbol{d}-\boldsymbol{r}^T\boldsymbol{d}, \tag{2.19}$$

where $\boldsymbol{d}$, $\boldsymbol{K}$ and $\boldsymbol{r}$ are the global displacement vector, the stiffness matrix, and the load vector. Equilibrium is obtained by using the principle of minimum total potential energy which requires stationarity of Π with respect to the displacement vector $\boldsymbol{d}$ at equilibrium

$$\frac{\partial\Pi}{\partial\boldsymbol{d}}=0, \tag{2.20}$$

which yields the well known equilibrium equation

$$\boldsymbol{K}\boldsymbol{d}=\boldsymbol{r}. \tag{2.21}$$

Substituting the developed finite element equations into (2.17) the problem of minimizing the work done by the external forces at equilibrium can be expressed as

$$\min_{\chi\in B} W(\boldsymbol{d}) \quad \text{subject to} \quad \boldsymbol{K}\boldsymbol{d}=\boldsymbol{r}, \tag{2.22}$$

where B is given by

$$B=\left\{\chi\,\middle|\,\int_\Omega \chi\,dx=V_{\text{fixed}}\right\}, \tag{2.23}$$

which expresses that the optimum design is to be determined for a prescribed volume of material, and χ denotes the design variable.

The given problem can be alternatively expressed in terms of the total elastic energy U by applying that at equilibrium $W=2U$. The equivalent form of the problem is thus

$$\min_{\chi \in B} U(\boldsymbol{d}) \quad \text{subject to } \boldsymbol{Kd}=\boldsymbol{r}. \tag{2.24}$$

Here, U can be given in a number of different ways, ie,

$$U=\frac{1}{2}\boldsymbol{d}^T\boldsymbol{K}\boldsymbol{d}=\sum_1^N \frac{1}{2}\int_{V_e}\varepsilon_e^T\boldsymbol{E}_e(x)\varepsilon_e dV_e$$

$$=\sum_1^N \frac{1}{2}\int_{V_e}\sigma_e^T\boldsymbol{C}_e(x)\sigma_e dV_e, \tag{2.25}$$

where $\boldsymbol{E}_e$ and $\boldsymbol{C}_e$ are finite element elasticity and compliance matrices, ε_e and σ_e element strain and stress vectors, V_e the volume, and N the total number of finite elements.

Considering the complementary energy expression at the right hand side of (2.25), the compliance matrix, and thus the material distribution problem, is controlled by a design variable that can be expressed by a switch function defined as

$$\chi(x)=\begin{cases}1 & \text{if} \quad x\in\Omega_s\\ 0 & \text{if} \quad x\in\Omega/\Omega_s\end{cases}, \tag{2.26}$$

where Ω denotes the entire design domain and Ω_s denotes the domain occupied by solid elastic material.

This implies that the topology optimization problem is formulated as a distributed, discrete valued design problem, a so-called 0-1 problem. However, it is by now well known that this distributed problem suffers from lack of existence of solutions, ie, it is ill-posed (see, Lurie [66], Kohn and Strang [266,267], Allaire and Kohn [126]). Numerically, the deficiency manifests itself by lack of convergence or by dependence of the topology on the size of the applied finite element mesh (see, Cheng and Olhoff [180,181], Olhoff *et al* [329], Cheng [176], Lurie *et al* [290]).

In order to obtain a well-posed problem, a regularization of the problem formulation is required. This can be done by introduction of microstructures with a continuous density of the base material as a design variable, see Section 3, and/or by including appropriate restrictions against formation of microstructure in the problem formulation as discussed in Section 4. In the latter case even the 0-1 problem becomes well-posed, and has recently been solved by Beckers [6,7,139] and Beckers and Fleury [140] by usage of dual methods.

2.5 Material models

In this section, we present some material models that allow the density of material to cover the complete range of values from 0 (void) over intermediate values (composite) to 1 (solid) and that provide regularization (well-posedness) of typical topology optimization problems when introduced in the mathematical formulation.

We first consider three material models with periodic, perforated microstructure, namely the *hole-in-cell*-microstructure and layered 2D microstructures (see Figs. 7 and 8), and the layered 3D microstructure (Fig. 9). These microstructural models provide regularization of the topology optimization problem via relaxation (extension) of the design space, and their periodicity implies that the effective mechanical properties of the microstructures can be determined via homogenization, *smear-out* or quasiconvexification techniques as will be discussed in Section 3. Figure 7 illustrates the parameterization of the perforated *hole-in-cell* and layered 2D microstructures which were first applied in Bendsøe and Kikuchi [150] and Bendsøe [142], respectively. The microstructures depicted in Figs. 6 and 7 all imply orthotropic material behavior.

In Subsection 2.5.4, we finally present the so-called SIMP material model (***S**olid **I**sotropic **M**icrostructure with **P**enalty*). This model also covers the complete range of density values from 0 to 1, but it does not provide regularization of the classical formulation of topology optimization problems. However, it has been proved mathematically by Ambrosio and Buttazzo [128] and Petersson [80] and will be discussed in Section 4 that the problem becomes well posed if the SIMP model is used in a formulation that includes a restriction in the form of, eg, an upper constraint value on the perimeter of the topology design of a 2D structure, or on the surface area of a 3D structure.

2.5.1 Hole-in-cell microstructures

Bendsøe and Kikuchi [150], Diaz and Bendsøe [194], and several others have applied a numerically evaluated anisotropic *hole-in-cell* microstructure as shown in Fig. 6*a* that consists of an isotropic material with rectangular holes. For the topology optimization, the orientation $\theta(x)$ of the microscopic cells and their geometry defined by $\mu_1(x)$ and $\mu_2(x)$, are applied as design variables. Thus, the model governs void and solid for $\mu_1(x)=\mu_2(x),=0$ and $\mu_1(x)=\mu_2(x)=1$, respectively, and composite for intermediate values of $\mu_1(x)$ and $\mu_2(x)$. The volume density $\rho(x)$ of material $0\leqslant\rho(x)\leqslant 1$ is given by

$$\rho(x)=1-\mu_1(x)\mu_2(x). \tag{2.27}$$

The components of the stiffness matrix for the microstructure can be obtained numerically on the basis of homogenization for different sets of values of μ_1 and μ_2. For expedience, the components of the effective stiffness matrix are normally represented as functions of μ_1 and μ_2 via approximation formulas.

2.5.2 Layered 2D microstructures

Referring to Figs. 6*b* and 7, we now consider the construction of a class of a layered planar microstructures which can be used for solution of a variety of topology optimization problems for 2D continuum structures.

The microstructures are obtained by a repetitive process in each step of which a new layering of given direction is added to the microstructure. The number of times this is performed is per definition the *rank* of the microstructure. Hence, given two isotropic materials with Cartesian elasticity tensors $E^+_{\alpha\beta\kappa\gamma} > E^-_{\alpha\beta\kappa\gamma}$, $(\alpha,\beta,\kappa,\gamma=1,2)$, $(E^{\alpha\beta\kappa\gamma}=E_{\alpha\beta\kappa\gamma})$, a first-rank microstructure is obtained by stacking alternately thin layers of the stiffer material (this material will be termed *stiff* in the following but has finite stiffness) with layers of the more compliant material in the proportion given by μ^{R1} and $1-\mu^{R1}$, respectively, along a

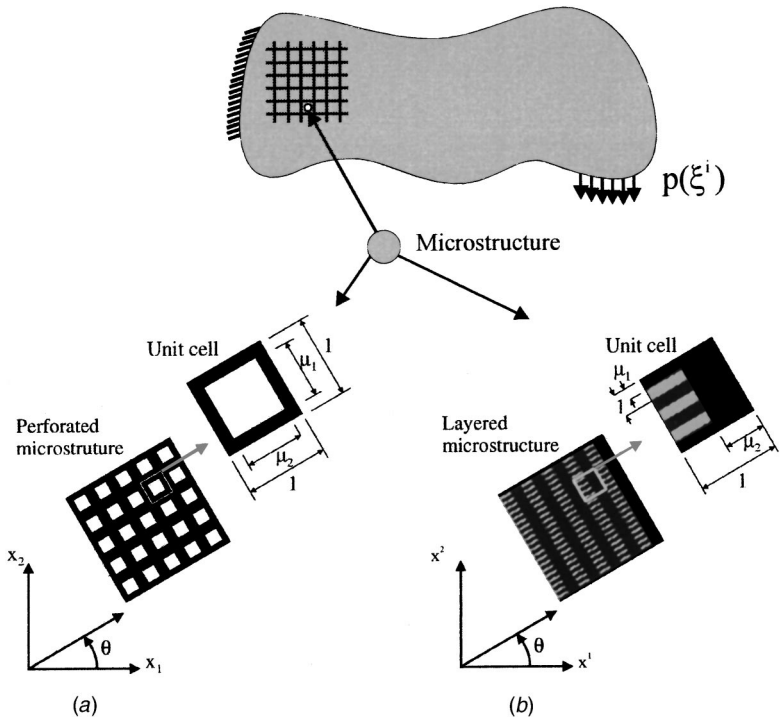

Fig. 6 Microstructures for 2D continuum topology optimization problems: *a*) Perforated microstructure with rectangular holes in square unit cells, and *b*) Layered microstructure constructed from two different isotropic materials

direction characterized by a unit normal n_α^{R1}. Similarly, a second-rank microstructure is obtained by stacking alternately thin layers of the stiff isotropic material and the first-rank microstructure in the proportion μ^{R2} and $1-\mu^{R2}$, respectively, along a new direction characterized by the unit normal n_α^{R2}. The process may be continued to build layered microstructures of any finite rank *Ri*, and the effective stiffness tensor for the resulting material may symbolically be obtained by the sequence

$$E_{\alpha\beta\kappa\gamma}^{R1}=E(\mu^{Ri},n_\alpha^{Ri},E_{\alpha\beta\kappa\gamma}^{+},E_{\alpha\beta\kappa\gamma}^{R(i-1)});$$
$$i=1,\ldots,I;\alpha,\beta,\ldots=1,2. \quad (2.28)$$

In the remaining part of this and the subsequent two Sections, 3 and 4, tensors like the elastity, stress, and strain tensors are assumed to be Cartesian tensors.

As indicated in Fig. 7, black and white domains are occupied by isotropic materials with the stiffness tensors $E_{\alpha\beta\kappa\gamma}^{+}$ and $E_{\alpha\beta\kappa\gamma}^{-}$, respectively, while gray domains represent areas occupied by layered materials composed of the two base materials.

It is a particular advantage of these layered planar microstructures that their effective material stiffness properties, in the limit where the width of the layers tends to zero, may be calculated analytically applying either a mathematically based homogenization procedure as used by eg, Bendsøe [142], or a more physically based smear-out procedure as used by, eg, Olhoff *et al* [329] and Thomsen [108].

The class of layered planar microstructures just described is of particular importance to problems of topology optimization of plane, 2D continuum structures, because second-rank planar microstructures with orthogonal layers are optimum for single load case stiffness design problems, while third-rank planar microstructures with non-orthogonal layers are optimum for multiple load case stiffness design problems

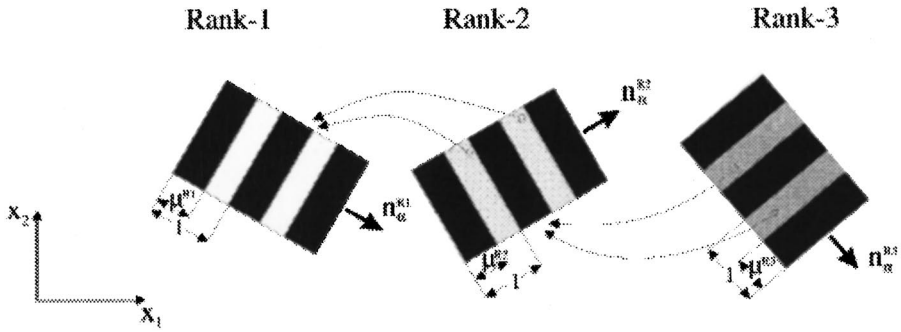

Fig. 7 Construction of first-, second-, and third-rank microstructures by successive layering along different directions

[134]. Certain properties of these optimum microstructures are discussed in Allaire and Aubry [124]. However, it is worth noting that the theory is restricted to compliance or eigenfrequency optimization (in the single or multiple loading case). For more general objective functions, the microstructures only provide a *partial* relaxation of the problem (see [123]). With regard to other topology optimization problems for 2D continuum structures parameterized by means of layered planar microstructures, it is worth mentioning that no further generality is obtained by application of more than a third-rank planar microstructure with non-orthogonal layers, as the whole range of effective stiffness properties for all finite rank planar microstructures is obtainable by application of third-rank planar microstructure with non-orthogonal layers. This follows from work by Avellaneda and Milton [135] and Lipton [280,281].

2.5.3 Layered 3D microstructures

Third-rank laminate microstructures for 3D elasticity were described first in Gibianski and Cherkaev [40]. They have recently been used for topology optimization of 3D continuum structures by Cherkaev and Palais [185], Allaire *et al* [125], Diaz and Lipton [195], Jacobsen *et al* [257], and Olhoff *et al* [326,330,331], and for multiple material optimization problems by Rovati and Taliercio [366] and Burns and Cherkaev [164]. Note that these third-rank microstructures are optimal only for optimization of the stiffness.

We now consider a 3D layered composite microstructure of rank-three as shown in Fig. 9. The three sets of layers are assumed to be mutually orthogonal, and the composite is made of two isotropic, linear elastic materials, and the volume fractions of these are given as m_1 and m_2 $(m_1=1-m_2)$.

The length scales (Fig. 8) describe the relative thickness of each layer which yields the following relation between volume density ρ and length scales for a rank-n material

$$\rho_n=\beta_n+(1-\beta_n)\rho_{n-1}, \tag{2.29}$$

where, in the case of a rank-3 material,

$$\beta_1=m_1\alpha_1, \quad \beta_2=\frac{m_1\alpha_2}{1-m_1\alpha_1}, \quad \beta_3=\frac{m_1\alpha_3}{1-m_1(1-\alpha_3)}. \tag{2.30}$$

The introduced parameter α_i, $(i=1,2,3)$, is the spatial thickness of layer i which means that it can be considered as a volume density for the layer (see [40]). By introducing this parameter the basic idea is to equalize the stresses in the different directions by varying the spatial thickness of each layer. The design variables for this 3D microstructure is the volume density ρ, the parameters α_i $(i=1,2,3)$, and angles governing the spatial orientation.

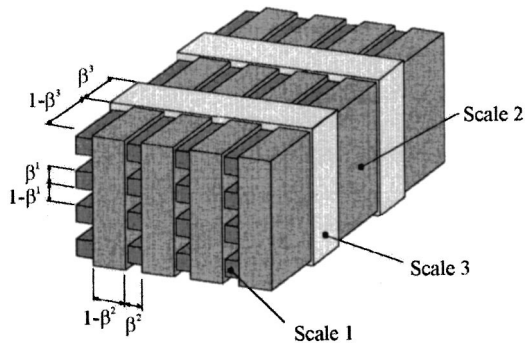

Fig. 8 Model of a spatial rank three laminate with β^i denoting the i-th length scale

2.5.4 SIMP model

For the SIMP (Solid Isotropic Microstructure with Penalty) material model (see Bendsøe [142], Zhou and Rozvany [423], Rozvany *et al* [369,370], Mlejnek and Schirrmacher [314], Mlejnek [313]), the elasticity tensor E_{ijkl} and the volume of a structure made of the material are given by

$$E_{ijkl}(x)=\rho(x)^pE^0_{ijkl}, \quad p>1; \quad \text{Volume}=\int_\Omega \rho(x)dx, \tag{2.31}$$

where $\rho(x)$, $x\in\Omega$, $0\leqslant\rho(x)\leqslant 1$ is a density function of the material and E^0_{ijkl} the elasticity tensor of a given solid isotropic reference material. The density function $\rho(x)$ enters the stiffness relation in a power $p>1$ which has the effect of penalizing intermediate densities $0<\rho<1$, since at such densities the SIMP material has lower stiffness than the reference material at the same cost.

Figure 9 displays the relative stiffness ratio E/E^0 vs. volume density ρ for different values of the penalization power p, and clearly illustrates that the use of the SIMP material model will force the topology design toward limiting values $\rho=0$ (void) and $\rho=1$ (solid) and thereby prompt the creation of more distinctive 0-1 designs. When applying the model, the value of the penalization power p is gradually increased from 1 to 4 during the topology design process (the so-called continuation technique, see [377]).

It is a drawback of the SIMP model that the topology designs obtained not only exhibit dependence on the value of p, but also on the finite element mesh applied. However, as will be discussed in Section 4, this drawback disappears, and topology optimization problems based on usage of the SIMP

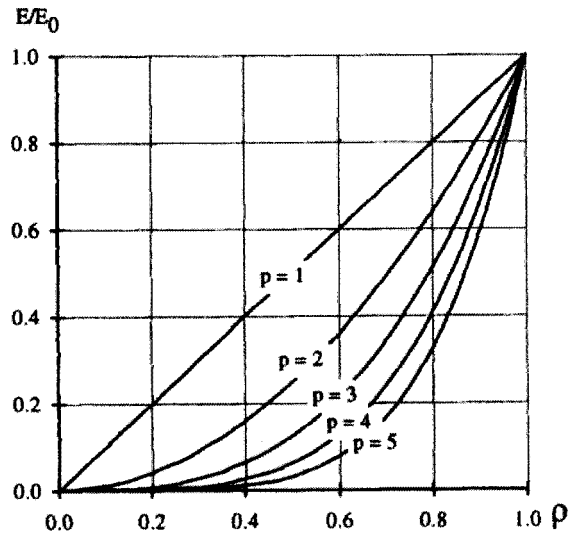

Fig. 9 Relative stiffness vs volume density for the SIMP material model for different values of the penalization power p

model become well posed if eg, a perimeter or surface area constraint is included in the formulation of the problem.

Even if such a constraint is not included in the formulation, the SIMP model can yield very nice results and the simplicity of the model greatly facilitates the implementation of topology design in commercial finite element codes. In research, the method has been very useful in investigations into extending the scope of topology optimization, where this simple model allows for emphasizing other aspects of the problems. In recent years this approach has been employed by Bendsøe [9], Bendsøe and Diaz [145], Duysinx and Bendsøe [201], Hinton *et al* [254], Magister and Post [294], Maute and Ramm [299–301], Maute [70], Petersson and Sigmund [345], Sigmund [379], Sigmund and Torquato [387], Sigmund *et al* [388], and Yang and Chen [415].

The SIMP model is very often called the *Artificial* or the *Fictituous* material model or interpolation scheme in the literature. Thus, up to now, it has not been apparent whether the 'SIMP material' of intermediate density, $0<\rho<1$, could be interpreted physically. However, in very recent work, Bendsøe and Sigmund [151] analyzed the SIMP and similar material models and compared them to variational bounds on effective properties of composite materials, such as the Hashin-Shtrikman bounds (see [251]).

The investigation by Bendsøe and Sigmund [151] led to the remarkable result that under fairly simple conditions on the penalization power p, any of the isotropic elasticity tensors of the SIMP model (2.31) can be physically realized as the elasticity tensor of a composite material made of void and an amount of the reference (base) material corresponding to the relevant density, ρ. For example, for a Poisson's ratio of the base material $\nu=1/3$, both for 2D and 3D problems a penalization power p satisfying $p>3$ ensures that the SIMP model can be physically realized within the framework of microstructured composite materials. Figure 10 depicts microstructures of material and void which realize the material properties of the SIMP model with $p=3$ for a base material with Poisson's ratio $\nu=1/3$. As stiffer material microstructures (that are closer to the *Hashin-Shtrikman* upper bound) can be constructed from the given densities ρ, non-structural areas are found at the cell centers. Thus, due to these very interesting recent results, when assuming proper values of p, we may refer to the SIMP model as a microstructured material model in the sequel.

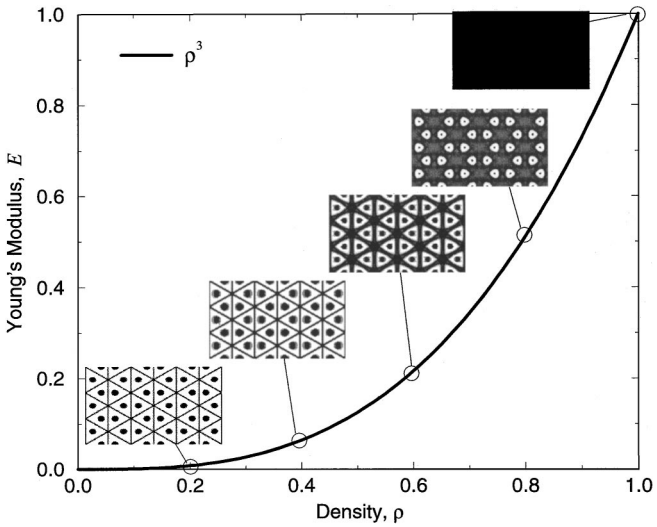

Fig. 10 Microstructures of material and void realizing the material properties of the SIMP model with $p=3$ for a base material with Poisson's ratio $\nu=1/3$ [151]

3 MICROSTRUCTURE APRROACHES: HOMOGENIZATION TECHNIQUES

The microstructure approach to achieve well-posedness of problems of topology optimization is based on the ability to model porous materials with microstructure such as those considered in Subsection 2.5.1-2.5.3. Each of these porous composite materials is constructed from a particular unit cell which at a macroscopic level consists of material and void, and the composite materials consist of infinitely many of such cells that are now assumed to be infinitely small and to be repeated periodically through the composite material. At this limit, we can also have continuously varying density of material through the porous composite material as required for topology optimization.

The resulting material can be described by effective, macroscopic material properties which depend on the geometry of the particular unit cell. These effective macroscopic properties can be computed on the basis of a mathematically based method of homogenization which will be briefly discussed in Section 3.1, but homogenization may also be carried out via *smear-out* or quasi-convexification techniques as will be illustrated in Sections 3.2 and 3.3, respectively.

3.1 Mathematically based homogenization techniques

This approach is based on analysis of the unit cell together with an asymptotic expansion of the displacement field of the composite material, see Bensoussan *et al* [12], Sanchez-Palencia [93], Bourgat [157].

Assuming that two coordinate systems, X and Y, are defined to describe the material on the macroscopic and on the microscopic scale, respectively, it is assumed that a periodic microstructure exists in the vicinity of an arbitrary point $\boldsymbol{x}$ of a linearly elastic structure, see Fig. 7. The periodicity is represented by a parameter δ which is very small, and the Cartesian elasticity tensor E^{δ}_{ijkl} is given in the form

$$E^{\delta}_{ijkl}(\boldsymbol{x})=E_{ijkl}(\boldsymbol{x},\boldsymbol{x}/\delta), \tag{3.1}$$

where $\boldsymbol{y}\rightarrow E_{ijkl}(\boldsymbol{x},\boldsymbol{y})$ is Y-periodic with unit cell $[0,1]\times\boldsymbol{R}$ of periodicity. Here, $\boldsymbol{x}$ is the macroscopic variation of the material parameters, while $\boldsymbol{x}/\delta$ gives the microscopic, periodic variations.

When the composite structure is subjected to macroscopic loading, the displacement field $\mathbf{v}^{\delta}(\boldsymbol{x})$ can be written in the form of an asymptotic expansion with respect to the cell size δ:

$$\mathbf{v}^{\delta}(\boldsymbol{x})=\mathbf{v}_0(\boldsymbol{x})+\delta\mathbf{v}_1(\boldsymbol{x},\boldsymbol{x}/\delta). \tag{3.2}$$

Here, the leading term $\mathbf{v}_0(\boldsymbol{x})$ is the macroscopic displacement field, which is an average over the cell and hence in-

dependent of the microscopic variable $\boldsymbol{y}$. It can be shown [12,93] that the effective displacement field $\mathbf{v}_0(\boldsymbol{x})$ will arise from the macroscopic loading if the effective (homogenized) elasticity tensor $E^H_{ijkl}(\boldsymbol{x})$ has the form

$$E^H_{ijkl}(\boldsymbol{x}) = \frac{1}{|Y|}\int_Y \left[E_{ijkl}(\boldsymbol{x},\boldsymbol{y}) - E_{ijpq}(\boldsymbol{x},\boldsymbol{y})\frac{\partial \chi^{kl}_p}{\partial y_q}\right] d\boldsymbol{y}. \quad (3.3)$$

Here, χ^{kl}_p is a microscopic displacement field which is given as the Y-periodic solution to the cell equilibrium equations

$$\int_Y E_{ijpq}(\boldsymbol{x},\boldsymbol{y})\frac{\partial \chi^{kl}_p}{\partial y_q}\frac{\partial \mathrm{v}_i}{\partial y_j} d\boldsymbol{y} = \int_Y E_{ijkl}(\boldsymbol{x},\boldsymbol{y})\frac{\partial \mathrm{v}_i}{\partial y_j} d\boldsymbol{y} \quad \text{for all } \mathbf{v} \quad (3.4)$$

where $\mathbf{v}$ are Y-periodic displacement fields.

The coefficients in the homogenized elasticity tensor E^H_{ijkl} can be determined by solving three and six prestrain analysis problems for the unit cell Y in cases 2D and 3D, respectively. In most cases this has to be done numerically using finite element analysis [157,233]. For the subsequent application in topology optimization, it is then expedient to represent the dependence of the components of the constitutive tensor on the microstructural parameters by means of approximation formulas.

Referring to Section 2, the constitutive tensor for the *hole-in-cell* microstructure must be determined numerically [76], whereas the tensor can be established analytically for the layered 2D-microstructure by the above approach. With a view to include presentation of other homogenization techniques in this paper, a smear-out and a quasi-convexification approach, respectively, will be presented subsequently by way of the layered 2D microstructure and the layered 3D microstructure described in Section 2.

3.2 Layered 2D microstructure: Smear-out technique

Referring to Subsection 2.4.2, we shall now demonstrate how the effective stiffness tensor for layered 2D microstructures can be derived analytically by a simple averaging technique based on the constitutive relationships between average stress and strain tensors and use of appropriate continuity and discontinuity conditions for components of these tensors at the interfaces between the two materials. Such so-called *smear-out* techniques have previously been used by, eg, Olhoff *et al* [329], for the derivation of effective bending stiffness tensors for microstructurally layered Kirchhoff plates, later by Thomsen [108] for the derivation of effective material stiffness tensors for first-rank planar disk microstructures, and recently also by Soto and Diaz [392–395] Soto [101] for the derivation of effective bending and transverse shear stiffness tensors for microstructurally layered Mindlin plates. In Lipton and Diaz [284], the extremal stiffness tensors for reinforced Midlin plates are derived from optimal bounds of the Hashin-Shtrikman type (see [251]).

3.2.1 Microstructure of first rank

Following the method used in Olhoff *et al* [329], we start by considering a small rectangular plane element Ω as depicted in Fig. 11. The size of this element, which consists of a finite number of parallel, alternating layers of the stiff and the compliant isotropic materials, respectively, is assumed to be small in comparison with the dimensions of the entire plane structure, but to be large relative to its underlying first-rank microstructure. The orientation of the element in the plane coordinate system x_1, x_2 (Fig. 11), is given by the unit vectors n^{R1}_α and t^{R1}_α which are perpendicular to and parallel with the layers, respectively, ie, $n^{R1}_\alpha n^{R1}_\alpha = 1$, $t^{R1}_\alpha t^{R1}_\alpha = 1$, and $n^{R1}_\alpha t^{R1}_\alpha = 0$. The stress-strain field within the element is assumed to be homogeneous from a macroscopic point of view, while at the microscale, ie, at the level of subdomains Ω^+ and Ω^-, the stress-strain field is assumed to be piecewise homogeneous. We shall denote the elasticity tensors for the stiff and compliant layers located in subdomains Ω^+ and Ω^-, by $E^+_{\alpha\beta\kappa\gamma}$ and $E^-_{\alpha\beta\kappa\gamma}$, respectively. Furthermore, assuming that plane stress conditions prevail, and taking the stiff and the compliant isotropic materials used in the layers to have the Young's moduli E^+ and E^- and a common Poisson's ratio ν, we have the following general relationships between the non-zero components of the elasticity tensors for the two types of layering

$$E^{(+/-)}_{1111} = E^{(+/-)}_{2222} = E^{(+/-)}_0; \quad E^{(+/-)}_{1122} = E^{(+/-)}_{2211} = \nu E^{(+/-)}_0,$$
$$E^{(+/-)}_{1212} = E^{(+/-)}_{1221} = E^{(+/-)}_{2121} = E^{(+/-)}_{2112} = \frac{1-\nu}{2} E^{(+\ -)}_0, \quad (3.5)$$

where the stiffness constants E^+_0 and E^-_0 for the stiff and the compliant layers, are given by

$$E^{(+/-)}_0 = \frac{E^{(+/-)}}{1-\nu^2}. \quad (3.6)$$

We now determine the effective elasticity tensor $E^{R1}_{\alpha\beta\kappa\gamma}$ for our first-rank microstructure shown in Fig. 11, by firstly considering the constitutive relationship for the small rectangular domain Ω,

$$\sigma^{avr}_{\alpha\beta} = E^{R1}_{\alpha\beta\kappa\gamma}\varepsilon^{avr}_{\kappa\gamma}. \quad (3.7)$$

Here, the Greek indices refer to the axes of a global coordinate system x_1x_2 embedded in the plane domain, see Fig. 11, and the tensors $\varepsilon^{avr}_{\kappa\gamma}$ and $\sigma^{avr}_{\kappa\gamma}$ are direct averages of strain and stress tensors for the small plane element Ω. Defining homogeneous strain tensors $\varepsilon^+_{\alpha\beta}$ and $\varepsilon^-_{\alpha\beta}$ and stress tensors

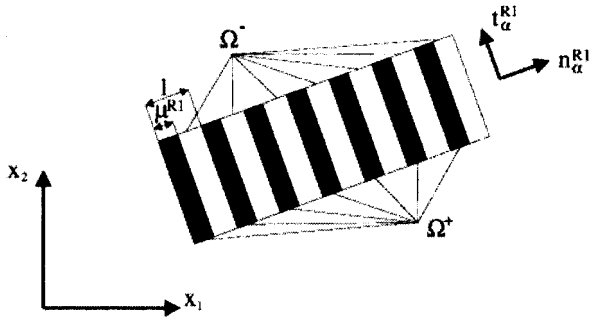

Fig. 11 Plane element with an underlying first-rank microstrucrure

$\sigma^+_{\alpha\beta}$ and $\sigma^-_{\alpha\beta}$ within subdomains Ω^+ and Ω^-, respectively, we have the following constitutive relations for the subdomains Ω^+ and Ω^-,

$$\sigma^+_{\alpha\beta}=E^+_{\alpha\beta\kappa\gamma}\varepsilon^+_{\kappa\gamma};\quad \sigma^-_{\alpha\beta}=E^-_{\alpha\beta\kappa\gamma}\varepsilon^-_{\kappa\gamma} \tag{3.8}$$

and the following expressions for the direct averages of the strain and stress tensors within the domain Ω,

$$\begin{aligned}\varepsilon^{avr}_{\alpha\beta}&=\mu^{R1}\varepsilon^+_{\alpha\beta}+(1-\mu^{R1})\varepsilon^-_{\alpha\beta};\\ \sigma^{avr}_{\alpha\beta}&=\mu^{R1}\sigma^+_{\alpha\beta}+(1-\mu^{R1})\sigma^-_{\alpha\beta}.\end{aligned} \tag{3.9}$$

The problem is now to establish an analytical expression for the effective elasticity tensor $E^{R1}_{\alpha\beta\kappa\gamma}$ as a function of the density variable μ^{R1} and the layering orientation n^{R1}_α, see Fig. 11. Such an expression can be derived by usage of Eqs. (3.7)–(3.9) and two sets of interface conditions that express the mechanics of the microstructure.

Firstly, from considerations of static equilibrium across the interfaces between adjacent subdomains Ω^+ and Ω^- we can write the following set of continuity/discontinuity conditions for the components of the stress tensors acting parallel and orthogonal to the interface,

$$\begin{aligned}&(\sigma^+_{\alpha\beta}-\sigma^-_{\alpha\beta})n^{R1}_\alpha n^{R1}_\beta=0;\quad (\sigma^+_{\alpha\beta}-\sigma^-_{\alpha\beta})t^{R1}_\alpha t^{R1}_\beta\neq 0;\\ &(\sigma^+_{\alpha\beta}-\sigma^-_{\alpha\beta})n^{R1}_\alpha t^{R1}_\beta=0.\end{aligned} \tag{3.10}$$

Similarly, by geometric compatibility considerations we may set up the following continuity/discontinuity conditions for the components of the strain tensors acting parallel and orthogonal to the interface:

$$\begin{aligned}&(\varepsilon^+_{\alpha\beta}-\varepsilon^-_{\alpha\beta})n^{R1}_\alpha n^{R1}_\beta\neq 0;\quad (\varepsilon^+_{\alpha\beta}-\varepsilon^-_{\alpha\beta})t^{R1}_\alpha t^{R1}_\beta=0;\\ &(\varepsilon^+_{\alpha\beta}-\varepsilon^-_{\alpha\beta})n^{R1}_\alpha t^{R1}_\beta\neq 0.\end{aligned} \tag{3.11}$$

However, these interface conditions may be written in the more compact form

$$\varepsilon^+_{\alpha\beta}-\varepsilon^-_{\alpha\beta}=\beta_1 n^{R1}_\alpha n^{R1}_\beta+\beta_2(t^{R1}_\alpha n^{R1}_\beta+n^{R1}_\alpha t^{R1}_\beta), \tag{3.12}$$

where the scalars β_1 and β_2 designate the jumps of those components of the strain tensor that exhibit discontinuity across the interfaces between the Ω^+ and Ω^- subdomains.

Equations (3.7)–(3.10) and (3.12) together with Eqs. (3.5)–(3.6) constitute the set of equations needed for the derivation of the effective stiffness tensor. The remaining part of the derivation consists of simple but cumbersome algebraic manipulations of these equations (the reader is referred to Krog [58] Krog and Olhoff [271]), which yield the following analytical expressions for the effective stiffness tensor for the first-rank 2D microstructure,

$$E^{R1}_{\alpha\beta\kappa\gamma}=E^+_{\alpha\beta\kappa\gamma}-(1-\mu^{R1})\left[(E^+_{\alpha\beta\kappa\gamma}-E^-_{\alpha\beta\kappa\gamma})^{-1}-\frac{\mu^{R1}}{E^+_0}\Lambda^{R1}_{\alpha\beta\kappa\gamma}\right]^{-1} \tag{3.13}$$

with specific expressions for elasticity entries defined in Eq. (3.4). Here, the tensor $\Lambda^{R1}_{\alpha\beta\kappa\gamma}$ contains information about layer orientation and is defined as

$$\begin{aligned}\Lambda^{R1}_{\alpha\beta\kappa\gamma}=&n^{R1}_\alpha n^{R1}_\beta n^{R1}_\kappa n^{R1}_\gamma+\frac{1}{2(1-\nu)}(t^{R1}_\alpha n^{R1}_\beta n^{R1}_\kappa t^{R1}_\gamma\\ &+n^{R1}_\alpha t^{R1}_\beta n^{R1}_\kappa t^{R1}_\gamma+t^{R1}_\alpha n^{R1}_\beta t^{R1}_\kappa n^{R1}_\gamma+n^{R1}_\alpha t^{R1}_\beta t^{R1}_\kappa n^{R1}_\gamma).\end{aligned} \tag{3.14}$$

It is worth mentioning that the isotropy of the elasticity tensor $E^+_{\alpha\beta\kappa\gamma}$ for the material in the subdomains Ω^+ has been used in the derivation of Eq. (3.13), while no such restriction has been imposed on the elasticity tensor $E^-_{\alpha\beta\kappa\gamma}$ for the material in the subdomains Ω^-. This important feature makes these equations applicable for calculation of effective elasticity properties of multi-rank microstructures.

3.2.2 Effective elasticity in matrix form

A convenient matrix description of the effective stiffness properties can be obtained if we introduce the following orthonormal basis of symmetric second order tensors

$$\xi^1=\frac{1}{\sqrt{2}}\begin{bmatrix}1&0\\0&-1\end{bmatrix};\quad \xi^2=\frac{1}{\sqrt{2}}\begin{bmatrix}0&1\\1&0\end{bmatrix};\quad \xi^3=\frac{1}{\sqrt{2}}\begin{bmatrix}1&0\\0&1\end{bmatrix}. \tag{3.15}$$

In this basis, any symmetric second order tensor is represented as a vector, and any symmetric fourth order tensor as a symmetric 3×3 matrix. Thus, the symmetric fourth order elasticity tensor $E_{\alpha\beta\kappa\gamma}$ for the plane disk may be represented as a symmetric 3×3 matrix $\boldsymbol{E}$ with components E_{ij} defined by

$$\boldsymbol{E}=[E_{ij}]=[\xi^i_{\alpha\beta}\xi^j_{\kappa\gamma}E_{\alpha\beta\kappa\gamma}]=\left[\begin{array}{c|c|c}\frac{1}{2}(E_{1111}+E_{2222})-E_{1122} & E_{1112}-E_{2221} & \frac{1}{2}(E_{1111}-E_{2222})\\ \hline & 2E_{1212} & E_{1112}+E_{2221}\\ \hline sym & & \frac{1}{2}(E_{1111}+E_{2222})+E_{1122}\end{array}\right]. \tag{3.16}$$

With this transformation at hand, we are able to transform the fourth-order tensor equation for the effective elasticity tensor in the preceding Section into a simple matrix equation. The *inverse transformation* for computation of the components of the original elasticity tensor from the components of the matrix E can be seen in Krog [58] and Krog and Olhoff [271]. Now, applying the transformation in Eq. (3.16) to the tensor equation for the effective elasticity tensor, $E^{R1}_{\alpha\beta\kappa\gamma}$ in Eqs. (3.13), and by using the following relation

$$\xi^i_{\alpha\beta}\xi^j_{\kappa\gamma}(E_{\alpha\beta\kappa\gamma})^{-1}=(\xi^i_{\alpha\beta}\xi^j_{\kappa\gamma}E_{\alpha\beta\kappa\gamma})^{-1}, \tag{3.17}$$

which holds for fourth order tensors with all major and minor symmetries, we get the following matrix equation:

$$\begin{aligned}\boldsymbol{E}^{R1}&=[E^{R1}_{ij}]=[\xi^i_{\alpha\beta}\xi^j_{\kappa\gamma}E^{R1}_{\alpha\beta\kappa\gamma}]\\ &=\boldsymbol{E}^+-(1-\mu^{R1})\left((\boldsymbol{E}^+-\boldsymbol{E}^-)^{-1}-\frac{\mu^{R1}}{E^+_0}\boldsymbol{\Lambda}^{R1}\right)^{-1}.\end{aligned} \tag{3.18}$$

Here $\boldsymbol{E}^+$, $\boldsymbol{E}^-$ and $\boldsymbol{\Lambda}^{R1}$ are (3×3) matrices obtained by using the transformations in Eq. (3.16) to the fourth order

tensors $E^{+}_{\alpha\beta\kappa\gamma}$, $E^{-}_{\alpha\beta\kappa\gamma}$ and $\Lambda^{R1}_{\alpha\beta\kappa\gamma}$. Adopting the notation introduced in Eqs. (3.5), and using the isotropy of the tensors $E^{+}_{\alpha\beta\kappa\gamma}$ and $E^{-}_{\alpha\beta\kappa\gamma}$, we get the following expressions for the matrices $\boldsymbol{E}^{+}$ and $\boldsymbol{E}^{-}$,

$$\begin{aligned}\boldsymbol{E}^{(+/-)}&=[E^{(+/-)}_{ij}]\\&=[\xi^{i}_{\alpha\beta}\xi^{j}_{\kappa\gamma}E^{(+/-)}_{\alpha\beta\kappa\gamma}]\\&=E^{(+/-)}_{0}\begin{bmatrix}1-\nu & 0 & 0\\ 0 & 1-\nu & 0\\ 0 & 0 & 1+\nu\end{bmatrix}\end{aligned} \tag{3.19}$$

Finally, taking the normal and tangential vectors, n^{R1}_{α} and t^{R1}_{α}, in the expression for the tensor $\Lambda^{R1}_{\alpha\beta\kappa\gamma}$ given in Eq. (3.14) as

$$n^{R1}_{\alpha}=\{\cos(\theta^{R1}),\ \sin(\theta^{R1})\}^{T}$$

and

$$t^{R1}_{\alpha}=\{-\sin(\theta^{R1}),\ \cos(\theta^{R1})\}^{T},$$

we obtain the following expression for the matrix $\boldsymbol{\Lambda}^{R1}$,

$$\boldsymbol{\Lambda}^{R1}=[\xi^{i}_{\alpha\beta}\xi^{j}_{\kappa\gamma}\Lambda^{R1}_{\alpha\beta\kappa\gamma}]=\begin{bmatrix}\frac{3-\nu(1+\nu)\cos(4\theta^{R1})}{4(1-\nu)} & -\frac{(1-\nu)\sin(4\theta^{R1})}{4(1-\nu)} & \frac{\cos(2\theta^{R1})}{2}\\ & \frac{3-\nu+(1+\nu)\cos(4\theta^{R1})}{4(1-\nu)} & \frac{\sin(2\theta^{R1})}{2}\\ sym & & \frac{1}{2}\end{bmatrix}. \tag{3.20}$$

The matrix expressions in Eqs. (3.18)–(3.20) constitute a simple set of matrix equations for the components of the effective elasticity tensor for the first-rank 2D microstructures described in Subsection 2.5.2.

3.2.3 Multi-rank layered 2D microstructures

Analytical expressions for the effective elasticity matrix for layered 2D microstructures of any finite rank may, as indicated in Eq. (2.28), be established iteratively. Thus the effective elasticity properties of a rank-$(i+1)$ microstructure may be determined by using the expressions for the effective elasticity matrix for a first-rank microstructure given in Eqs. (3.18)–(3.20) with the effective elasticity for a rank-i microstructure as the elasticity of the compliant material.

Following derivations in Soto [101] (see also, [280,281]), we obtain the following expression for the effective elasticity matrix [58,101,196,269],

$$\boldsymbol{E}^{R1}=\boldsymbol{E}^{+}-(1-\rho^{R1})\left[(\boldsymbol{E}^{+}-\boldsymbol{E}^{-})^{-1}-\frac{\rho^{R1}}{E^{+}_{0}}\sum_{i=1}^{I}p_{i}\boldsymbol{\Lambda}^{Ri}\right]^{-1}, \tag{3.21}$$

where the factors p_i for the rank-I microstructure obey the relationship

$$\sum_{i=1}^{I}p_{i}=1;\quad p_{i}\geqslant 0,\quad i=1,\ldots,I \tag{3.22}$$

and the layer orientation matrix $\boldsymbol{\Lambda}^{Ri}$ is given by

$$\boldsymbol{\Lambda}^{Ri}=[\xi^{i}_{\alpha\beta}\xi^{j}_{\kappa\gamma}\Lambda^{Ri}_{\alpha\beta\kappa\gamma}]=\begin{bmatrix}\frac{3-\nu-(1+\nu)\cos(4\theta^{Ri})}{4(1-\nu)} & -\frac{(1+\nu)\sin(4\theta^{Ri})}{4(1-\nu)} & \frac{\cos(2\theta^{Ri})}{2}\\ & \frac{3-\nu+(1+\nu)\cos(4\theta^{Ri})}{4(1-\nu)} & \frac{\sin(2\theta^{Ri})}{2}\\ sym & & \frac{1}{2}\end{bmatrix}, \tag{3.2}$$

where (compare with Eq. (3.20) and Fig. 6), θ^{Ri} is the angle between the global x_1 axis and the unit normal vector n^{Ri}_{α} to the layering made at the i-th step of the construction of the rank-I microstructure.

Notice that Eq. (3.21) gives a mathematical expression for the effective elasticity matrix for a rank-I layered 2D microstructure where the microstructure is described in terms of $(2I+1)$ parameters, namely the total density ρ^{R1} of stiff material in the microstructure, the I new density variables p_i, and the I layer orientations in the microstructure given by the angles of rotation θ^{Ri}, $i=1,\ldots,I$ through Eq. (3.23). The new density variables p_i, $i=1,\ldots,I$, of which only $I-1$ are mutually independent in view of Eq. (3.22), are defined by

$$p_{i}=\frac{(1-\rho^{R(i-1)})\mu^{Ri}}{\rho^{RI}},\quad i=1,\ldots I. \tag{3.24}$$

3.2.4 Special case: Second-rank 2D microstructure with orthogonal layers

Historically, the second-rank 2D matrix laminates where introduced first by Lurie and Cherkaev [67] for the heat conductivity problems and subsequently for elasticity problems by Gibianski and Cherkaev [39]. The latter paper derived the properties of the second-rank laminates and provided proof of the optimality of these microstructures for the problem of an elastic plate which is mathematically identical to the plane elasticity problem; the paper contains the complete solution to this problem along with numerical examples, see also Lurie and Cherkaev [289] and Cherkaev and Gibianski [182–184].

Second-rank layered microstructures with orthogonal layers play an important role in the design parametrization of topology optimization problems for planar disks, because such microstructures are optimum for single load case stiffness design problems for planar disks. In the sequel, we therefore write the analytical expressions for the components of the effective membrane stiffness tensor for second-rank disk microstructures with orthogonal layers. The tensor is expressed relative to a fixed material coordinate system $x'_1x'_2$ with axes parallel to the layering directions of the microstructure, see Fig. 12, and the results will therefore only depend on the two density variables μ^{R1} and μ^{R2}. The dependence on the layer directions are described via a third design variable θ which gives the overall rotation of the orthotropic microstructure relative to a fixed global coordinate system x_1x_2, see Fig. 12. The dependence of the effective stiffness tensor on this design variable is simply accounted for via transformation formulas for rotation of anisotropic materials [114] and Tsai *et al* [112], Tsai and Pagano [408].

From Eqs. (3.21), (3.22) and (3.24) we get the following expression for the effective membrane elasticity matrix for a second-rank 2D microstructure with non-orthogonal layers,

$$\boldsymbol{E}^{R2}=\boldsymbol{E}^{+}-(1-\mu^{R1})(\boldsymbol{1}-\mu^{R2})\times \left[(\boldsymbol{E}^{+}-\boldsymbol{E}^{-})-\frac{\mu^{R1}\boldsymbol{\Lambda}^{R1}+(1-\mu^{R1})\mu^{R2}\boldsymbol{\Lambda}^{R2}}{E_0^{+}}\right]^{-1}. \tag{3.25}$$

The elasticity matrices $\boldsymbol{E}^{+}$ and $\boldsymbol{E}^{-}$ which characterize the constituent layers of the microstructure are defined in Eq. (3.19), while the geometric matrices $\boldsymbol{\Lambda}^{R1}$ and $\boldsymbol{\Lambda}^{R2}$ which depend on the normal vectors n_α^{R1} and n_α^{R2} are defined in Eq. (3.23). Taking the latter to be orthogonal and given by the angles $\theta^{R1}=0$ deg and $\theta^{R2}=90$ deg with respect to the x_1' axis we obtain the following expressions for the geometric matrices for a second-rank disk microstructure with orthogonal layers,

$$\boldsymbol{\Lambda}^{R1}=\begin{bmatrix}\frac{1}{2} & 0 & \frac{1}{2}\\ 0 & \frac{1}{1-\nu} & 0\\ \frac{1}{2} & 0 & \frac{1}{2}\end{bmatrix};\quad \boldsymbol{\Lambda}^{R2}=\begin{bmatrix}\frac{1}{2} & 0 & -\frac{1}{2}\\ 0 & \frac{1}{1-\nu} & 0\\ -\frac{1}{2} & 0 & \frac{1}{2}\end{bmatrix}. \tag{3.26}$$

With the definitions in Eq. (3.19) and Eq. (3.26) and the expression in Eq. (3.25), we can now write an analytical expression for the effective elasticity matrix for the microstructure. By an inverse transformation we have then established the expressions given below for the non-zero components of the effective membrane elasticity tensor for a second-rank 2D microstructure with orthogonal layers, where the density variables μ^{R1} and μ^{R2} have been written by the short-hand symbols μ_1 and μ_2,

$$E_{1111}^{R2}=\frac{E_0^{R2}+E_1^{R2}(\mu_2-\mu_1\mu_2-\mu_2^2+2\mu_1\mu_2^2-\mu_1^2\mu_2^2)}{E_2^{R2}+E_3^{R2}};$$

$$E_{2222}^{R2}=\frac{E_0^{R2}+E_1^{R2}(\mu_1-\mu_1^2)}{E_2^{R2}+E_3^{R2}};$$

$$E_{1122}^{R2}=\frac{\nu E_0^{R2}+\nu E_1^{R2}(\mu_1\mu_2-\mu_1^2\mu_2)}{E_2^{R2}+E_3^{R2}};$$

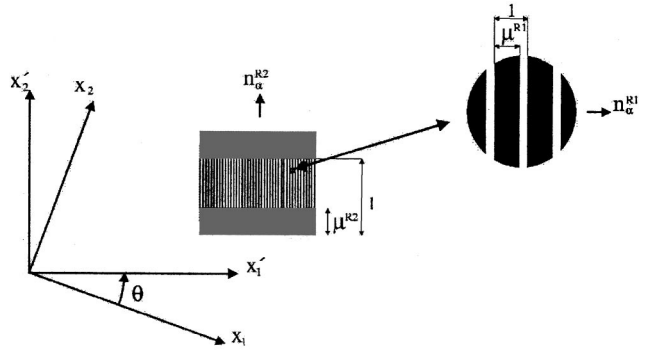

Fig. 12 Second-rank microstructure with orthogonal layers

$$E_{1212}^{R2}=\frac{(1-\mu)E_0^{-}E_0^{+}}{2E_4^{R2}} \tag{3.27}$$

with

$$\begin{aligned}
&E_0^{R2}=E_0^{-}(E_0^{+})^2,\\
&E_1^{R2}=(1-\nu^2)(E_0^{-}-E_0^{+})^2E_0^{+},\\
&E_2^{R2}=(E_0^{+})^2+E_0^{+}(E_0^{-}-E_0^{+})(\mu_i+\mu_2-\mu_1\mu_2),\\
&E_3^{R2}=(1-\nu^2)(E_0^{-}-E_0^{+})^2(\mu_1\mu_2-\mu_1^2\mu_2),\\
&E_4^{R2}=E_0^{+}+(E_0^{-}-E_0^{+})(\mu_1+\mu_2-\mu_1\mu_2).
\end{aligned} \tag{3.28}$$

Corresponding expressions for the effective bending and transverse shear stiffness tensors for a second-rank Mindlin plate microstructure with orthogonal layers are given in Krog [58] and Krog and Olhoff [269].

In topology optimization of disks, we may now apply a design parameterization where the material in each domain of the finite element discretized structure is modeled as an orthotropic material with the appropriate stiffness properties of the second-rank microstructure written above. This yields a convenient finite parameter, continuous formulation of the topology optimization problem. At this point, we shall not discuss the type of behavioral objective and constraint functions which may be considered using such a design parameterization, but only present the following general formulation of the topology optimization problem:

Objective:

$$\min_{\mu_{1e},\mu_{2e},\theta_e} \text{or} \max[f(\mu_{1e},\mu_{2e},\theta_e)] \qquad e=1,\ldots,N_e.$$

Subject to:

$$\begin{aligned}
&g_i(\mu_{1e},\mu_{2e},\theta_e)\leqslant 0 && e=1,\ldots,N_e, i=1,\ldots,p,\\
&h_j(\mu_{1e},\mu_{2e},\theta_e)=0 && e=1,\ldots,N_e, j=1,\ldots,q,\\
&0\leqslant\mu_{1e}\leqslant 1 && e=1,\ldots,N_e,\\
&0\leqslant\mu_{2e}\leqslant 1 && e=1,\ldots,N_e.
\end{aligned} \tag{3.29}$$

Here f, g_i, and h_j are objective and constraint functions for the optimization, and N_e denotes the total number of finite elements of the discretized structure. It is important to realize that this problem is inherently a very large scale problem; the number of design variables equals three times the number of finite elements of the discretized structure. This naturally imposes some restrictions on the type of objective and constraint functions that may be considered, and the problem generally requires usage of special optimization procedures in order to deal with the many design variables in an efficient way.

3.2.5 Moment formulation

While the second-rank 2D microstructure with orthogonal layers considered in the preceding subsection is optimum for single load case stiffness design problems for disks, a third-rank microstructure with non-orthogonal layers is optimum for the corresponding multiple load case design problem for disks. For other types of planar design problems, where the

optimum microstructure is unknown, one should use as general a microstructure as possible, but also here a design parameterization based on a third-rank microstructure with non-orthogonal layers seems reasonable; the full range of effective stiffness properties for all finite-rank 2D microstructures are described by only five independent variables, and the effective stiffness properties may be calculated analytically using the expressions in Eqs. (3.21), (3.22), and (3.23).

However, a design parametrization of stiffnesses directly in terms of layer directions is often associated with problems of nonconvexity as there exist local optimum solutions with respect to the layer directions (Pedersen [341–343]), and this implies that usual solution methods based on sensitivity analysis and mathematical programming normally fail.

To illustrate how these problems can be overcome, in the following we therefore consider a special restatement of the expressions for the effective stiffness properties of planar microstructures in terms of so-called *geometric moment variables*. Moment formulations for description of effective stiffness properties of composite laminates and layered microstructures were introduced by Tsai and Pagano [408] and Francfort and Murat [225] and later applied by Miki [306] as an effective parameterization to render laminate optimization problems in a convex formulation, and by Avellaneda and Milton [135] in the derivation of bounds on the elastic stiffness tensors for layered planar microstructures of arbitrary rank. There is an immediate connection between the use of moment variables in topology design and in design of laminates ([35,45,219,220,221,229,232,244,245,307], and references cited therein for optimum design of laminates).

In relation to topology optimization problems, moment formulations have been used by eg, Lipton [280,281], Diaz *et al* [196], Krog [58], Soto [101], and Krog and Olhoff [269,271] for the description of effective stiffness properties of microstructurally layered Kirchhoff and Mindlin plates, and by Lipton and Diaz [282] and Diaz and Lipton [195,199] for description of effective stiffness properties of three dimensional microstructures. The moment formulation for microstructurally layered Mindlin plates considered here follows the developments by Diaz *et al* [196] and Soto [101] and it is attractive for the following reasons:

- As shown in the afore-mentioned papers, the moment formulation yields a full description of the effective stiffness properties for all finite-rank 2D microstructures using only five design variables.
- For a fixed strain field, the strain energy density has been found to be concave in the set of variables used to describe the anisotropy of the microstructure [196,280,281]. Thus, for stiffness design problems, the possibility of convergence to local extrema is eliminated in the computation of optimum layer orientations.
- For other types of problems than stiffness design problems, application of periodic functions of layering orientations generally is avoided in the expressions for the effective stiffness properties, so difficulties with local extrema with respect to layer orientations also can be expected to be eliminated for those problems.

To establish the moment formulation for a general rank-I layered planar microstructure we now in the set of Eqs. (3.21), (3.22), and (3.23) for the effective stiffness matrix perform a variable substitution in which we condense all information on the layer densities and orientations given by the design variables p_i and θ^{Ri}, $i=1,\ldots,I$, into four new variables, the moment variables $m_1,\ldots,m_4$, which we define as

$$
\begin{aligned}
m_1 &= \sum_{i=1}^{I} p_i \cos(2\theta^{Ri}),\\
m_2 &= \sum_{i=1}^{I} p_i \sin(2\theta^{Ri}),\\
m_3 &= \sum_{i=1}^{I} p_i \cos(4\theta^{Ri}),\\
m_4 &= \sum_{i=1}^{I} p_i \sin(4\theta^{Ri}).
\end{aligned}
\tag{3.30}
$$

These moment variables together with the condition $\Sigma_{i=1}^{I} p_i = 1$ in Eq. (3.22) and the expressions in Eqs. (3.23) allow us to define the folowing matrix

$$
\boldsymbol{M} = \sum_{i=1}^{I} p_i \boldsymbol{\Lambda}^{Ri}
= \left[\begin{array}{c|c|c}
\dfrac{3-\nu-(1+\nu)m_3}{4(1-\nu)} & -\dfrac{(1+\nu)m_4}{4(1-\nu)} & \dfrac{m_1}{2} \\ \hline
 & \dfrac{3-\nu+(1+\nu)m_3}{4(1-\nu)} & \dfrac{m_2}{2} \\ \hline
sym & & \dfrac{1}{2}
\end{array}\right],
\tag{3.31}
$$

which we may use to rewrite the expression for the effective elasticity (stiffness) matrix in Eq. (3.21) in the following convenient form

$$
\boldsymbol{E}^{RI} = \boldsymbol{E}^{+} - (1-\rho^{RI})\left((\boldsymbol{E}^{+}-\boldsymbol{E}^{-})^{-1} - \frac{\rho^{RI}}{E_0^{+}}\boldsymbol{M} \right)^{-1}. \tag{3.32}
$$

Hence, by the variable substitution in Eq. (3.30) we have obtained a very simple expression which gives the full range of effective stiffness properties of all finite-rank planar microstructures using only five design variables, namely the density ρ^{R1} of layers of stiff material in the microstructure and the four moment variables $m_1,\ldots,m_4$ defined in Eqs. (3.30). It follows from Eqs. (3.30) that the moment variables, in general, must satisfy the simple side constraints

$$
-1 \leq m_i \leq 1, \quad i=1,\ldots,4. \tag{3.33}
$$

The moment variables $m_1,\ldots,m_4$ are obviously not mutually independent due to the trigonometric relations between the functions that define the moments, and therefore there

exist some additional conditions which restrict the combinations of the moment variables to some feasible domain. This set of additional constraints on the moment variables was first established by Avellaneda and Milton [135] via the solution to the trigonometric moment problem treated in Krein and Nudelman [57]. Hereby, the following two additional constraint equations for the moment variables were derived:

$$g_1(m_1,m_2)=m_1^2+m_2^2\leqslant 1$$

$$g_2(m_1,m_2,m_3,m_4)=2m_1^2(1-m_3)+2m_2^2(1+m_3)+(m_3^2+m_4^2)-4m_1m_2m_4\leqslant 1. \tag{3.34}$$

For topology and layout optimization problems for 2D continuum structures, we may now apply a design parameterization where the material in each subdomain of a finite element discretized structure is modeled as an anisotropic material with stiffness properties given by Eqs. (3.30)–(3.32). The general topology or layout optimization problem may then be stated as follows.

Objective:
$$\min_{\rho_e^{R1},m_{1e},m_{2e},m_{3e},m_{4e}} \text{or} \max \quad [f(\rho_e^{R1},m_{1e}m_{2e},m_{3e},m_{4e})] \qquad e=1,\ldots,N_e.$$

Subject to:

$$g_i(\rho_e^{R1},m_{1e},m_{2e},m_{3e},m_{4e})\leqslant 0, \qquad e=1,\ldots,N_e, i=1,\ldots,p,$$

$$h_j(\rho_e^{R1},m_{1e},m_{2e},m_{3e},m_{4e})=0, \qquad e=1,\ldots,N_e, j=1,\ldots,q,$$

$$g_{1e}(m_{1e},m_{2e})\leqslant 1, \qquad e=1,\ldots,N_e,$$

$$g_{2e}(m_{1e},m_{2e},m_{3e},m_{4e})\leqslant 1, \qquad e=1,\ldots,N_e,$$

$$0\leqslant \rho_e^{R1}\leqslant 1, \qquad e=1,\ldots,N_e,$$

$$-1\leqslant m_{1e}\leqslant 1, i=1,\ldots,4, \qquad e=1,\ldots,N_e, \tag{3.35}$$

where f, g_1, and h_j are the objective and constraint functions for the optimization, g_{1e} and g_{2e} are local element constraints which must be satisfied by the set of moment variables associated with each finite element, and N_e denotes the total number of elements in the finite element discretized structure. As compared with the optimization problem formulated in Eqs. (3.29) in Subsection 3.2.4, the optimization problem in Eqs. (3.35) is much larger both in terms of the number of design variables and constraint equations. It should be noted that the solution to the optimization problem in Eqs. (3.35) directly yields the optimum material densities, and hence the global distribution of material over the structure. The solution also contains the optimum values of the moment variables, but these do not directly yield the optimum layer densities and orientations. A method for determining the local microstructure that corresponds to a given combination of the moment variables can be found in eg, Lipton [280,281], Diaz *et al* [196], and Soto [101].

3.3 Layered 3D microstructures: Quasiconvexification

We now consider the layered 3D microstructure discussed in Section 2.5.3 and shown in Fig. 8, and subsequently follow the analysis in Gibianski and Cherkaev [40] in establishing analytical expressions for the complementary energy density $\bar{U}^*$ and elastic properties of this 3D microstructure that can be shown to be optimum in terms of stiffness subject to any given 3D state of stress. This is achieved by construction of an upper and a lower bound $\bar{U}_l^*\leqslant\bar{U}^*\leqslant\bar{U}_u^*$ for the complementary elastic energy density $\bar{U}^*$ of the optimum microstructure. The upper bound $\bar{U}_u^*$ will be established by minimization of the complementary energy density of a bi-material matrix layered composite of any rank, and the lower bound $\bar{U}_l^*$ (which is valid for any bi-material microstructure) will be developed by means of quasiconvexification. The optimum characteristics of the microstructure for topology optimization for maximum stiffness (minimum compliance) are derived subsequently by utilizing the fact (Gibianski and Cherkaev [40]) that in the limit where the compliance of one of the two materials tends to infinity in order to mimic void, the above mentioned bounds coincide with $\bar{U}^*$ so that $\bar{U}_l^*=\bar{U}^*=\bar{U}_u^*$, and from this follow the desired analytical results. The composite in Fig. 8 is assumed to be made of two materials with 6×6 dimensional compliance matrices denoted by $\boldsymbol{C}_1$ and $\boldsymbol{C}_2$, respectively. The compliance matrices which are the inverted elasticity matrices are given by

$$\boldsymbol{C}(\kappa,\mu)=\left[\begin{array}{ccc:ccc} \frac{3\kappa+\mu}{9\kappa\mu} & \frac{2\mu-3\kappa}{18\kappa\mu} & \frac{2\mu-3\kappa}{18\kappa\mu} & 0 & 0 & 0 \\ \frac{2\mu-3\kappa}{18\kappa\mu} & \frac{3\kappa+\mu}{9\kappa\mu} & \frac{2\mu-3\kappa}{18\kappa\mu} & 0 & 0 & 0 \\ \frac{2\mu-3\kappa}{18\kappa\mu} & \frac{2\mu-3\kappa}{18\kappa\mu} & \frac{3\kappa+\mu}{9\kappa\mu} & 0 & 0 & 0 \\ \hdashline 0 & 0 & 0 & \frac{1}{2\mu} & 0 & 0 \\ 0 & 0 & 0 & 0 & \frac{1}{2\mu} & 0 \\ 0 & 0 & 0 & 0 & 0 & \frac{1}{2\mu} \end{array}\right] \tag{3.36}$$

where κ and μ are the bulk and shear moduli respectively, and where the indices of the two materials have been omitted. The effective elastic properties of the resulting anisotropic material depend on the material properties of the two constituents given by $\boldsymbol{C}_1,\boldsymbol{C}_2$, the normals $\boldsymbol{n}$ to the material interfaces, and the volume fractions m_1 and m_2 ($m_2=1-m_1$) of the two materials.

As a function of the parameter α_i representing the spatial thickness of layer i in the microstructure, the expression for the optimum compliance tensor $\boldsymbol{C}_M$, for a matrix layered composite of any rank n is given by

$$\boldsymbol{C}_M=\boldsymbol{C}_1+\boldsymbol{Q}^{-1}, \tag{3.37}$$

where

$$\boldsymbol{Q}=\frac{1}{m_2}(\boldsymbol{C}_2-\boldsymbol{C}_1)^{-1}+\frac{m_1}{m_2}\sum_{i=1}^{n}\alpha_i N_i, \tag{3.38}$$

$$\boldsymbol{N}_i=\boldsymbol{N}(\boldsymbol{n}_i)=\boldsymbol{p}_i(\boldsymbol{p}_i^T\boldsymbol{C}_1\boldsymbol{p}_i)^{-1}\boldsymbol{p}_i^T,$$

$$\sum_{i=1}^{n}\alpha_i=1,\quad \alpha_i\geqslant 0.$$

The projection matrix $\boldsymbol{p}_i$ controls discontinuous stress components across the material interfaces, and $\boldsymbol{n}_i$ is the normal to the i-th layer. Inserting this result in the expression for the complementary energy density, we get the following equation for a minimum value of the upper bound energy density $\overline{U}_u^*$ with respect to the variables α_i and $\boldsymbol{n}_i$

$$\overline{U}_u^*=\sigma^T\boldsymbol{C}_1\sigma+\min_{\alpha_i,\boldsymbol{n}_i}\sigma^T\boldsymbol{Q}^{-1}\sigma, \tag{3.39}$$

where σ is a 6×1 vector of stress components defined by $\sigma=(\sigma_{11},\sigma_{22},\sigma_{33},\sigma_{12},\sigma_{13},\sigma_{23})^T$. Assuming that we are dealing with a rank three material that is oriented along the principal stress directions, we can write

$$\sum_{i=1}^{3}\alpha_i N_i=\frac{2\mu_1}{3\kappa_1+4\mu_1}\begin{bmatrix}\boldsymbol{B}_1 & 0\\ 0 & \boldsymbol{B}_2\end{bmatrix}, \tag{3.40}$$

where the matrices $\boldsymbol{B}_1$ and $\boldsymbol{B}_2$ are given by

$$\boldsymbol{B}_1=\begin{bmatrix}2(3\kappa_1+\mu_1)(\alpha_2+\alpha_3) & (3\kappa_1-2\mu_1)\alpha_3 & (3\kappa_1-2\mu_1)\alpha_2\\ (3\kappa_1-2\mu_1)\alpha_3 & 2(3\kappa_1+\mu_1)(\alpha_1+\alpha_3) & (3\kappa_1-2\mu_1)\alpha_1\\ (3\kappa_1-2\mu_1)\alpha_2 & (3\kappa_1-2\mu_1)\alpha_1 & 2(3\kappa_1+\mu_1)(\alpha_1+\alpha_2)\end{bmatrix},$$

$$\boldsymbol{B}_2=\begin{bmatrix}(3\kappa_1+\mu_1)\alpha_3 & 0 & 0\\ 0 & (3\kappa_1+4\mu_1)\alpha_2 & 0\\ 0 & 0_1 & (3\kappa_1+4\mu_1)\alpha_1\end{bmatrix}, \tag{3.41}$$

respectively.

Referring to Gibianski and Cherkaev [40] and the initial discussion in this section, the expression for maximum value of the lower bound $\overline{U}_l^*$ on the complementary energy density $\overline{U}^*$ of any microstructure made of two elastic materials with volume fractions m_1 and $m_2=1-m_1$ and compliance matrices $\boldsymbol{C}_1$ and $\boldsymbol{C}_2$, is given by

$$\overline{U}_l^*=\max_{\alpha_j}\sigma^T\beta\sigma \tag{3.42}$$

with the compliance matrix $\beta=[\boldsymbol{C}_1,\boldsymbol{C}_2,\phi(a_j)]$ defined by

$$\beta=[[m_1(\boldsymbol{C}_1-\phi)^{-1}+m_2(\boldsymbol{C}_2-\phi)^{-1}]^{-1}+\phi]. \tag{3.43}$$

where

$$\phi=\begin{bmatrix}\alpha_1^2 & -\alpha_1\alpha_2 & -\alpha_1\alpha_3 & 0 & 0 & 0\\ -\alpha_1\alpha_2 & \alpha_2^2 & -\alpha_2\alpha_3 & 0 & 0 & 0\\ -\alpha_1\alpha_3 & -\alpha_2\alpha_3 & \alpha_3^2 & 0 & 0 & 0\\ 0 & 0 & 0 & \alpha_2^2+\alpha_3^2 & 0 & 0\\ 0 & 0 & 0 & 0 & \alpha_1^2+\alpha_3^2 & 0\\ 0 & 0 & 0 & 0 & 0 & \alpha_1^2+\alpha_2^2\end{bmatrix} \tag{3.44}$$

is the non-convex matrix function that makes $\overline{U}_l^*$ quasiconvex. Here, a_j, $(j=1,2,3)$, are scalar parameters, and the maximization in Eq. (3.42) is to be carried out with respect to these. The parameters a_1, a_2 and a_3 must satisfy the constraints of positive definiteness of the matrices $\boldsymbol{C}_i-\phi(a_1,a_2,a_3)$, $i=1,2$, which ensure positive definiteness of the compliance matrix β, Eq. (3.43), and hence positive complementary energy for all σ in Eq. (3.42).

In the case of topology optimization, where the compliant material is considered as void, the expressions for the effective properties of the microstructure simplify considerably so that the optimum properties can be expressed in explicit analytic form [40]. Thus, letting $\boldsymbol{C}_2\to\infty$ to mimic void, the term $(\boldsymbol{C}_2-\phi)^{-1}$ of $\beta(\boldsymbol{C}_1,\boldsymbol{C}_2,\phi(a_j))$ in Eq. (3.43) vanishes, and the following expression for $\overline{U}_l^*$ is obtained

$$\overline{U}_l^*=\max_{\alpha_j}\sigma^T\left[\left(1+\frac{m_2}{m_1}\right)\boldsymbol{C}_1-\frac{m_2}{m_1}\phi\right]\sigma$$

$$=\sigma^T\boldsymbol{C}_1\sigma+\frac{m_2}{m_1}\max_{\alpha_j}\sigma^T\boldsymbol{G}\sigma \tag{3.45}$$

with $\boldsymbol{G}=\boldsymbol{C}_1-\phi$. Assuming that $\boldsymbol{n}_i$ are oriented along the principal directions of σ, it is only the upper 3×3 blocks of $\boldsymbol{C}_1$ and $\boldsymbol{G}$ that have an influence upon the resulting bound. The lower bound $\overline{U}_l^*$ for the complementary energy density can then be formulated as

$$\overline{U}_l^*=\hat{\sigma}^T\hat{\boldsymbol{C}}_1\hat{\sigma}+\frac{m_2}{m_1}\max_{\alpha_j}\hat{\sigma}^T\hat{\boldsymbol{G}}\hat{\sigma}, \tag{3.46}$$

where $\hat{\sigma}$ indicates principal stresses, and $\hat{\boldsymbol{G}}$, $\hat{\boldsymbol{C}}_1$ indicate the upper-left 3×3 blocks of the 6×6 matrices $\boldsymbol{G}$ and $\boldsymbol{C}_1$ respectively. If a_i is chosen optimally we can write

$$\overline{U}_l^*=\hat{\sigma}^T\left(\hat{\boldsymbol{C}}_1+\frac{m_2}{m_1}\hat{\boldsymbol{G}}\right)\hat{\sigma}. \tag{3.47}$$

Assuming that σ is oriented along the principal directions such that $\sigma^1=(\sigma_1,\sigma_2,\sigma_3,0,0,0)$ and by defining principal stress ratios ω and η as

$$\omega=\frac{\sigma_1}{\sigma_3},\quad \eta=\frac{\sigma_2}{\sigma_3}\quad \text{where}\quad \sigma_3\geqslant|\sigma_2|\ \text{ and }\ \sigma_3\geqslant|\sigma_1| \tag{3.48}$$

the optimum values of the parameters a_j can be derived in explicit analytical form by assuming that the optimum solution lies on the edges or vertices of the design space. The expressions for the optimum parameters a_j change with changing stresses, and it turns out that the entire stress domain is covered by nine different sets of expressions for the optimum parameters a_j. These expressions can be used to determine the optimum α_i associated with the upper bound (Gibianski and Cherkaev [40]).

Considering the upper bound $\overline{U}_u^*$ in Eq. (3.39) with $\boldsymbol{Q}$ given in Eq. (3.38), and letting $\boldsymbol{C}_2\to\infty$, the first term of $\boldsymbol{Q}$ equals zero. Moreover, assuming that the rank three micro-

structure is oriented along the principal stress directions, the second term in the expression for $\boldsymbol{Q}$ simplifies, and the following expression for $\overline{U}_u^*$ is obtained

$$\overline{U}_u^* = \hat{\sigma}^T \hat{\boldsymbol{C}}_1 \hat{\sigma} + \min_{\alpha_i} \hat{\sigma}^T \hat{\boldsymbol{Q}}^{-1} \hat{\sigma}. \tag{3.49}$$

Provided that α_i, $i=1,2,3$, are chosen optimally we can write

$$\overline{U}_u^* = \hat{\sigma}^T [\boldsymbol{C}_1 + \hat{\boldsymbol{Q}}^{-1}] \hat{\sigma} = \hat{\sigma}^T \hat{\boldsymbol{C}}_M \hat{\sigma}, \tag{3.50}$$

where $\hat{\boldsymbol{C}}_M$ is the optimum effective compliance matrix. In Eqs. (3.49) and (3.50), the vector $\hat{\sigma}$ and the matrices $\boldsymbol{C}_1$, $\hat{\boldsymbol{Q}}$ and $\hat{\boldsymbol{C}}_M$ are all expressed in the basis $\boldsymbol{n}_i$ oriented along the principal directions of σ. It is shown in Gibianski and Cherkaev [40] that the two bounds $\overline{U}_u^*$ and $\overline{U}_l^*$ coalesce for an optimum microstructure which implies that for any admissible a_j the following difference is equal to zero

$$\overline{U}_u^*(\sigma) - \overline{U}_l^*(\sigma) = \max_{a_j} \min_{\alpha_i} \sigma^T (\boldsymbol{Q}^{-1}(\alpha_i) - \boldsymbol{G}(a_j)) \sigma = 0, \tag{3.51}$$

which after some algebra can be reduced to

$$(\hat{\boldsymbol{Q}}(\alpha_j) \hat{\boldsymbol{G}}_j - \boldsymbol{I}) \hat{\sigma} = 0, \tag{3.52}$$

where $\boldsymbol{I}$ is the unit matrix. In order to solve this problem, we first determine the eigenvalues of the 3×3 matrix $\hat{\boldsymbol{Q}}(\alpha_i) \hat{\boldsymbol{G}}_i$. It can be shown that for all matrices $\hat{\boldsymbol{Q}}(\alpha_i) \hat{\boldsymbol{G}}_i$ the corresponding eigenvalues are equal to (0, 0, 1) and the corresponding eigenvector yields a set of equations which upon solution yields the optimum a_j that satisfy Eq. (3.52).

The solution of this problem reveals that the relation between the principal stresses and the optimum microstructure changes for different stresses and that the entire stress domain is divided into nine sub-domains (Fig. 13) with different relations. The expressions for the individual domains are listed in Eq. (3.53) where ν denotes Poisson's ratio.

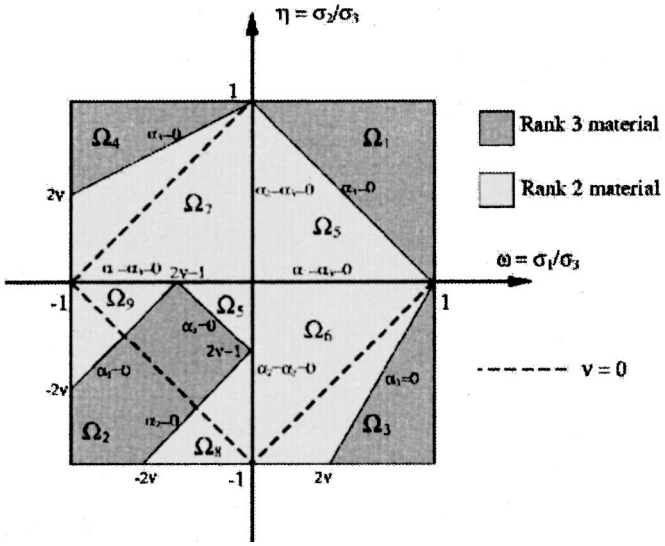

Fig. 13 The domain Ω with individual sub-domains Ω_1

$$\alpha_1 = \frac{1-\omega+\eta}{1+\omega+\eta}, \quad \alpha_2 = \frac{1+\omega-\eta}{1+\omega+\eta}, \quad \alpha_3 = \frac{\omega+\eta-1}{1+\omega+\eta}, \quad \text{if } \sigma \in \Omega_1$$

$$\alpha_1 = \frac{-\omega+\eta-(1-2\nu)}{(1-2\nu)(\omega+\eta-(1+2\nu))},$$

$$\alpha_2 = \frac{\omega-\eta-(1-2\nu)}{(1-2\nu)(\omega+\eta-(1+2\nu))},$$

$$\alpha_3 = \frac{\omega+\eta+(1-2\nu)}{\omega+\eta-(1+2\nu)}, \quad \text{if } \sigma \in \Omega_2$$

$$\alpha_1 = \frac{1-\omega-(1-2\nu)\eta}{(1-2\nu)(1+\omega-(1-2\nu)\eta)},$$

$$\alpha_2 = \frac{1+\omega+(1-2\nu)\eta}{1+\omega-(1+2\nu)\eta},$$

$$\alpha_3 = \frac{\omega-(1-2\nu)\eta-1}{(1-2\nu)(1+\omega-(1-2\nu)\eta)}, \quad \text{if } \sigma \in \Omega_3;$$

$$\alpha_1 = \frac{\eta-1-\omega(1-2\nu)}{(1-2\nu)(1-(1+2\nu)\omega+\eta)},$$

$$\alpha_2 = \frac{1-\omega(1-2\nu)-\eta}{(1-2\nu)(1-(1+2\nu)\omega+\eta)},$$

$$\alpha_3 = \frac{1+\omega(1-2\nu)+\eta}{(1-(1+2\nu)\omega+\eta)}, \quad \text{if } \sigma \in \Omega_4;$$

$$\alpha_1 = \frac{\eta}{\omega+\eta}, \quad \alpha_2 = \frac{\omega}{\omega+\eta}, \quad \alpha_3 = 0, \quad \text{if } \sigma \in \Omega_5;$$

$$\alpha_1 = \frac{\eta}{\omega-\eta}, \quad \alpha_2 = \frac{\omega}{\omega-\eta}, \quad \alpha_3 = 0, \quad \text{if } \sigma \in \Omega_6;$$

$$\alpha_1 = \frac{\eta}{\omega-\eta}, \quad \alpha_2 = \frac{\omega}{\omega-\eta}, \quad \alpha_3 = 0, \quad \text{if } \sigma \in \Omega_7;$$

$$\alpha_1 = \frac{1}{1-\omega}, \quad \alpha_2 = 0, \quad \alpha_3 = \frac{\omega}{\omega-1}, \quad \text{if } \sigma \in \Omega_8$$

$$\alpha_1 = 0, \quad \alpha_2 = \frac{1}{1-\eta}, \quad \alpha_3 = \frac{\eta}{1-\eta}, \quad \text{if } \sigma \in \Omega_9. \tag{3.53}$$

Equations (3.53) constitute the analytically derived solution to the local microstructure optimization problem. From Fig. 13, it is clear that if the size of all principal stresses are in the same range, the resulting microstructure is a rank three laminate, whereas the resulting microstructure is a rank two laminate if one principal stress is considerably less than the two others.

3.3.1 Parametric study of the microstructure

Parametric studies of the effective properties of microstructures can be used to reveal valuable information about stability and response of the microstructures under certain conditions. Extensive parametric studies have thus been performed by a number of researchers for the ranked laminates, but these have almost exclusively been devoted to pla-

nar rank 2 laminates (Bendsøe [9], Sigmund [377]). The relation between the effective properties of the layered 3D microstructure and some of the used parameters have been studied by Gibianski and Cherkaev [40], Cherkaev and Palais [185], Jacobsen *et al* [257], and Olhoff *et al* [330].

In this context, it is important to note [330] that the 3D laminate generally does not suffer from the problem of lack of shear stiffness which is the case for the 2D laminate (see, eg, [9]). Considering Eqs. (2.19) and (3.40), it is clear that the microstructure possesses a finite stiffness in all tensor directions if the microstructure is of third rank.

Due to the large number of parameters in the 3D case, it is useful to perform a numerical analysis in order to obtain an overall picture of the material properties (Jacobsen *et al* [257], Olhoff *et al* [330]). Hence, with the results for the rigorous 3D microstructural model of the preceding section at hand, we may compare the relative energy (stiffness) of this microstructure to that of the non-penalized model used for isotropic materials (ie, isotropic material with $p=1$ in Eq. (3.21) and Fig. 9). A plot of the relative energy $E_{\mathrm{rel}} = \overline{U}^*_{\mathrm{iso}}/\overline{U}^*_{\mathrm{aniso}}$ vs. the volume density ρ of material is shown in Fig. 14.

The energy density of the anisotropic material is not uniquely defined because it varies with varying stresses, but if we vary the stress field within the admissible limits for a fixed volume density ρ of material, we get the results shown in Fig. 14. The upper limit of the gray region corresponds to a rank 1 material while the lower limit corresponds to a rank 3 material. An essential observation is that in all points except of $\rho=0$ and $\rho=1$, the energy density of the ranked optimum anisotropic material is always higher than (in the special case of a uniaxial stress, equal to) that of the isotropic material model. This indicates that the commonly used assumption of a linear material density to stiffness relation overestimates the stiffness of a given structure if intermediate densities occur. This is in perfect agreement with results obtained by Sigmund [377] for plane laminates.

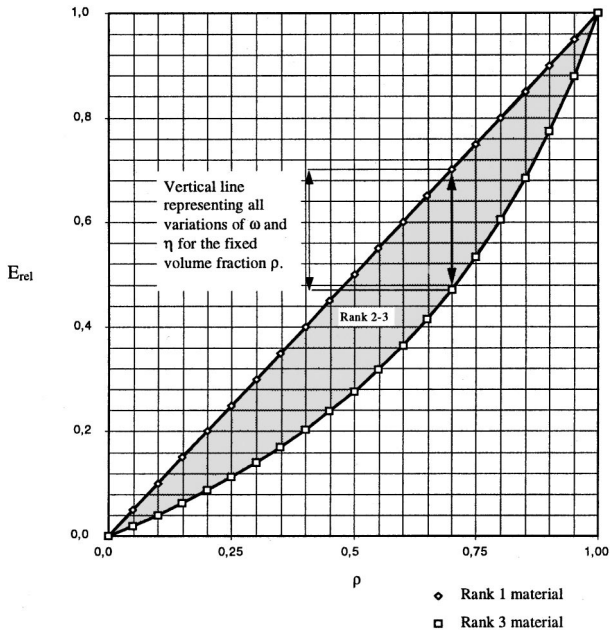

Fig. 14 Relative energy $E_{rel}=\overline{U}^*_{iso}/\overline{U}^*_{aniso}$ *vs* the volume density ρ of material for the entire range of principal stress ratios ω and η

3.4 Discussion and examples

3.4.1 Mesh independence of solutions

We now illustrate numerically by way of an example that the layered 2D and 3D microstructures considered in Sections 3.2 and 3.3 provide full relaxation of problems of maximum stiffness topology design for a single case of loading. As discussed in Section 2.4, topology and layout optimization are often not well-posed because the design space is not closed in the appropriate sense. A remedy to ensure closure of the set of feasible designs is then to relax, ie, regularize, the mathematical formulation of the problem by introducing composites with perforated, periodic microstructures as admissible materials for the structural design [9,66,176,180,181,266,267,290,329]. Numerical indications of the need for regularization of a given problem are lack of convergence and dependence of the design on the size of the applied finite element mesh. In particular, if the problem is not properly regularized it is not possible to obtain a limiting, numerically stable design by consecutively decreasing the mesh size [176,180,181,329].

To illustrate the mesh dependence of topologies obtained by using the 3D microstructures of Section 3.3, we consider for convenience a planar design domain with loading and support conditions as depicted in Fig. 15*a*. The problem is modeled by usage of 8-node 3D isoparametric finite elements and solved using three different mesh sizes, whereby solutions as shown in Figs. 15*b*,*c*, and *d* are obtained [330]. It is seen that the topology is consistent.

The results clearly indicate mesh independence of the topology and the existence of a well-defined limiting design for any further mesh refinement. This witnesses that the applied microstructures have provided full relaxation of the problem. It is worth noting that the solutions in Fig. 15 con-

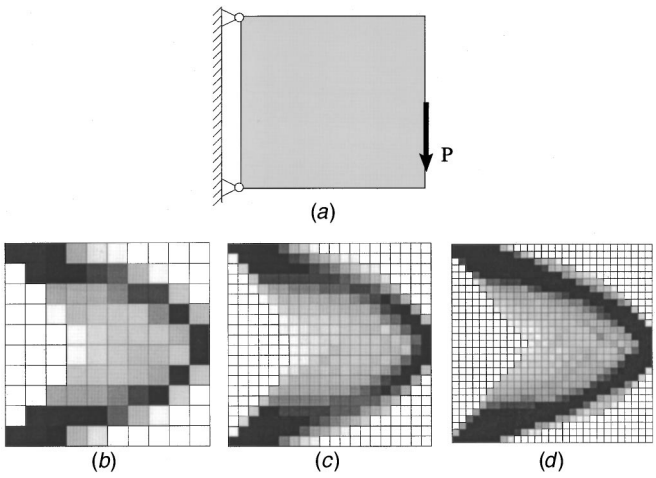

Fig. 15 Example of finite element mesh refinement [330]: *a*) Admissible design domain, loading and support conditions for example problem, and *b*, *c*, *d*) Topology results obtained for different mesh sizes

sist of composite in large sub-domains, and that the designs in Figs. 15*c* and *d* strongly resemble that of a Michell truss (Michell [305]). This is not surprising since the Michell truss is the optimum solution to the problem depicted in Fig. 15*a* provided that the amount of available material is much less than the amount prescribed in the current example.

3.4.2 2D topology examples

Consider now a simple maximum stiffness topology design problem for a 2D structure [271]. The structure is to be confined within a rectangular design domain and to be subjected to a concentrated load and be supported as shown in Fig. 16. The volume fraction of available material relative to the admissible design domain is taken to be 0.45. The design domain is dicretized into a 60×20 mesh of 8-node 2D isoparametric finite elements, and we consider two cases where the material within each of the elements is modelled by either a second-rank 2D microstructure with orthogonal layers as considered in Section 3.2.4 or by a layered microstructure of arbitrary rank governed by the moment formulation in Section 3.2.5.

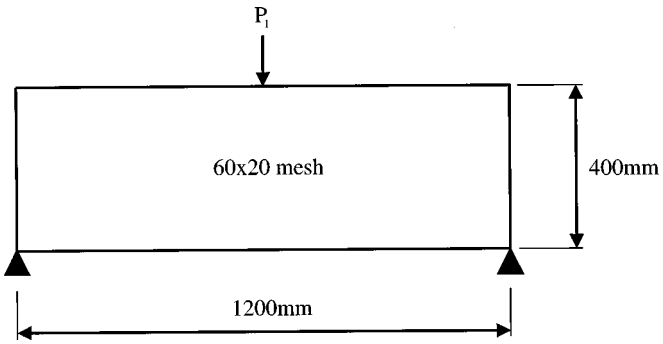

Fig. 16 Design domain, load, and support conditions for the 2D example problems

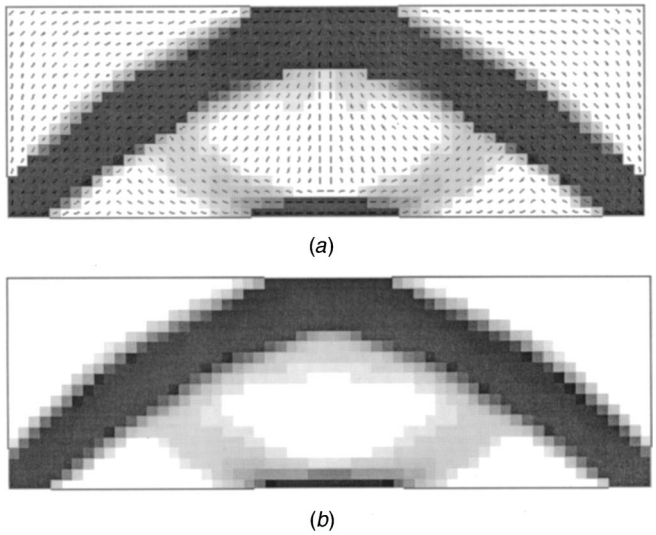

Fig. 17 Optimum solution to example problems [271]; *a*) Solution by usage of second-rank 2D microstructures with orthogonal layers. The direction of the principal material stiffness is also shown; *b*) Solution based on layered microstructure of arbitrary rank governed by the moment formulation

The two optimization problems have been solved using the two iterative approaches outlined in Sections 3.2.4 and 3.2.5, respectively, and Figs. 17*a* and *b* show the optimum topologies obtained. These two optimum solutions are found to have the same stiffness (total elastic energy) and are also seen to be almost identical. This is to be expected as the optimum microstructure for the solution of the problem considered here is a second-rank microstructure (Section 3.2.4), and this microstructure is contained as a special case of the layered microstructure of arbitrary rank covered by the moment formulation in Section 3.2.5.

3.4.3 3D topology examples

We now consider two full 3D topology optimization examples (Olhoff *et al* [330]), where the solution is based on usage of the optimum 3D material microstructure discussed in Section 3.3.

The first example is presented in Fig. 18. Here, Fig. 18*a* shows a cubic design domain which is subjected to four parallel concentrated loads *P* at the upper surface and equipped with simple supports at the four corners of the lower surface. The volume fraction of available material relative to the design domain is chosen to be 0.08 in this example. Figure 18*b* illustrates the optimum topology solution to the problem which is a quadrupod consisting of four legs of quite distinctly solid material, each transferring one of the applied concentrated loads to the nearest simple support, and a substructure made of composite material which interconnects the upper parts of the four legs.

Figure 19 displays an example, cf, Olhoff *et al* [330], of an oblong box-formed design domain for which the available volume fraction of material is taken to be 0.30. The two ends of the domain are clamped, and a concentrated bending moment *M* acts at the center. Figure 19*b* shows the topology solution obtained after usage of a commonly used method of penalization (Rozvany *et al* [90], Olhoff and Rozvany [75]) of intermediate densities $0<\rho<1$ of material that makes a 0-1 solution more advantageous, but the solution is seen to consist still of a large part of composite material. In Fig. 19*c*,

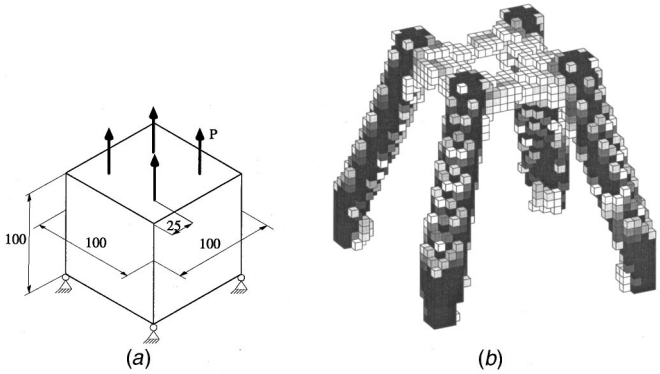

Fig. 18 Cubic design domain subjected to four point loads *P*. (Material volume fraction=0.08): *a*) Design domain with loading and support conditions, *b*) Quadrupod solution to the problem with material densities less than 0.8 removed

elements with material densities below 0.5 have been removed from the solution as a means to visualize the topology.

3.4.4 Discussion

As is clearly illustrated by the results in Figs. 16 and 19, it is a characteristic feature that the structures of optimum topology obtained by the approach of relaxation generally consist of composite material in large sub-domains. There are two reasons for this. Firstly, as discussed in Section 3.3.1, depending on the state of stress, composite materials are generally much more efficient than isotropic, solid materials, and therefore largely manifest themselves in optimum solutions. Secondly, it is characteristic that application of the optimum 2D or 3D microstructures considered in Sections 3.2 and 3.3 as a basis for topology optimization actually prompts a larger content of composite material in the resulting solution, as compared with use of non-optimum microstructures.

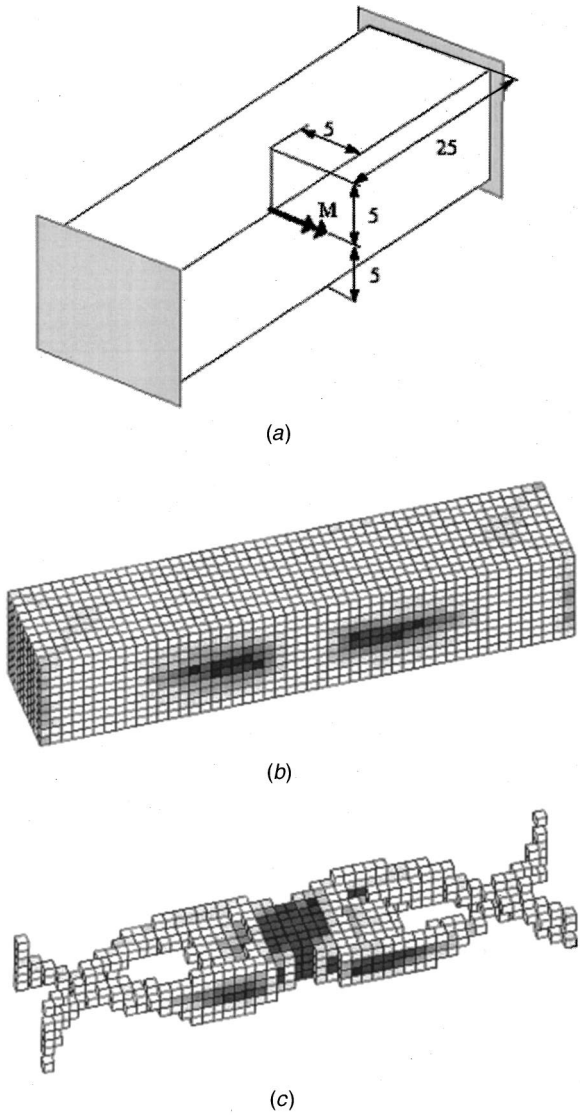

Fig. 19 Oblong box-shaped design domain with clamped ends and a concentrated bending moment M acting in the center (Olhoff *et al* [330]): (Material volume fraction=0.3): *a*) Design domain with loading and support conditions; *b*) Topology solution represented with all material densities present; and *c*) Solution depicted with densities below 0.5 removed

Hence, optimum microstructures must always be chosen as a basis for topology optimization when it is our desire to obtain or acquire knowledge of the global optimum solution associated with the highest possible value of the performance index. The not surprisingly large structural sub-domains of composite material that are a consequence of such a desire, however, often make it difficult to visualise the overall structural topology of such a solution and to devise simplified, sub-optimum (0-1) designs or designs that are attractive from the point of view of manufacture.

In the subsequent Section 4, we shall consider how the introduction of appropriate restrictions in the formulation of topology optimization problems may lead to more distinct (0-1) topology designs that are easier to manufacture, but also associated with a lower value of the performance index.

4 OTHER APPROACHES TO ACHIEVE WELL-POSED PROBLEM FORMULATIONS: PERIMETER METHOD AND FILTERING TECHNIQUES

As discussed at the end of Section 2.4.2, the distributed, discrete valued black-white (0-1) topology optimization problem stated by Eqs. (2.22) [or (2.24)], (2.23) and (2.26) of determining the stiffest (minimum compliance) structure under a single loading condition by distributing a fixed volume V_{fixed} of homogeneous, isotropic, linearly elastic material within an admissible design domain Ω, is ill-posed. In this formulation, Ω_s is the solid part of Ω where material is present, and the design variable χ is a binary indicator function with $\chi=1$ denoting solid and $\chi=0$ denoting void. Attempts to solve this problem do not converge to macroscopic patterns of solid and void. Instead, rapid spatial oscillations appear in the function χ as the compliance is reduced. Although a limiting value of the compliance can be determined, the solution tends toward a design with an infinite number of vanishing small holes, rather than a finite number of macroscopic holes.

One way of achieving a well-posed problem is to *extend* the design space (via *relaxation*) to include materials with perforated microstructure of variable density covering the entire spectrum from solid to void, and to derive their effective mechanical properties by homogenization as considered in Section 3. Numerical methods based on a complete relaxation (ie, incorporating *optimum* microstructures as considered in Subsections 2.5.2, 2.5.3 and Section 3) are convergent with respect to mesh refinement, but they yield solutions with large sub-domains of perforated material which are undesirable from the point of view of manufacturing, see Section 3.3 and, eg, [260]. Numerical methods based on partial relaxations (cf the *Hole-in-Cell* microstructures [150] considered in Subsection 2.5.1) generate implicit penalties against intermediate densities. They behave similarly to methods with explicit penalties.

This section will focus on another way to achieve a well-posed mathematical formulation for topology optimization,

namely to restrict the design space such as to remove the possibility of rapid oscillations in the density of material in the structure. Approaches of this kind have been studied in Haber *et al* [237–239], Beckers [7,139], Duysinx [25], and Beckers and Fleury [140], where a constraint is imposed on the perimeter of the structure (see the following Section 4.1), in Petersson and Sigmund [345] where a pointwise constraint is imposed on the gradient of the density of material (see Section 4.2), and in Sigmund [97,379], Sigmund and Torquto [379], and Sigmund and Petersson [387] where an image processing inspired filter is used to maintain a certain minimum length scale in the structure (Section 4.3). In Borrwall and Petersson [17], a regularized intermediate density control is used.

4.1 Perimeter method

In Haber *et al* [237–239] and Jog and Haber [259], a new method is introduced that achieves a well-posed continuum optimization problem by restricting the design space to exclude rapidly oscillating designs. These authors defined the perimeter of a design as the measure of the boundary of the solid region: $|\partial\Omega_s|$. Designs with fewer, larger holes have lower perimeter measures than designs of equal volume with more numerous smaller holes. Chattering designs are characterized by unbounded perimeter measures, so an upper-bound constraint on the perimeter effectively excludes chattering solutions from the feasible design space. Furthermore, a perimeter bound controls the number and sizes of holes in a macroscopic design without otherwise restricting the shape or layout of the holes. Thus, Haber *et al* [237–239] appended an upper bound constraint on the perimeter $|\partial\Omega_s| \leqslant \overline{P}$ (where $\overline{P}$ is a designer-specified value) to the abovementioned problem stated by Eqs. (2.22) [or (2.24)], (2.23) and (2.26). An existence proof for a topology design problem similar to this perimeter constrained problem is presented by Ambrosio and Buttazzo [128].

Finite element discretizations of the discrete valued, perimeter constrained topology optimization problem generate integer programming problems that until very recently were considered too large for direct solution. However, Beckers [7] recently overcame this difficulty by developing a very efficient discrete mathematical programming method working in the dual space, and she has subsequently published several solutions to these large-scale, discrete valued problems [7,139,140] with global design objectives and constraints. Both these papers and Fernandes *et al* [216] consider 3D problems with a *perimeter* constraint.

Haber *et al* [237–239] used a continuous approximation to the problem by replacing the indicator function χ with a distributed interpolation parameter ρ, $0 \leqslant \rho_{\min} \leqslant \rho \leqslant 1$, for the volume density of material, and introduced a penalty on intermediate values of ρ to suppress transitional material in the final design. The small lower bound $\rho_{\min}$ on ρ ensures that the energy is positive definite, and the volume of structural material is simply given by $\int_\Omega \rho d\Omega$.

As a representation of the perimeter measure $|\partial\Omega_s|$ that is compatible with the continuous interpolation model, Haber *et al* [237–239] adopted the Total Variation $TV(\rho)$ of ρ, as this is a suitable measure approaching the perimeter in the limit as the amount of transitional material is forced to zero [33]. In anticipation of a piecewise-continuous finite element model for ρ, Haber *et al* [237–239] partitioned the admissible design domain Ω into a set of open, disjoint regions Ω_α so that $\Omega = \bigcup_\alpha \Omega_\alpha$, and accounted for the possibility that ρ may be discontinuous across sets of measure zero (eg the finite element boundaries). The total variation of the scalar function ρ can then be expressed [117] as

$$TV(\rho) = \int_{\Omega/\Gamma_J} |\nabla\rho| d\Omega + \int_{\Gamma_J} |\langle\rho\rangle| d\Gamma, \tag{4.1}$$

where $\Gamma_J = \Omega / \bigcup_\alpha \Omega_\alpha$ is the jump set of ρ, and $\langle\rho\rangle$ is the jump in ρ across Γ_J.

The total variation in Eq. (4.1) is used to express the "perimeter" P of the material volume density function ρ via the formula

$$P \equiv \int_{\Omega/\Gamma_J} g_n(\nabla\rho, \xi) d\Omega + \int_{\Gamma_J} j(\langle\rho\rangle, \xi) d\Gamma, \tag{4.2}$$

where the functions g_n and j are defined by

$$\begin{aligned} g_n(\boldsymbol{w}, \xi) &\equiv \left[(1 + 2\xi)\boldsymbol{w}^T\boldsymbol{w} + \frac{\xi^2}{h^2} \right]^{1/2} - \frac{\xi}{h}; \\ j(r, \xi) &\equiv [(1 + 2\xi)r^2 + \xi^2]^{1/2} - \xi \end{aligned} \tag{4.3}$$

and are smooth approximations to $|\boldsymbol{w}|$ and $|r|$, respectively. Isotropy properties of the *perimeter*, P are discussed by Petersson *et al* [344]. In Eq. (4.3), h is a characteristic mesh dimension (eg, the size of a finite element). The smoothing, based on the parameter ξ in Eq. (4.3), circumvents numerical problems associated with the non-differentiability of the magnitude and absolute value operators appearing in the expression for the total variation in Eq. (4.1). Note that $\lim_{\xi \to 0} g_n(\nabla\rho, \xi) = |\nabla\rho|$ and $\lim_{\xi \to 0} j(\langle\rho\rangle, \xi) = |\langle\rho\rangle|$. Further, the approximations are exact in the limit of a discrete approximation to an integer design, even for $\xi > 0$. That is, for all $\xi \geqslant 0$, $g_n(\nabla\rho, \xi) \to |\nabla\rho|$ as $|\nabla\rho| \to 0$ or $1/h$, and $j(\langle\rho\rangle, \xi) \to |\langle\rho\rangle|$ as $|\langle\rho\rangle| \to 0$ or 1.

Haber *et al* [237–239] use an optimality criterion method to solve the design problem. The constraint $|\partial\Omega_s| \leqslant \overline{P}$ is treated with an interior penalty method, and the prescribed volume constraint is enforced with a *Lagrange* multiplier. The modified problem considered has the form

$$\sup_{\rho} \inf_{\boldsymbol{u}} \Pi + \alpha S_1 + \beta S_2 - \lambda \left[\int_\Omega \rho d\Omega - V_{\text{fixed}} \right], \tag{4.4}$$

in which Π is the total potential energy, $\boldsymbol{u}$ the displacement field, α and β are positive scalars, S_1 is a function that penalizes intermediate values of ρ, S_2 is an interior penalty function for the constraint $|\partial\Omega_s| \leqslant \overline{P}$, and λ is the Lagrange multiplier associated with the volume constraint.

Figure 20 illustrates the use of the perimeter method to control the optimum topology and to achieve mesh independent solutions (Haber *et al* [239]). The results are obtained for the beam example first considered in Olhoff *et al* [327]: a simply supported beam with a midspan load on the top sur-

face. Solid material is prescribed around the periphery, and $V_{\text{fixed}} = 0.60|\Omega|$. The results in Figs. 20*a* and *b* are based on a perimeter bound $\bar{P} = 30L$. While the coarse mesh in Fig. 20*a* is not able to completely resolve the design, the optimum topology is essentially the same as the one obtained with the refined mesh in Fig. 20*b*. The characteristic Michell truss layout is evident. A simpler optimum topology is obtained by reducing the perimeter bound to $\bar{P} = 24L$ in Figs. 20*c* and *d*. The same optimum topology is clearly evident in Figs. 20*c* and 20*d*, demonstrating the ability of the perimeter method to generate mesh independent solutions. An even simpler design is obtained by further reducing the perimeter bound to $\bar{P} = 22L$ in Figs. 20*e* and *f*. Figure 20*g* shows a very simple topology obtained by setting $\bar{P} = 18L$.

The compliance values obtained on different meshes cannot be directly compared, because the discretization error associated with a coarser mesh artificially reduces the compliance. However, the trade-off between stiffness (low compliance) and perimeter is clearly evident when designs obtained on the same mesh are compared (Figs. 20*a*, *c*, *e*, and *g* for the coarse mesh and Figs. 20*b*, *d*, and *f* for the refined mesh). Improved stiffness can be achieved at the cost of design complexity; the compliance increases as the perimeter bound is decreased to achieve a simpler design. On the other hand, the results show that designs with simple, practical topologies can be achieved with a relatively small increase in compliance.

It may be concluded that the perimeter method yields high-quality numerical solutions and has the following distinct advantages:

Firstly, solutions are convergent with respect to mesh refinement; finer meshes offer improved resolution without altering the design. Next, the SIMP material model (see Subsection 2.4.2) or any other reasonable interpolation can be used to model material properties for intermediate values of ρ. The complexities and limitations of the homogenization method are circumvented; so the perimeter method is easy to implement and is extensible to general constraint and objective functions. Finally, the perimeter method allows the designer to control the number and scale of the holes, and the designer can vary $\bar{P}$ to explore alternative designs.

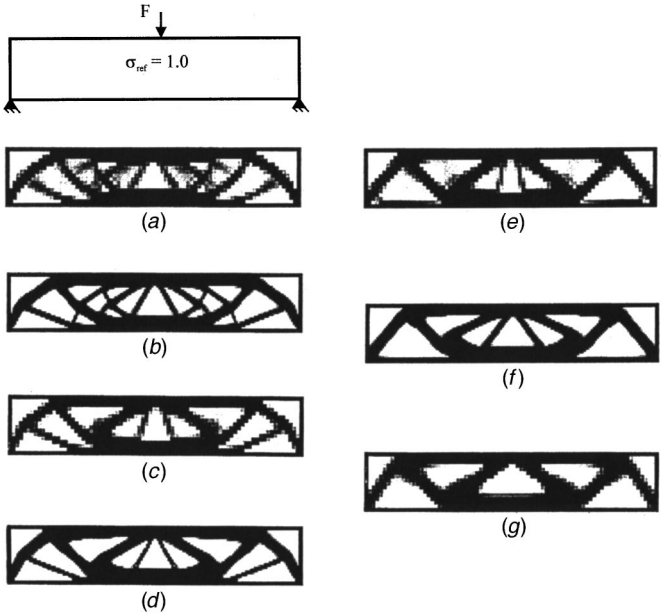

Fig. 20 Solutions for a beam problem [327] with perimeter control (from [239]): *a*) $\bar{P} = 30$ L, coarse mesh; *b*) $\bar{P} = 30$ L, fine mesh; *c*) $\bar{P} = 24$ **L**, coarse mesh; *d*) $\bar{P} = 24$ L, fine mesh; *e*) $\bar{P} = 22$ L, coarse mesh; *f*) $\bar{P} = 22$ L, fine mesh: and *g*) $\bar{P} = 18$ L, coarse mesh

4.2 Local constraint on gradient of material density

Introduction of a local gradient constraint on thickness variation of solid plates was first done by Niordson [321]. The following approach with a local constraint on the gradient of the volume density ρ of material in a 2D topology optimization problem presupposes that ρ is sufficiently smooth *and* defined for intermediate values. This is the case when, eg, the SIMP material model in Section 2.5.4 is applied to the ill-posed topology optimization problem stated by Eqs. (2.22) [or (2.24), (2.23), and (2.26)], and for this type of problem proof of existence, mesh independence and numerical implementation of a scheme introducing local gradient constraint on density variation was given by Petersson and Sigmund [345].

The constraint on the local density variation is written as the following pointwise constraint on the derivatives of the function ρ:

$$\left|\frac{\partial \rho}{\partial x_\alpha}\right| \leqslant \mathrm{c}, \quad \alpha = 1,2. \tag{4.5}$$

The convergence proof implies that checkerboards (see Subsection 6.1.3) and other numerical anomalies will be eliminated, or at least, they can be made arbitrarily weak using this scheme. However, implementation of this scheme results in up to $2N$ extra constraints in the topology optimization problem, and the method must therefore be considered to be too slow for practical design problems [345].

4.3 Filtering techniques

Based on filtering techniques from image processing, Sigmund [97,377] suggested a filter that prevented creation of checkerboards in numerical solutions to topology optimization problems (see Subsection 6.1.3) by modifying the design sensitivities used in each iteration of the algorithm solving the discretized problem. This filter makes the design sensitivity of a given element depend on a weighted average over the element itself and its eight neighbors.

As an extension of the checkerboard filter just mentioned, Sigmund [377,379] developed a method of mesh independent filtering which modifies the design sensitivity of any specific element based on a weighted average of the element sensitivities in a fixed neighborhood. It should be mentioned that this filter is purely heuristic, but it produces results very similar to local gradient constrained results, cf Petersson [79], Petersson and Sigmund [345] (see the preceding section), requires little extra CPU-time, and is very simple to implement compared to the other approaches. Similar ideas

of weighted averages have been used to ensure mesh independence in bone mechanics simulation [316].

The mesh independence scheme works by modifying the element sensitivities as follows

$$\frac{\partial \hat{f}}{\partial \rho_k} = (\rho_k)^{-1} \frac{1}{\sum_{i=1}^{N} \hat{H}_i} \sum_{i=1}^{N} \hat{H}_i \rho_i \frac{\partial f}{\partial \rho_i}. \tag{4.6}$$

Here, the convolution operator (weight factor) $\hat{H}_1$ is written as

$$\hat{H}_i = r_{\min} - \mathrm{dist}(k,i), \quad \{i \in N \,|\, \mathrm{dist}(k,i) \leq r_{\min}\}, \quad k = 1, \ldots, N, \tag{4.7}$$

where the operator $dist(k,i)$ is defined as the distance between the center of element k and the center of element i. The convolution operator $\hat{H}_i$ is zero outside the filter area. The convolution operator for element i is seen to decay linearly with the distance from element k.

This means that instead of applying the real sensitivities (eg, $\partial f/\partial \rho_k$), the filtered sensitivities computed by Eq. (4.6) are used. It is worthwhile noting that the *filtered* sensitivity in Eq. (4.6) converges to the original sensitivity when $r_{\min}$ approaches zero and that all sensitivities will be equal (resulting in an even distribution of material) when $r_{\min}$ approaches infinity.

For minimum compliance topology optimization the existence issue for the mesh independence filter has just been proved by Bourdin [20], and applications in several papers on material and mechanism design [97,377,379–381,387,388] show that the method in practice produces mesh independent designs and eliminates checkerboarding. The existence issue for the mesh independence filter has yet to be proved, but applications in several papers on material design and mechanism design show that the method in practice produces mesh independent designs.

4.4 Discussion of methods

As discussed in Sigmund and Petersson [386], the perimeter, local gradient and mesh independence filter methods produce very similar designs, but there are some notable differences.

The perimeter method [7,139,140,237–239] in Section 4.1 involves a global constraint and will allow the formation of locally very thin members. The local gradient approach [345,386] and the filtering schemes [97,377,379–381,387,388] involve local constraints and will generally remove thin structural members.

Predicting the value $\overline{P}$ of the perimeter constraint for a new design problem must be determined by experiments, since there is no direct relation between local scale in the structure and the perimeter bound. If the perimeter bound is too tight, there may be no solution to the optimization problem. This problem is particularly difficult for three-dimensional problems. In contrast, the gradient and filtering schemes define a local length scale under which structural variation is filtered out. This local length scale corresponds to a lower limit on bar/beam widths and can easily be defined when, eg, manufacturing is taken into consideration.

Another important difference is the implementation aspect. The perimeter control scheme requires an extra constraint added to the optimization problem. Although the addition of one extra constraint to the optimization problem should not be a problem for advanced large-scale mathematical programming algorithms, practice has shown that implementation of the constraint can give some convergence problems, see Duysinx [25]. The local gradient constraint scheme is considered impractical due to the addition of $2N$ extra constraints to the optimization problem [386]. The great advantage of the filtering scheme is that it requires no extra constraints in the optimization problem. Furthermore, it is very easy to implement, and experience shows that its implementation even stabilizes convergence [97,377,379–381,387,388]. The only disadvantage of the filtering method is that it is based on heuristics.

The perimeter and mesh independence filter methods have both been applied to 3D problems with success [7,139,388]. The comparisons above also hold true for 3D problems.

5 MACROSTRUCTURE APPROACHES

In Subsection 2.2.1, we discussed the principle differences between the two conceptual processes of topology optimization, Material or Micro-structure approaches vs. Geometrical or Macro-structure approaches. The considerations in the present section are focused on Macro-structure techniques. These techniques assume that the structure entirely consists of solid, isotropic or anisotropic material, and the topological optimization is always carried out in connection with a kind of shape variation technique.

Thus, within the Macro-structure approach, the structural topology is changed by two different categories of procedures, namely by *degenerating and/or growing a structure or by inserting holes in a structure,* and these procedures will be discussed in this section.

The methodology of degenerating and/or growing a structure, which will be discussed in Section 5.1, recognizes that an optimal design is a subset of the admissible design domain, and that the solution can be achieved by appropriately removing and/or adding material from/to this domain, see Fig. 21*b* (where only material removal is considered). This concept seems to have been envisioned first by Maier [295] and Rossow and Taylor [365]. The concept underlies the theory and algorithm embodied in the SHAPE program [4,132,133] for the shape optimum design of continuum structures, and a rule-based application of the concept may be found in the work of Rodriguez and Seireg [363]. Notice that the concept also underlies the evolutionary methods published by, eg, Mattheck [68,69], Mattheck *et al* [298], Hartzheim *et al* [250], Xie and Steven [412], Querin [85], Querin *et al* [86], Young *et al* [418], and Liu *et al* [285–287].

The approach of inserting new holes in a structure (see Fig. 21*a*) is based on the so-called *Bubble Method* and will be discussed in Section 5.2. Here, the boundaries of the structure are taken as parameters, and the shape optimization

of new holes (bubbles) and of the other variable boundaries of the structure is carried out as a parameter optimization problem (see [95,209,212,404]).

Garreau *et al* [230] have developed a special topological sensitivity analysis whose aim it is to obtain an asymptotic expansion of a criterion with respect to the creation of a small hole, ie a bubble. Such an expansion is obtained, for example, for linear elasticity by using an adaptation of the adjoint method and a domain truncation technique, respectively. Sokolowski and Zochowski [99] give some mathematical justifications to this topological sensitivity in the plane stress case with free boundary conditions on the hole, and generalize it to various cost functions.

5.1 Techniques by degenerating and/or growing a structure

5.1.1 Variable thickness sheets

The *variable thickness sheet model* for optimization of shape and topology was first suggested by Rossow and Taylor [365]. The sheet is assumed to be planar and to be subjected to in-plane loading, and the sheet domain is divided into a large number of small sub-domains, whose thicknesses are used as design variables with a view to minimize the structural compliance for given total volume. Clearly, if the optimization procedure yields thicknesses that are equal to prescribed minimum constraint values very close to zero, this implies changes of the shape of the planar sheet, and if (vanishing) thicknesses are found in the interior of the sheet domain, topology changes are implied.

It is worth noting that if for planar problems we set the power $p=1$ in Eq. (2.31), then (2.31) simply reduces to govern a variable thickness sheet where the density function ρ is precisely the thickness of the sheet. It should be emphasized as well that the variable thickness sheet design problem (with $p=1$ in (2.31)) can be also interpreted as a problem where we seek the optimum design over all isotropic materials with a continuously varying Young's modulus and a given Poisson's ratio.

With $p=1$ in (2.31) for a variable thickness sheet design problem, both the specific stiffness and volume of the structure depend linearly on the design variable ρ. This implies the important property that existence of solutions can be proved for the variable thickness sheet design problem [173], and means that there is no need for relaxation and introduction of materials with microstructure for this simple planar design problem.

Let us finally remark that the idea behind the penalized density approach in (2.31) may become clearer if we think of a variable thickness sheet for which intermediate thicknesses $0<\rho<1$ are penalized by the penalization power $p>1$. This makes sense for planar problems, where the extra dimension in the 3D space makes it possible to make a physical interpretation of a possible resulting intermediate density. But for fully 3D problems this interpretation is not possible, and intermediate densities cannot be directly interpreted physically.

5.1.2 SHAPE method

The optimization procedure applied in the SHAPE method is based on the Lagrange multiplier method, and thus belongs to the class of optimality criteria (OC) methods. The SHAPE method was developed by Atrek [4,130,131] and is very similar to the optimization technique for the *variable thickness sheet problem* developed by Rossow and Taylor [365]. The SHAPE method is also based on the idea that the admissible domain for shape and topology optimization is divided into a large number of smaller sub-domains, and is combined with a technique of cutting away elements (sub-areas of the structure) with thicknesses that end up being equal to the prescribed lower limit value.

For a more detailed description of the theoretical basis of the SHAPE method, the reader is referred to Atrek [4,131], Atrek and Agarwal [132], Atrek and Kodali [133]. The element volumes are used as design variables. Their current values, which are obtained in the optimization calculations, are transformed internally into 0-1 decisions, ie, elements are either maintained within the structure, or they are removed completely. It should be emphasized that some of these problems are ill-posed with dependence of the results on the size of the finite element mesh and that the method is heuristic for all problems other than variable thickness (or Young's modulus) sheets with in-plane loads.

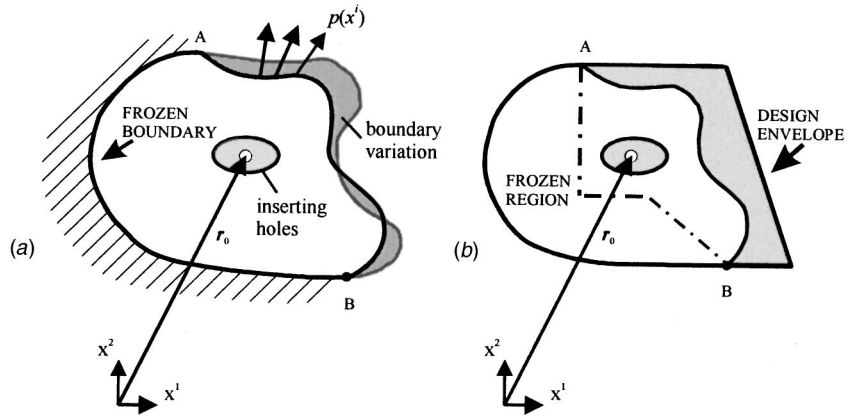

Fig. 21 *a*) Shape and topology optimization by boundary variation and inserting holes; and *b*) Shape and topology optimization by material removal

The volume of the structure is chosen as *objective function* and subjected to minimization. The constraints, ie, user-defined bound values on the structural responses (stresses, displacements), are considered by an *active-set strategy* so that only the currently critical constraints are processed in an optimization step. The number and selection of critical constraints in the active set is adjusted in each optimization step.

The quality of the optimization is estimated by an optimality criterion function termed *virtual volume* defined by

$$V_v = \frac{V}{F_{\min}} \tag{5.1}$$

with

$$F_{\min} = \min\left(\frac{r_j^*}{r_j}\right) \quad j = 1, \ldots, m, \tag{5.2}$$

where V_v = virtual volume; V = total volume in the current state; $F_{\min}$ = most critical factor; r_j^* = boundary value for the structural response r_j; r_j = current jth structural response; m = number of considered structural responses. Thus, the virtual volume denotes the ratio between the current volume and the ''most critical factor,'' the latter being the most unfavorable ratio between the prescribed bound value for a response and the response itself, when we consider all the responses. If the virtual volume is larger than the actual volume, then one or more of the constraints are violated. A lower virtual volume always indicates a better optimization result.

The optimality criterion plays a particularly important role for the determination of the most effective design as it facilitates the optimization toward the global optimum. Since the optimization is highly nonlinear, the optimization algorithm may be unable to find the global optimum without additional measures. For example, once a reliably optimized design has been determined, it has to be checked whether it is a local optimum. SHAPE uses the virtual volume as optimality criterion as well as sensitivity analysis for determining the most effective design. After each optimization step, ie, after removing the corresponding elements, the virtual volume is determined. Based on the results of a sensitivity analysis, some elements are then again added to the optimized structure whereupon the virtual volume is recalculated. If it decreases in spite of the increase of the actual volume, a better design is achieved since a substantially improved structural response is obtained with a smaller increase of the weight. The subsequent optimization steps then use the design with the lowest virtual volume, thus avoiding the optimization process to develop towards a local minimum.

Applications. Two examples shall show the application of SHAPE to planar and solid problems. The first one deals with a 2D model of a bridge under a single load case, and the second with the optimization of an automobile component under multiple static load cases. Further examples can be found in Atrek [4,131], Cristescu and El-Yafi [189], Atrek and Kodali [133], Atrek and Agarval [132], Henkel *et al* [253], Botkin [156], Bennet and Botkin [11,152,153].

Example 1: Bridge [131].

Figure 22 shows the admissible design domain for a simple bridge modeled by triangular plane-stress elements. The only load case consists of a uniformly distributed load ($q = 10.0$) applied under the roadway (Fig. 22*a*), representing the self-weight of the roadway. The dimensions of the design domain are $20 \times 10 \times 0.1$. The roadway and the abutments (supports) are frozen, and the rest of the model is free to change during the optimization. The material constants are Young's modulus $= 1.0 \times 107$ and Poisson's ratio $= 0.3$.

The following results were obtained:

a) The bridge was first topology-optimized for a maximum admissible von Mises-stress of 50.0 units. The resulting topology is shown in Fig. 23*a*. No distinction was made between compressive and tensile stresses, although in a practical design environment, stability considerations require the admissible compressive stress to be related to the slenderness ratio. This can be implemented easily by imposing separate stress limits on the negative and positive values of the principal stresses. The limit on the compressive stress can be modified as the design progresses, based on stability considerations.

b) The same design domain is used again for topology optimization, but this time with a limit on the maximum deflection. This limit is chosen as the maximum value obtained for the optimum design in Fig. 23*a*. The resulting topology is shown in Fig. 23*b*. As expected, the stresses for this design are much higher than those for the design in Fig. 23*a*.

c) Optimization subject to both the stress and deflection constraint resulted in a topology very similar to that in Fig.

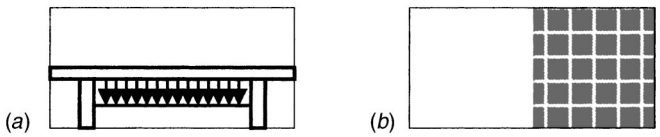

Fig. 22 *a*) Sketch of roadway, loading and supports of a bridge; and *b*) Admissible design domain

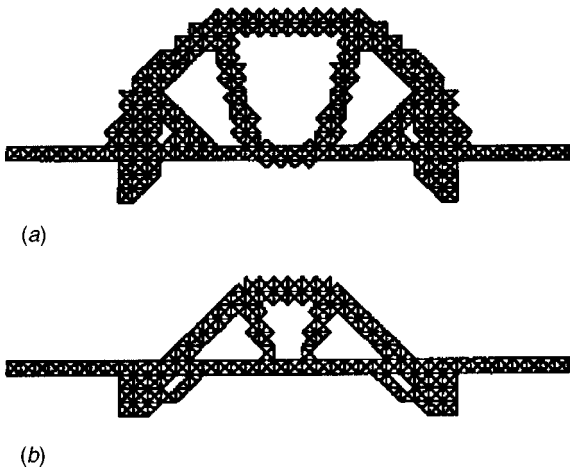

Fig. 23 *a*) Optimum topology of bridge for maximum stress constraint; and *b*) Optimum topology of bridge for maximum deflection constraint

23*a*, where the deflection constraint was only incidentally *active* at the optimum and the topology determined by the stress constraints.

Example 2: Piston rod [253]

Proceeding from an admissible design domain in the form of an enveloping model (Fig. 24*a*), the optimal design is to be determined for the piston rod under consideration. Exploiting the existing symmetry, only one half of the piston rod has been modeled in the FE-modeling. The three-dimensional FE-model consists of 19,400 tetrahedron elements with a total of 5145 nodes. The areas depicted in black are ''frozen,'' ie, they remain unchanged during the optimization.

Optimization is carried out for extreme piston positions in the upper and lower dead center, as well as for an intermediate position. The loading includes both the piston force acting at the smaller ring and the forces of inertia due to the accelerated mass of the driving rod. The direction of the contact forces acting in the rings depends on the position of the piston and is simulated for each load case by equivalent pressure forces on the inner sides of the rings. As the inertia forces of the rod change with the decrease of material, the equivalent pressure forces have to be adapted in the course of the optimization.

Since, proceeding from the admissible design domain, a new design is to be sought in the optimization, additional constraints have to be defined as, eg, arising from fitting the rod. The inner sides of the rings shall remain unchanged during optimization, and hence each first element ring has been ''frozen'' in the bigger and smaller rod ring. Optimization is admitted only on the basis of the existing surfaces to avoid generation of inner cavities. On the other hand, the possibility of generating holes in the driving rod is guaranteed.

As stress constraint, an upper limit of 450 MPa is prescribed for the admissible von Mises reference stress in all elements. The maximum von Mises reference stress in the initial model amounts to 433 MPa. The load decrease can be seen in the optimized structure. In order to strengthen the highly stressed rings, material remains at the periphery of the rings, while material is removed in the middle of the driving rod where the loading is lower. Holes are generated at the connecting points of the rings. The admissible boundary stress is achieved in all areas of the structure.

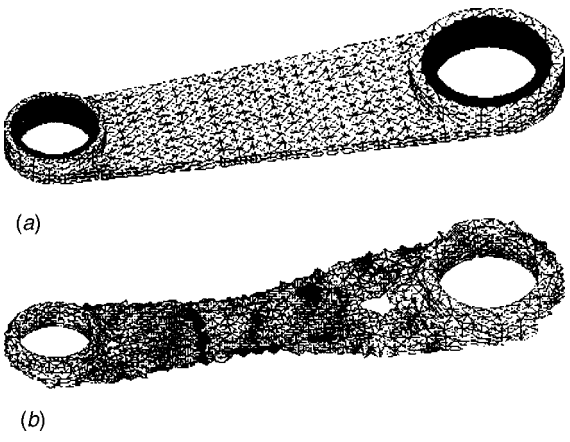

Fig. 24 *a*) Admissible design domain for a piston rod; and *b*) Optimal design for extreme piston position in upper dead center

A very similar piston rod with basic dimensions and loads was originally shape optimized by Bennet and Botkin [152].

5.1.3 Optimization by simulation of biological growth: CAO-/SKO-method

The CAO (**C**omputer **A**ided **O**ptimization) and the SKO (**S**oft **K**ill **O**ption) methods were developed and augmented at the Karlsruhe Research Center, and based on simulation investigations of biological growth and their application to engineering problems. For details, refer to Metzger [71] and Mattheck [68,69]. As is known from design methodology, overstressing is the starting point of damages within the single components and often the entire system. If neither overstressed nor understressed areas are to exist within a component, it has to be demanded that at any point equal maximum stresses must occur. The latter statement is termed the *axiom of constant stress*, or of *fully stressed design*.

The above considerations led to the development of the *CAO-method* [68,69,138], which is a commonplace shape optimization method based on fully stressed design and ideas of the variable thickness sheet model (cf, Subsection 5.1.1); in particular the method applies Young's modulus of the material to play the role of thickness. In order to make this approach a tool for optimum topology design, the method is combined with a basic technique of cutting away understressed sub-domains (elements) of the structure, the so-called SKO technique.

As mentioned in Subsection 5.1.1, for variable thickness sheets, the thickness and the Young's modulus have the same influence on the in-plane stiffness and stresses, so the approach of Mattheck [68,69] and Mattheck *et al* [298] of using Young's modulus to cut away under-stressed areas is completely analogous to the earlier usage of the thickness for shape and topology changes proposed by Rossow and Taylor [365] and applied by Atrek and Kodali [133].

By combining the two optimization procedures SKO and CAO within an integrated design procedure, the principles of lightweight construction (minimum use of material) can be realized by simultaneously achieving durable constructions [376]. In a first step of the computational procedure, SKO determines and eliminates redundant, ie, non-loadbearing areas from the initial structure for CAO, and in a second step, CAO is used to achieve a constant stress distribution on the surface. The resulting design is characterized by maximum strength with the lowest possible consumption of material.

It should be emphasized that the method is heuristic for all problems other than variable thickness (or Young's modulus) sheets with in-plane loads. The SKO and CAO procedures remove inefficient material to optimize the use and efficiency of the remaining material in the structure, and are intuitive and very simple approaches [283]. Applications of the CAO- and SKO-methods in industrial practice can be found in Hartzheim and Graf [248,249] and Hartzheim *et al* [250].

Applications

Example 1: *2D continuum structures (Mattheck et al [298])* Figure 25 presents some applications of the SKO-method in terms of a given rectangular design domain subjected to different support conditions and load cases. The isolines of the distribution of Young's modulus form the contours of the structure optimized for the respective load. By introducing a reference stress it is possible to obtain solutions with varying fineness for the same load case (see Figs. 25*a*,*b*). Equally, one can prescribe a subdomain with a fixed value of Young's modulus in order to determine an optimal support for a loaded plate (see Fig. 25*c*).

Example 2: *Thin-walled, curved structure (Hartzheim et al [250])*
A simple application of topology optimization is the generation of holes in thin-walled, curved sheet metal structures in order to save weight. Figure 26 shows the bracket for a gearshift guide control where it is the task to determine an appropriate number and positioning of interior holes without causing damage to the structure. This problem is approached by usage of the SKO-method and the assumption of a homogeneous stress distribution along the boundaries of the holes.

Figure 26 shows the single steps from the initial to the optimized design, where only the bottom of the U-profile in the sloping area has been defined as the admissible design domain. The practical application of the result led to a weight reduction of 16%.

5.1.4 Optimization by Bi-directional Evolutionary Structural Optimization (BESO) method

The method of Evolutionary Structural Optimization (ESO) is a forerunner of the BESO method cited above and is very similar to the SKO-method. Thus, ESO is a numerical procedure which is integrated into a finite element program and was developed by Xie and Steven [412], see the textbook by Steven and Xie [105]. The computer code is known as EVOLVE [86]. Both ESO and BESO is a combination of an entirely intuitive-heuristic and a gradient-based approach to structural optimization. ESO seeks the optimum design by removing the lowest stressed material from an oversized structure. Each time elements are removed, the structure is re-analyzed to obtain the new load paths. This is repeated until the result is a fully stressed design where all the members support the same maximum stress. The method is very similar to those of Atrek *et al* and Mattheck *et al* (cf, Subsections 5.1.2 and 5.1.3).

The ESO method described above requires that the structural modifications per cycle be kept very small [85,350–352,421,422], and the computational cost easily became a significant problem. Thus, development of a more efficient way of performing an evolutionary structural optimization was undertaken. The new technique developed was the bidirectional ESO (BESO) method, where the initial physical structure contained the minimum number of elements necessary for all the load cases and support cases. This method involves adding material where the structure is over-stressed and simultaneously removing material where the structure is under-stressed in an iterative manner until a fully stressed design in achieved.

The BESO approach was first performed on structures modelled by 2D plate elements, see van Gemert [113]. Querin *et al* [352] dealt with the implementation of the bidirectional evolutionary structural optimization (BESO) method for 3D brick elements and multiple load cases for 2D and 3D. In conducting this research, a program was developed (based on EVOLVE by Querin *et al* [86]) that produced the optimal 3D finite element model of a structure under given loading conditions and the optimal 2D and 3D models under multiple load cases. For 3D examples, the time to optimize a structure was reduced compared to the traditional ESO method. This reduction in time was achieved by beginning the process with a minimum amount of material and allowing the structure to *grow* into the optimized design. Additionally, the BESO method allowed the optimal solution to be approached in a more reliable manner than the ESO method, with the added capability of handling multiple load cases for both 2D and 3D examples in a more reliable manner. A detailed description of the BESO method can be found

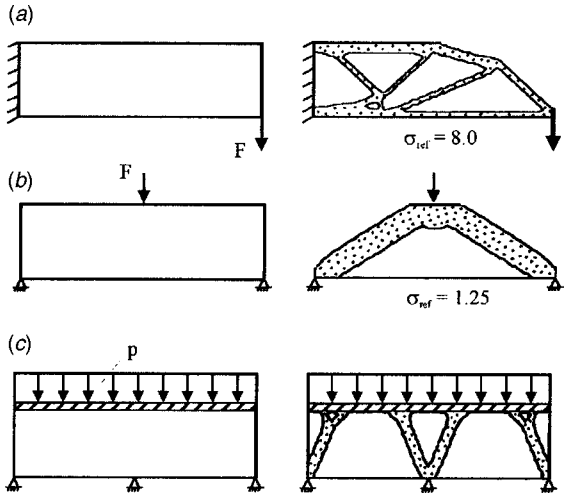

Fig. 25 Examples of application of the SKO-method (rectangular design domain, different load cases, and boundary conditions): *a*) Cantilevered structure with tip load; *b*) Bridge structure with single load acting at the center; and *c*) Supporting structure for a prescribed (hatched) area subject to uniformly distributed load

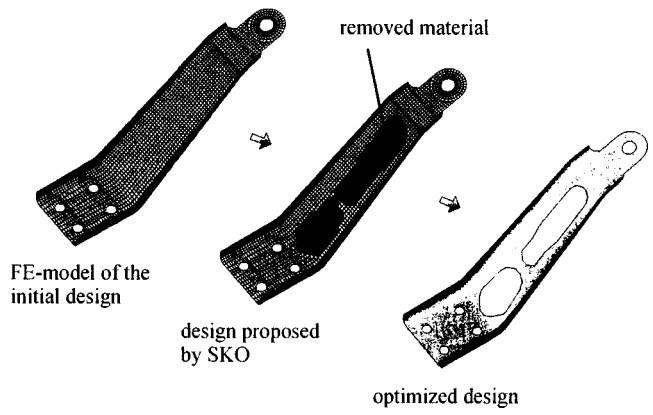

Fig. 26 Bracket for a gearshift guide control

in Young [417], Young *et al* [418], and an overview of the activities in the area of evolutionary structural optimization (ESO) can be obtained from Steven *et al* [103,104] and Querin *et al* [353].

It should be emphasized that the ESO-type methods are heuristic and a very recent evaluation [424] of these methods have shown that they may fail seriously even for simple and not atypical problems.

Applications.

Example: 3D structure [352]

This example concerns a box-shaped admissible design domain which is clamped at one end and subjected to a concentrated load at the other. Figure 27 presents the evolutionary history for this example. The history of the structure shows the growth in thickness at the clamped end and the spreading of the material to form two main arms to support the load. This general exterior shape is similar to the analytical Michell structure (compare [305] and Fig. 15 of this article) as is the internal cross-brace that forms for this type of loading [367]. The applied finite element mesh is relatively coarse and the final result is by no means representative of the exact manufacturable product, but just an indication of the early capabilities of BESO.

5.1.5 Optimization by Metamorphic Development (MD) method

Aforementioned macrostructure techniques for the optimization of continuum structures like the method of material removal [4] or the *Evolutionary Structural Optimization* (ESO) method [412] proceed from a dense mesh of finite elements. These methods have the drawback that the resulting design may only be formed by degenerating a ground mesh whose best size may not be known a priori. Although the capability of adding or reinstalling elements has been implemented in the ESO-method [352], this growth is still restricted to the area/volume defined by the ground mesh.

Another intuitive and heuristic topology optimization method called *Metamorphic Development* (MD), has recently been proposed by Liu *et al* [285,286,288]. The method does not only apply for trusses and continuum structures, but also for combined truss/continuum structures, and can be used to solve different kinds of optimization problems, such as

1) Minimizing the structural mass subject to structural response constraints, and
2) minimizing the structural compliance (or the total elastic energy) subject to constraints on the total structural mass and structural responses.

The MD procedure starts from a very basic description of the structure, ie, just the specification of a minimum number of nodes and elements connecting the applied loads and support points (topology design domain). Thus, a dense FE-ground mesh is not required. The optimum is sought through both growth and degeneration, ie, by adding to and removing from the structure both nodes and elements, with the aim of ensuring satisfactory or improved overall performance. The metamorphic development is controlled by so-called growth factors (positive or negative) related to the current structural performance. In the optimization procedure, growth is guided to occur only in certain parts, called *growth cones*, of the current structure. Such a growth cone is a local section of structural *surface* (either interior or exterior), where high strain energy, high compliance and/or high stresses occur. The strain energy, compliance and/or stresses in growth cones can be reduced by putting more structural material in these areas. Conversely, structural elements which carry only a small load are considered to be used inefficiently and can be removed. The structural growth in the growth cones may be described (see Fig. 28) in terms of various network topologies (see [285,286]).

The growth factors mentioned above, which may be positive or negative, are used as a control measure to dynamically regulate the rates of growth and degeneration, ie, to control the sizes of the growth cones and the structural parts to be removed.

The optimization procedure possesses a hierarchical structure as indicated in Fig. 29. First, the structural compliance, see (2.17), is minimized, while the structural mass is disregarded until the structural response constraints are all satisfied. Then, the structural mass is minimized subject to constraints on the structural response. In the first optimization step, a positive growth factor is used and more elements are added than removed in each iteration. Conversely, in the second step, a negative growth factor is used and more elements are removed than added in each iteration. During the MD-

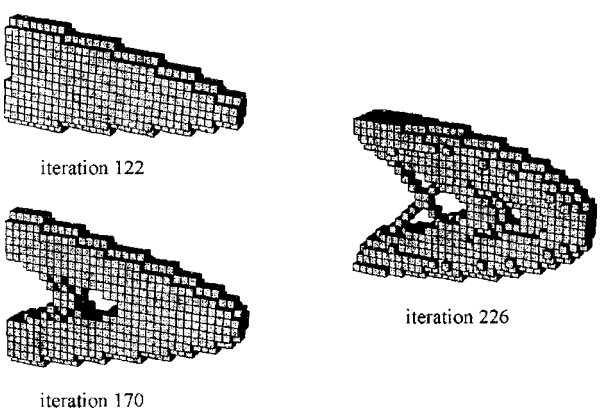

Fig. 27 Evolutionary history

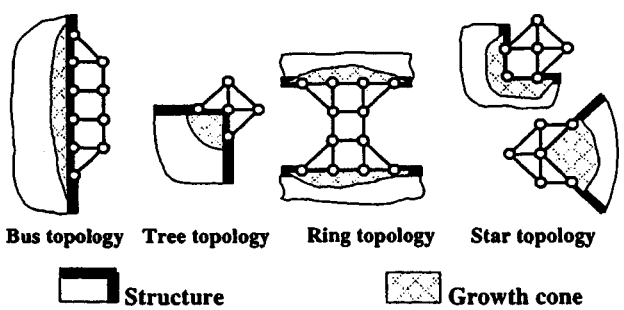

Fig. 28 Structural growth in growth cones by network topologies

procedure, the two optimization schemes may be adopted alternately depending on the current structural performance. The reader is referred to Liu *et al* [285–288] for more details on the optimization procedure.

5.2 Techniques by inserting holes

5.2.1 Basic variational formulations and concepts

As already mentioned in 1.2 and 2.2, the topology optimization method addressed in this chapter uses an iterative introduction, positioning, and hierarchically structured shape optimization of new holes. This means that the boundaries of the structure are taken as design parameters, and that the shape optimization of new holes and of other variable boundaries of the component is carried out as a parameter optimization [209,210,211,235,364]. Another similar method is to obtain an asymptotic expansion of a criterion with respect to the creation of a small hole by means of topological sensitivity analysis [6,230].

Step 1: Global domain variation by direct shape strategy

Shape optimization problems can be solved by means of indirect and direct strategies. In indirect strategies, the necessary conditions for the optimal shape are derived using variational principles, and the resulting differential equations are then solved, in general by means of approximation methods because of their nonlinearity.

The direct solution strategy is easier to apply in many applications. Here, the shape optimization problem is transformed into a parameter optimization problem using approximation functions.

Based on the general description of a shape optimization problem, a boundary variation problem can be formulated as follows [29,174,373]:

$$F^*[\Gamma^*_{var}(\xi^\alpha)] = \underset{\Gamma_{var}}{\text{Min}}\{F[\Gamma_{var}(\xi^\alpha)] | \Gamma_{var}(\xi^\alpha) \in X\} \qquad (5.3)$$

with

$$X = \{\Gamma_{var}(\xi^\alpha) \in \Re^3 | \boldsymbol{H}[\Gamma_{var}(\xi^\alpha)] = \boldsymbol{H}^0, \; \boldsymbol{G}[\Gamma_{var}(\xi^\alpha)] \geqslant \boldsymbol{G}^0\},$$

and the following notations

F	=	objective functional,
$\Gamma_{var}(\xi^\alpha)$	=	variable boundary of the structure,
$\Gamma^*_{var=}(\xi^\alpha)$	=	optimal boundary configuration of the structure,
ξ^α	=	Gaussian surface parameters $\alpha = 1,2$,
$\boldsymbol{H},\boldsymbol{G}$	=	equality and inequality operators,
$\boldsymbol{H}^0$, $\boldsymbol{G}^0$	=	bounds of the equality and inequality operators,
X	=	admissible design space,
$\Re^3$	=	three-dimensional topology domain.

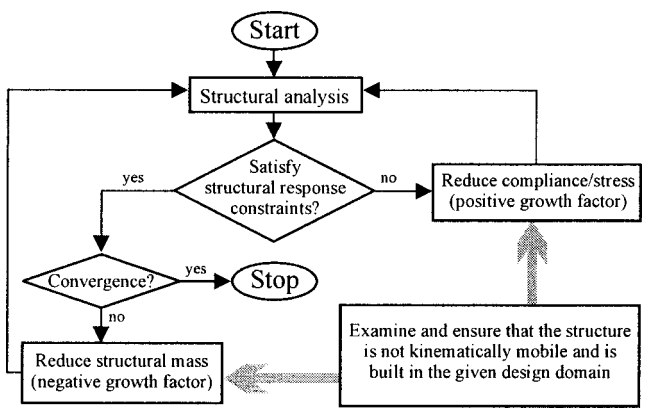

Fig. 29 Flow chart of the MD method

This problem formulation assumes that the boundaries of a three-dimensional space are represented by surfaces, and that the two Gaussian surface parameters ξ^α ($\alpha = 1,2$) uniquely describe each point on the boundary. For the curve representation of a two-dimensional domain, one merely requires one describing parameter ξ.

The boundary of a body $\Gamma_{var}(\xi^\alpha)$ is described by the approximation functions $\boldsymbol{r}(\xi^\alpha,\boldsymbol{x})$. The shape optimization problem (5.1) can thus be written as a parameter optimization problem:

$$F^*[\boldsymbol{r}^*(\xi^\alpha,\boldsymbol{x}^*)] = \underset{\boldsymbol{R}(\xi^\alpha,\boldsymbol{x})}{\text{Min}}\{F[\boldsymbol{r}(\xi^\alpha,\boldsymbol{x})] | \boldsymbol{r}(\xi^\alpha,\boldsymbol{x}) \in X\} \qquad (5.4)$$

with

$$X = \{\boldsymbol{r}(\xi^\alpha,\boldsymbol{x}) \in \Re^3 | \boldsymbol{H}[\boldsymbol{r}(\xi^\alpha,\boldsymbol{x})] = \boldsymbol{H}^0, \; \boldsymbol{G}[\boldsymbol{r}(\xi^{>a},\boldsymbol{x})] \geqslant \boldsymbol{G}^0\},$$

and with the additional notations:

$\boldsymbol{r}(\xi^\alpha,\boldsymbol{x})$	approximation functions for the description of the component boundaries,
$\boldsymbol{r}^*(\xi^\alpha,\boldsymbol{x}^*)$	optimal configuration of the approximation functions,
$\boldsymbol{x}$	vector of the design variables.

The use of general approximation functions $\boldsymbol{r}(\boldsymbol{x})$ like NURBS (**N**on-**U**niform-**R**ational-**B**-**S**plines) [215] allows one to vary the structural boundaries by the vector of the design variables $\boldsymbol{x}$ only. The vector consists of the parameters of the approximation functions as, the coordinates of the control points of splines.

The global variation of the domain complies with the homeomorphical mapping rules. Thus, the interrelations between the elements constituting the domain are maintained, ie, the topology class of the domain is unchanged (shape optimization) (Fig. 30*a*). The solutions of the global domain variation are based on the theory of the *variation with variable domain* [23,54,116,136,155], where a domain functional is considered that can be expressed by an arbitrary function f_Γ:

$$L_\Gamma = \int_\Omega f_\Gamma d\Omega. \qquad (5.5)$$

Using Green's rule, the variation of this domain functional can be written as an integral of the product of a function f_Γ and the variation of the boundary δs (distance be-

tween the initial and new boundary considered in the direction of the normal) along the boundary of the domain Γ:

$$\delta L_\Gamma = \int_\Gamma f_\Gamma \delta s \, d\Gamma = 0. \tag{5.6}$$

This problem formulation corresponds to the first variation of the functional L_Γ. The majority of numerical methods for domain variation is based on this first variation. In order to explicitly determine the function f_Γ, one can employ existing methods based on the formulation of the problem by means of the Lagrange function, the variation of multidimensional problems, and on the fundamental equations of structural mechanics [83].

Step 2: Local domain variation by hole positioning

By means of the local domain variation, the topology class is changed by inserting small holes (topology optimization) (Fig. 30*b*). The aim of a local domain variation is to determine the optimal position of a new insert (hole) within the structure. By that, the topology class is increased. Thus, the confinement to the existing topology class is no longer given.

The insertion of a hole changes the states of stresses and deformations in the elastic body. If an infinitesimally small hole is inserted, it can be treated as a singular disturbance. Two elastic bodies described by the domains Ω^p and Ω^{p+1} (Fig. 21*a*,*b*) possess identical characteristics, ie, the domain Ω^{p+1} has an infinitesimal hole with the coordinate vector $\boldsymbol{r}$ and the radius r_h in the case of a circular hole (see Fig. 30*b*). The difference of an optimization functional F for the two bodies then reads as follows:

$$\Delta F_\nu = F_\nu(\Omega^{p+1}) - F_\nu(\Omega^p), \tag{5.7}$$

where it is assumed that ΔF_ν vanishes if $r_h \to 0$. This assumption is to be checked for each ΔF_ν by means of a convergence test. If ΔF_ν does not vanish for $r_h \to 0$, a minor

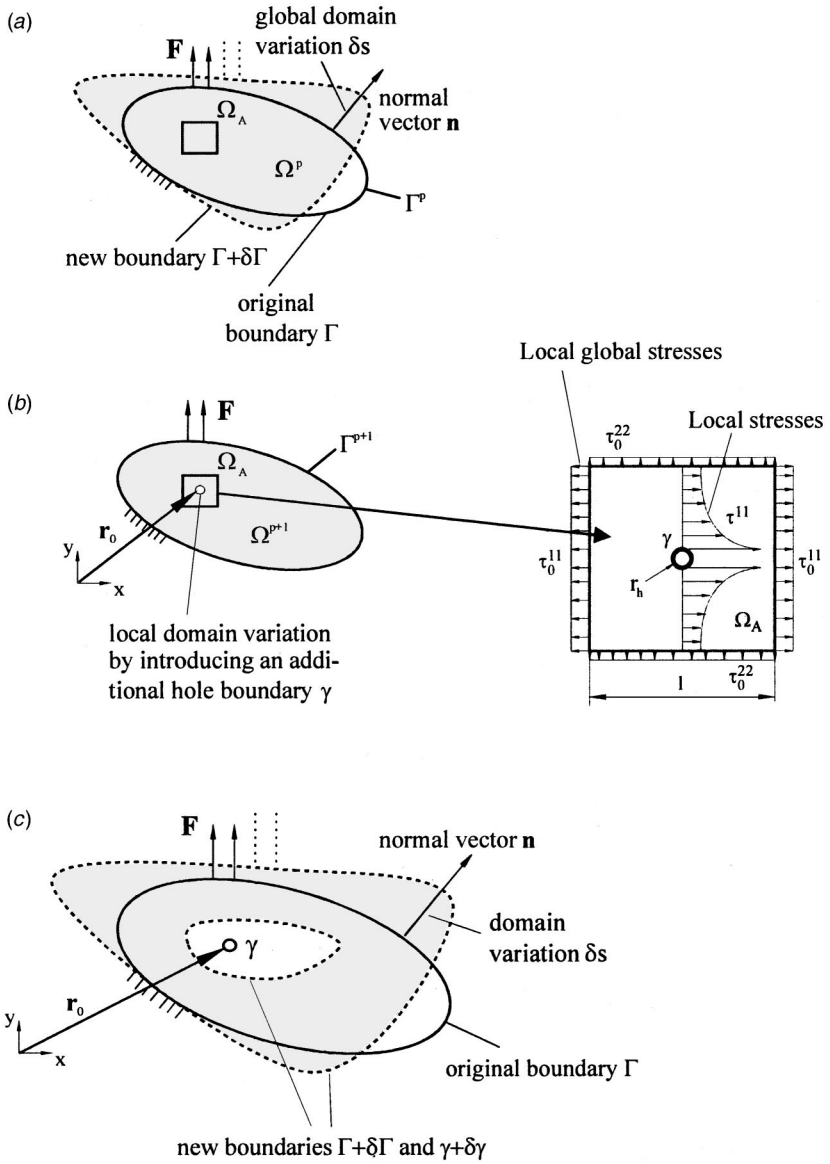

Fig. 30 Variation of the topology and domain by inserting a circular hole (bubble): *a*) Global variation; *b*) Local variation; and *c*) Total (combined) variation

disturbance gains strong influence on the domain functional. In this case (which will not be treated in this article), we are dealing with an ill-posed problem that has to be solved by special methods [3,118,355]. For a well-posed problem (ie, ΔF_ν vanishes for $r_h \to 0$), the radius of the circular hole r_h around $r_h = 0$ can be expanded in a *Taylor* series:

$$\Delta F_\nu = \left(\frac{\partial \Delta F_\nu}{\partial r_h}\right)_{r_h=0} r_h + \left(\frac{\partial^2 \Delta F_\nu}{\partial r_h^2}\right)_{r_h=0} \frac{r_h^2}{2!} + \cdots + \left(\frac{\partial^n \Delta F_\nu}{\partial r_h^n}\right)_{r_h=0} \frac{r_h^n}{n!}. \tag{5.8}$$

The first term, which does not equal zero, describes the sensitivity of the functional with respect to the positioning of the infinitesimal hole. The solution can be simplified by introducing an evaluation domain Ω_A (Fig. 30*b*), where the radius of the hole shall be substantially smaller than the dimensions of the evaluation domain, and these dimensions shall be much smaller than the component dimensions ($r_h \ll l \ll L$). The new hole causes a stress peak in the vicinity of the boundary of the hole, but it decays rapidly according to the *Principle of de Saint Venant*.

Based on the above assumptions we define that

- the global stress field of the component remains practically unchanged by the infinitesimal hole (the global stress field depends on the outer shape of the component and on the external loads),
- a local stress concentration is generated in the vicinity of the hole so that the local stress field in the small evaluation domain Ω_A depends on the shape of the bubble and on the mean value of the global stress in the domain.

Thus, it is sufficient to evaluate Ω_A in order to determine the optimal position. By means of Green's rule, the variation of the domain integral is to be reduced to a boundary integral, and the local variational problem can be written as an integral of a function f_γ over the boundary γ of the inserted, infinitesimal hole or bubble:

$$\delta L_\gamma = \int_\gamma f_\gamma \delta s_h d\gamma = 0, \tag{5.9}$$

where the function f_γ depends on the considered objective and constraint functions of the optimization problem, and on the mechanical conditions.

Step 3: Variation of the total problem

The variation of the total problem can be written as the sum of the global domain variation (5.6) and the local domain variation (5.9) (Fig. 30*c*)

$$\delta L = \int_\Gamma f_\Gamma \delta S d\Gamma + \int_\gamma f_\gamma \delta s_h d\gamma = 0. \tag{5.10}$$

As discussed in Section 2.4.1, the generalized optimization problem is expressed by the Lagrange functional (2.16 *a,b*). For a detailed description of the single steps for evaluating the variation problem, the reader is referred to Eschenauer *et al* [209], Eschenauer and Schumacher [212]), and Schumacher [95]. After a number of variation steps, the necessary conditions can be stated for the total problem. The conditions are the single subproblems, ie the variation of the stress boundaries δL_σ, the variation of the displacement boundaries δL_d, and of the unloaded boundaries δL_0:

$$\delta L = \delta L_\sigma + \delta L_d + \delta L_0 = 0. \tag{5.11}$$

After some reformulations, we finally perform the variation over the unloaded boundaries of the new hole (bubble) as

$$\delta L_0 \hat{=} \delta L_\gamma = \int_{\Gamma_0} \left[1 + \sum_{n=1}^{N} \lambda_n g_n - (\psi_i \sigma^{ij})\Big|_j\right] \delta S d\Gamma = \int_{\Gamma_0} \phi_1(\sigma_1, \sigma_2)\, \delta S d\Gamma = 0. \tag{5.12}$$

The above expression yields an analytical relation for the hole positioning called the *characteristic function*. Various constraints can be introduced in (5.10). In accordance with Sections 2.3 and 2.4 we consider a constraint on the *compliance* which in this case corresponds to the complementary energy of the structure according to (2.7*b*):

$$g_1 \hat{=} \overline{U^*} = \frac{1}{2} C_{ijkl} \sigma^{ij} \sigma^{kl} \hat{=} \frac{1}{2} \sigma^T \boldsymbol{C} \sigma. \tag{5.13}$$

It is obvious that apart from this global energy functional local (pointwise) constraints like stresses or failure criteria can and should be regarded, a fact that naturally leads to a greater numerical expense.

For further calculation, the variation of the hole volume and the variation of the mean compliance are separated:

$$\delta L_\gamma = \delta\Omega - \lambda (\delta L_\gamma)_1 = 0. \tag{5.14}$$

The first term is constant because the inserted hole possesses an arbitrary best constant volume variation $\delta\Omega$. For hole positioning the variation of the complementary energy of mean compliance $(\delta L_\gamma)_1$ is employed:

$$(\delta L_\gamma)_1 = \int_\gamma \overline{U^*} \delta s d\Gamma = \int_\gamma \left(\frac{1}{2} \sigma^T \boldsymbol{C} \sigma\right) \delta s d\Gamma = 0. \tag{5.15}$$

To calculate the complementary energy, we require the local stresses at the boundary of the hole in dependence on the global state of stresses.

In (5.14), $\delta\Omega$ is a virtual, infinitesimally small value. But in (5.11) and (5.12) the variation over the boundary of the hole $\delta L_\gamma = \delta L_0$ as well as the variation over the boundary of the stress functional δL_γ and the boundary of the displacement functional δL_d must equal zero. For arbitrary admissible variation δs, the characteristic function ϕ_1 in (5.12) which depends on the coordinates x^1 and x^2, must become zero. Since in most cases this does not occur, the new hole is inserted at the point in the disk, where the characteristic function Φ_1 takes the minimum value.

The entire body can be analyzed to find the minimum because of the simple structure of the characteristic function. No further optimization step is necessary. In case of using a

finite-element-model, all nodes existing in the topology domain are analyzed, which finally results in the optimal positioning vector $\boldsymbol{r}^*(x,y)$.

Another optimization functional is the consideration of local stress hypotheses which we can formulate with the integral function F_2 (where σ_0 is a feasible stress value):

$$F_2=\left(\frac{1}{\Omega}\int_\Omega f_2 d\Omega\right)^n \quad \text{with} \quad f_2=\left(\frac{\sigma_r}{\sigma_0}\right)^n \tag{5.16}$$

into which we can substitute the criterion according to *von Mises*:

$$\sigma_r=\frac{1}{\sqrt{2}}[(\sigma^{11}-\sigma^{22})^2+(\sigma^{11}-\sigma^{33})^2+(\sigma^{22}-\sigma^{33})^2 + 6(\sigma^{12})^2+6(\sigma^{13})^2+6(\sigma^{23})^2]^{1/2}.$$

By substituting this functional into Eq. (5.12), we obtain the following variation expression

$$(\delta L_\gamma)_2=\int_\gamma\left[(1-n)\left(\frac{\sigma_r}{\sigma_0}\right)^n\right]\delta s\, d\Gamma. \tag{5.17}$$

In order to determine the characteristic function, we have to solve this integral relation over the hole contour γ.

5.2.2 Optimization by means of positioning criteria: Bubble-method

Numerical procedure. As discussed in Section 5.2.1, the optimal behavior of a solid body after shape optimization of the outer boundaries can be increased by positioning a new hole or bubble, that means by changing the topology. Therefore, the coordinates of the optimal position of $\boldsymbol{r}^*$ of such a bubble must be determined. For complex optimization functionals, the positioning is carried out by means of numerical search procedures (MP algorithms).

The bubble method is numerically realized by means of the optimization procedure SAPOP (**S**tructural **A**nalysis **P**rogram and **O**ptimization **P**rocedure), see Eschenauer *et al* [208]. For that purpose, SAPOP had to be augmented by the corresponding positioning model. Figure 31 presents the flowchart of the Bubble-method. For solving large scale problems, SAPOP is adapted to parallel computers (see [231]).

Using FE-analysis during the optimization process, the FE-mesh has to be produced in each iteration by a free mesh generator. If the positioning criterion in the bubble method decides to form an open hole (bubble) at the boundary of the contour, a notch is created. If the hole is positioned within the solid structure, the method generates a closed hole (bubble). The potential of applying the bubble method depends on the works in classical shape optimization. SAPOP offers a large number of different optimization strategies and algorithms which facilitate an effective application of the bubble method (see [95,208,212,268]).

Procedure of inserting holes. In the following, criteria shall be presented for positioning circular holes in a 2D-structure (disks, plates), and a spherical hole in a 3D-structure (for more details see [50,95,212]).

Example 1: *Positioning of a circular hole in a thin disk*
If a circular shaped hole in a 2D-structure (thin disk) is considered, we determine the following boundary stresses written in polar coordinates in dependence on the global principal stresses σ_1,σ_2:

$$\sigma_{\varphi\varphi}=(\sigma_1+\sigma_2)-2(\sigma_1-\sigma_2)\cos 2\varphi, \quad \sigma_{rr}=\tau_{r\varphi}=0. \tag{5.18}$$

With this equation we determine the complementary energy density $\bar{U}^*$ and obtain the integral over the hole contour γ (Eq. 5.15). The characteristic function depends on the stress state σ_1,σ_2 in the component:

$$\Phi_{1D}(\sigma_1,\sigma_2)=\frac{1}{2E}[(\sigma_1+\sigma_2)^2+2(\sigma_1-\sigma_2)^2]. \tag{5.19}$$

This function has to be evaluated for each point of the structure. The bubble is to be positioned at that point of the structure where the characteristic function attains a minimum; thus, the positioning vector $\boldsymbol{r}(x^1,x^2)$ is determined.

Example 2: Positioning of a circular hole in a thin plate
The consideration of mean compliance in the case of plate problems subjected to transverse loads (Kirchhoff's theory) leads to the following characteristic function for a circular hole (same procedure as for a disk):

$$\Phi_{1Pl}(\sigma_{1,top},\sigma_{2,top})=\frac{1}{6E}\left[(\sigma_{1,top}+\sigma_{2,top})^2 + \left(\frac{2(1+\nu)}{3+\nu}\right)^2(\sigma_{1,top}-\sigma_{2,top})^2\right] \tag{5.20}$$

with the principal stresses $\sigma_{1,top}$, $\sigma_{2,top}$ at the top of the plate ($z=+t/2$, t-plate thickness). In this context, the positioning

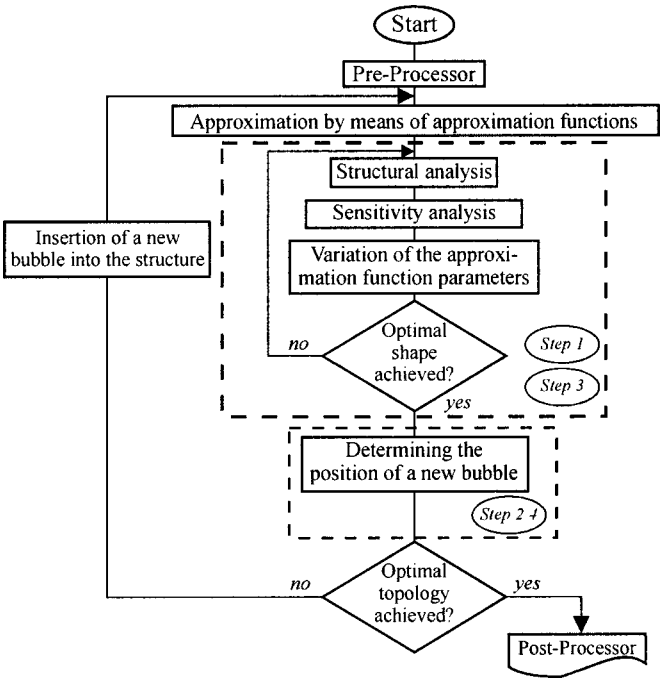

Fig. 31 Flowchart of the bubble method

of holes in the quadratic plates in Fig. 32 presents an impressive example. Depending on the type of support, different hole positions are obtained. In the case of the simply supported plate (Fig. 32*a*), the holes are positioned at the middle of the boundaries. For a plate with clamped edges (Fig. 32*b*), the holes are positioned in the plate corners. In physical interpretation, this means that the simply supported plate requires the edges for the stiffness, while the plate with clamped boundaries uses the shortest distance to transfer the load to the support (see Fig. 32*a*,*b*)

Example 3: Positioning of a spherical hole in a 3D-body
For treating 3D (spatial) bodies, it is necessary to position a 3D hollow sphere. Here, the characteristic function is derived in the same manner as for disks and plates.

The stresses at the boundary of the sphere (boundary of the bubble) are analogous to the plane solutions, and they are to be determined in dependence on the three principal stresses. Based on procedures for an explicit solution of partial differential equations, Neuber [74] gives general solution methods for the calculation of stresses in bodies with spheres. The special case of a sphere in an infinite body subjected to uni-axial tension dates back to Leon [275]. The stresses at the boundary of the sphere read for the first global principal stress σ_1 (Fig. 33):

$$\sigma_{\varphi\varphi_1}=\frac{\sigma_1}{14-10\nu}(30\sin^2\varphi-3-15\nu), \tag{5.21a}$$

$$\sigma_{\vartheta\vartheta_1}=\frac{\sigma_1}{14-10\nu}(30\nu\sin^2\varphi-3-15\nu). \tag{5.21b}$$

The remaining stress components on the surface of the sphere are equal to zero. It can be observed that the stress increase caused by the 3D bubble is lower than in the corresponding plane case. By superposing three global principal stresses perpendicular to each other, one obtains:

$$\sigma_{\varphi\varphi}=\frac{1}{14-10\nu}[\sigma_1(30\sin^2\varphi_1-c)+\sigma_2(30\sin^2\varphi_2-c)+\sigma_3(30\sin^2\varphi_3-c)], \tag{5.22a}$$

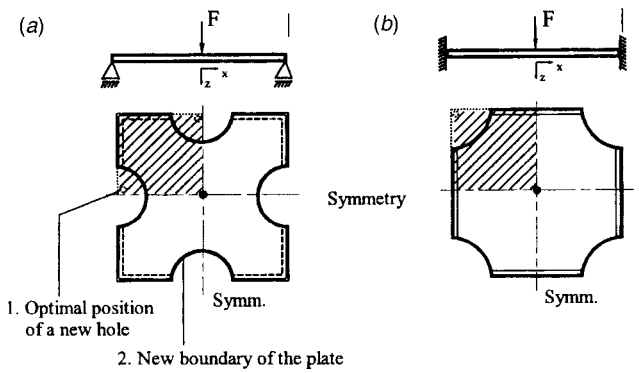

Fig. 32 Hole positioning in plates with different supports

$$\sigma_{\vartheta\vartheta}=\frac{1}{14-10\nu}[\sigma_1(30\nu\sin^2\varphi_1-c)+\sigma_2(30\nu\sin^2\varphi_2-c)+\sigma_3(30\nu\sin^2\varphi_3-c)] \tag{5.22b}$$

with

$$\varphi_1=\arccos\frac{x^1}{r}=\varphi,$$

$$\varphi_2=\arccos\frac{x^2}{r}=\arccos(\sin\varphi\cos\vartheta),$$

$$\varphi_3=\arccos\frac{x^3}{r}=\arccos(\sin\varphi\sin\vartheta),\quad c=3+15\nu.$$

The variational functional (5.15) leads to the following form:

$$(\delta L_\gamma)_{1\mathrm{SV}}=\frac{8r^2}{2E}\int_0^{\pi/2}\int_0^{\pi/2}(\sigma_{\varphi\varphi}^2+\varphi_{\vartheta\vartheta}^2-2\nu\sigma_{\varphi\varphi}\sigma_{\vartheta\vartheta})\times\sin\varphi\,d\vartheta\,d\varphi\,\delta s. \tag{5.23}$$

The index 1SV denotes the application of a sphere *S* in a 3D domain (volume) with respect to the complementary energy $\bar{U}^*$.

After integration, one obtains the functional in dependence on the three principal stresses:

$$\Phi_{1\mathrm{SV}}=\frac{8r^2}{2E(14-10\nu)}[c_a(\sigma_1^2+\sigma_2^2+\sigma_3^2)+c_b(\sigma_1\sigma_2+\sigma_1\sigma_3+\sigma_2\sigma_3)]\delta s \tag{5.24}$$

with

$$c_a=1920\pi(1-\nu^2)-160\pi c(1-\nu^2)+8\pi c^2(1-\nu),$$

$$c_b=1440\pi(1-3\nu^2)+160\pi c(2\nu^2+\nu-1)+8\pi c^2(1-2\nu).$$

The coefficients c_a and c_b have been calculated numerically using 10-th order polynomial approximations.

Hence, the characteristic function for the positioning of a sphere reads:

$$\Phi_{1\mathrm{SV}}(\sigma_1,\sigma_2,\sigma_3)=\frac{1}{2E(14-10\nu)}[c_a(\sigma_1^2+\sigma_2^2+\sigma_3^2)+c_b(\sigma_1\sigma_2+\sigma_1\sigma_3+\sigma_2\sigma_3)]. \tag{5.25}$$

Applications

Example 1: *Cantilever disk [212]*
The task in this example is to find a best-possible initial design for a prescribed topology domain (Fig. 34). A disk is clamped at the left-hand side and is subjected to a load on the right-hand side. The optimization problem consists of a minimization of the complementary energy of the component, ie, minimization of the mean compliance, while considering a volume constraint as equality condition. A triangular disk is chosen as initial design in the half-occupied topology domain. In this case, the problem reads as follows:

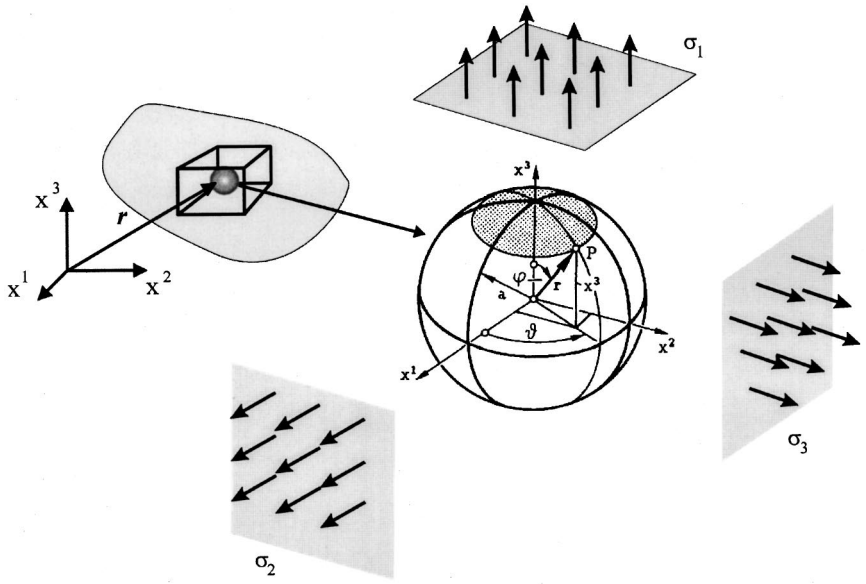

Fig. 33 Sphere in an infinite body

$$\operatorname*{Min}_{x \in \mathfrak{R}^n} \left\{ U^*(\boldsymbol{x}) \,\middle|\, V(\boldsymbol{x}) = \frac{1}{2} V_{\text{domain}}, \quad \boldsymbol{h}(\boldsymbol{x}) = \boldsymbol{0} \right\} \tag{5.26}$$

with $U^*(\boldsymbol{x})$ complementary energy,
$V(\boldsymbol{x})$ volume of the structure,
$\boldsymbol{h}(\boldsymbol{x})$ vector of q equality constraints.

Remarks on the solution procedure. If a shape optimization is carried out on this structure, a shape as presented in *Genus 1* is achieved (Fig. 34). If a bubble is positioned at the point of the minimum of the characteristic function (in the middle of the supported edge) and a new shape optimization is carried out, we obtain *Genus 2*. By positioning the next bubble at the

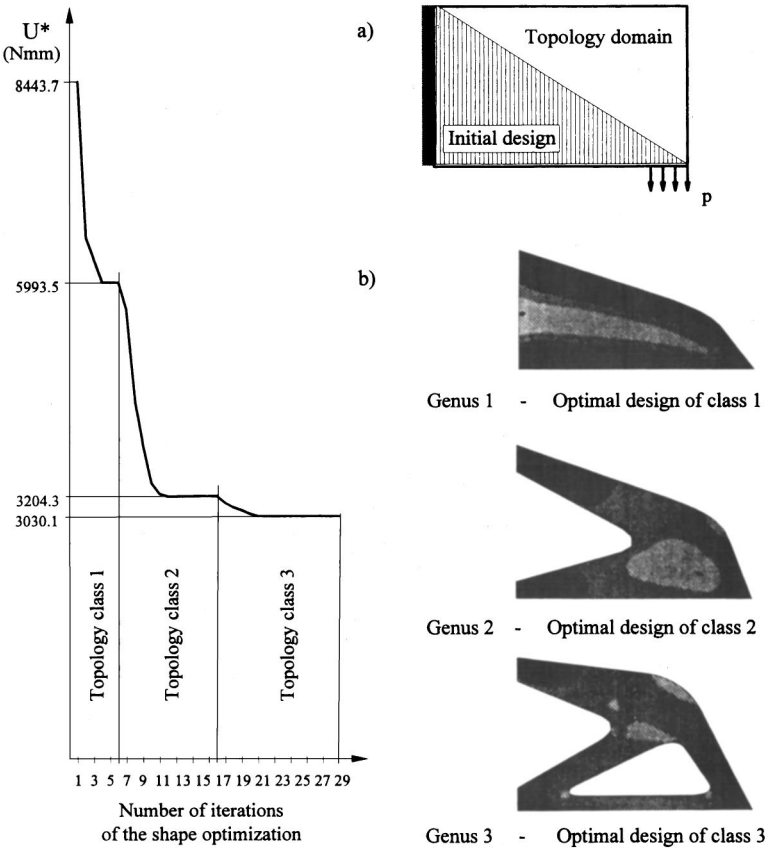

Fig. 34 Optimization of a cantilever disk within three topology classes

point of the minimum of the characteristic function, *Genus 3* is achieved. In the present example, the optimization is terminated at this point.

Example 2: Panel back-up structure of a radio telescope mirror [212]

The following considerations address an example from the field of radio telescope design. Radio-astronomical observations in the millimeter and sub-millimeter range require highly precise telescopes [203,205,207]. The reflector of these types of telescopes consists of a large number of single panels mounted on a supporting back-up structure (Fig. 35).

The panel back-up structures have a substantial influence on the structural deviations, since they deform due to weight and wind, and due to temperature influences. In Eschenauer *et al* [207], it is shown how a best-possible panel truss structure can be determined by means of parameter studies. However, these investigations are normally very time consuming. When one of the topology approaches is applied, the development process can be carried out more efficiently. In the following, the bubble method will be used.

Here, a two-dimensional substitute model (Fig. 35) is dealt with. For this purpose, two topology domains (versions) are chosen to determine the best-possible initial designs for two given topology domains. The first topology domain has a depth of 150 mm (version 1), and the second one has a depth of 250 mm (version 2). In both versions, the topology domain has a width of $b = 1000$ mm. This structure is subjected to a loading that is composed of deadweight and wind load. In a first step, the topology optimization shall be performed with vertical surface loads as illustrated in Fig. 35.

As a measure of accuracy we take the *mean displacement of the surface*. Provided that no temperature influence occurs, the displacement is linearly dependent on the complementary energy. The volume of the panel structure must not be larger than the volume of a structure with a rectangular base of 1000 mm. The results for the topology optimization of version 1 are shown in Fig. 36*a*. The minimum of the characteristic function for positioning a triangular hole can be found in the lower corner of the structure. Thus, one obtains a shape optimization of the outer boundary in the same topology class. The subsequent holes are positioned at the marked points. This leads to notches as the holes are positioned at a nonvariable boundary of the structure. The topology optimization is terminated when the next following hole is positioned at the boundary of the original bubble. Further optimization then requires a refinement of the approximation function of the original bubble. Figure 36*b* illustrates the results of the topology optimization for version 2, which yields substantially improved results for higher topology classes. Here, the suitable choice of the topology domain

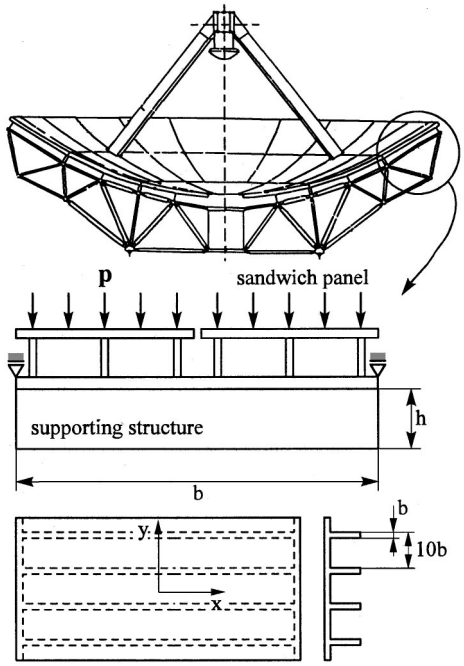

Fig. 35 Panel truss back-up structure of a 30m-Millimeter-Radio Telescope MRT (Version 1: h = 150 mm; Version 2: h = 250 mm)

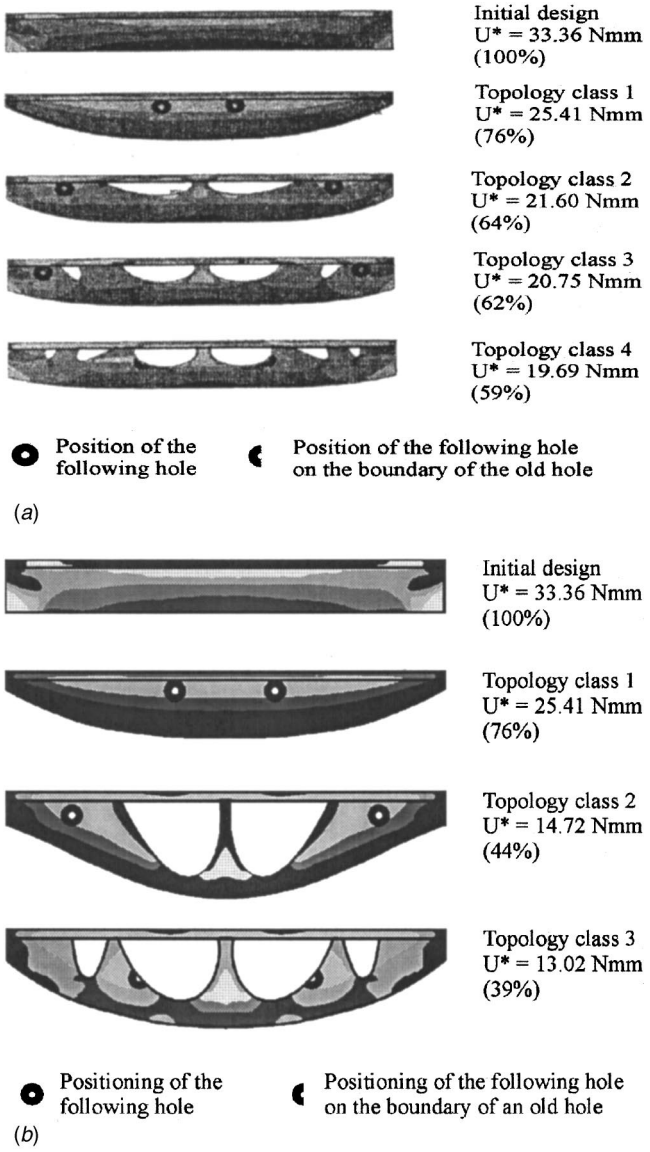

Fig. 36 Topology classes with two different initial domains: *a*) Version 1; *b*) Version 2

gains a decisive influence on the optimal structure of the component. Figure 37 shows the curves of deformations for the intermediate results of version 2. It becomes obvious that a substantial reduction of the deformations in the middle of the panel surface can be achieved in the course of the optimization process.

The results found by means of the bubble method confirm the parameter study in Eschenauer *et al* [207]. Comparing the computing times of the two procedures, the computing time for the parameter study amounted to several weeks, whereas the time required for one optimization run is only about four hours, using a DEC-AXP-3000 workstation.

Example 3: Casing of a handsaw grip [212]

The bubble method was practically applied to the topology optimization of the casing of a handsaw grip, and in particular to its internal stiffeners (Eschenauer and Schumacher [212]). In order to avoid stress peaks, a reduction of special parts of the cross-sections with local stress peaks in a crash shall be avoided. In a first approach, we again use the complementary energy for optimization. By minimizing the complementary energy in the grip, the stresses are smoothened and stress peaks can be reduced. For the computation, the grip is clamped at the motor suspension and is subjected to a horizontal load at the rear end of the grip. The structural model is shown in Fig. 38.

In the optimization, holes at the inner side of the grip are positioned and optimized with regard to shape. In order to ensure an effective optimization calculation, a special geometry definition is employed for the bubbles to be inserted. The coordinates of the corner points of the bubbles are prescribed by means of two curvilinear coordinate systems (move variables on the outer hull of the grip), and the size of the corresponding bubbles is kept variable by scaling factors. Furthermore, they are additional design variables in the optimization process.

The step-wise positioning and shape optimization of new bubbles provide helpful information on the optimal position and arrangement of stiffeners. Further details on the optimization process can be found in Schumacher [95]. The optimization history with the final optimal designs within different topology classes is presented in Fig. 39.

Example 4: *Conceptual layout of a wing rib [27]*

Wing ribs stabilize the profile of the wing of an aeroplane (see Fig. 40*a*), and they connect the spars and the plating of the supporting structure. The ribs are clamped at the spars at 15% and 75% of the wing depth. The plating is mounted on their outer sides. For reasons of assemblage, the wing ribs must have recesses in the inner part of a wing. These notches shall be optimized by means of a shape and a topology optimization.

The following load cases shall be dealt with in the example (see Fig. 40*a*):

1) Air-induced forces along the rib length→Pull-out after gliding flight (Fig. 40*b*)
2) Tank pressure (2 bar) (Fig. 40*c*)

The loads are defined on a parameterized geometry model that is independent of the finite element mesh. The outer cover (wall-thickness 5 mm) and the spars (wall-thickness 5

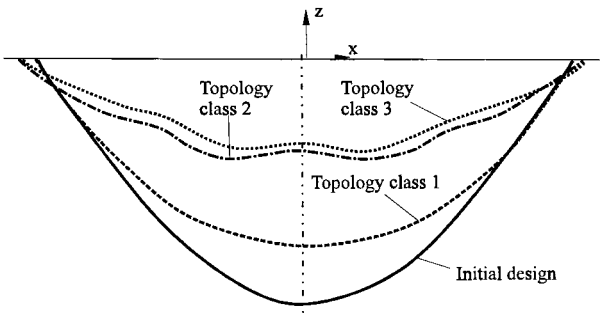

Fig. 37 Deformation of the intermediate results of version 2 (magnifying factor 2000)

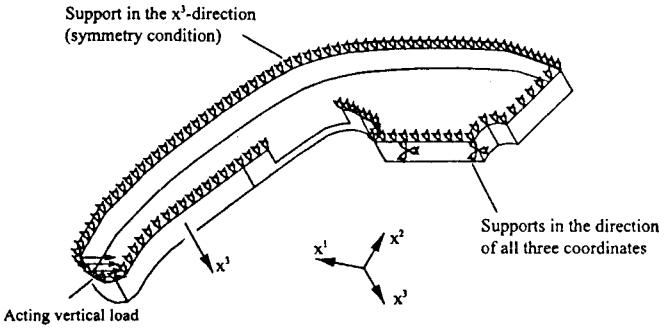

Fig. 38 Structural model of a handsaw grip

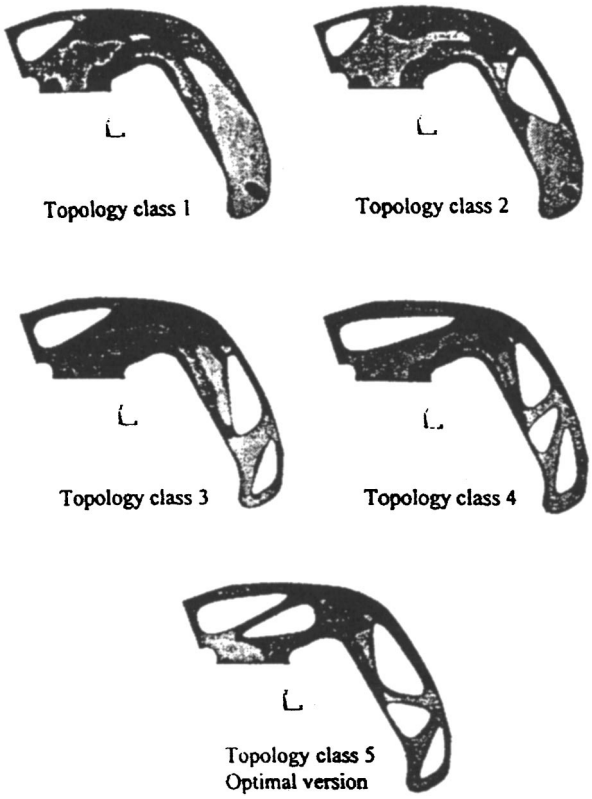

Fig. 39 Optimization history in single topology classes

mm) are simulated by means of beam elements. As an example, calculation is carried out for a stiffener thickness of 5 mm and a stiffener distance of 1000 mm.

The geometric center of gravity of the inserted triangular bubble is placed at a point determined by the positioning criterion. The side of the triangle closest to the boundary shall be parallel to the boundary. The coordinates of the corner points of the bubble are guided along the curvilinear coordinate systems of the stiffener boundaries. The sizes of the respective bubbles are kept variable by means of scaling factors, and they are used as design variables in the optimization process.

For the first optimization, we consider Load case 1 (pull-out after gliding flight). The topology optimization classes are presented in Fig. 41. With unchanged volume, the complementary energy (as a measure of mean compliance) could be reduced from 61818.5 Nmm (class 1) to 60697.6 Nmm (class 3).

LC 2 (tank pressure) is treated in a second optimization process. The first two topology classes are presented in Fig. 42. With unchanged volume, the complementary energy could be reduced from 57725.6 Nmm (class 1) to 17264.6 Nmm (class 2). In the present example, superposition of the pull-out load and of the tank-pressure load leads to the results for the pull-out load, as the sensitivities of the hole positions and their shapes are very low in the load case tank pressure.

This example was part of the investigations undertaken in the scope of the Research and Development project *Dynaflex* of the German Federal Ministry of Research and Technology, Bonn, Germany [27].

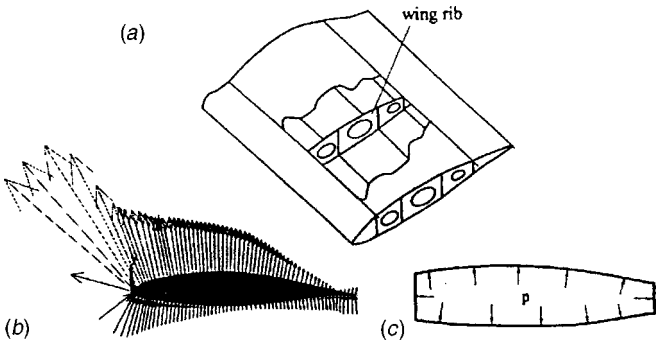

Fig. 40 *a*) Principle sketch of a wing rib of an aeroplane; *b*) Load case 1: Pull-out after gliding flight; and *c*) Load case 2: Tank pressure (2 bar)

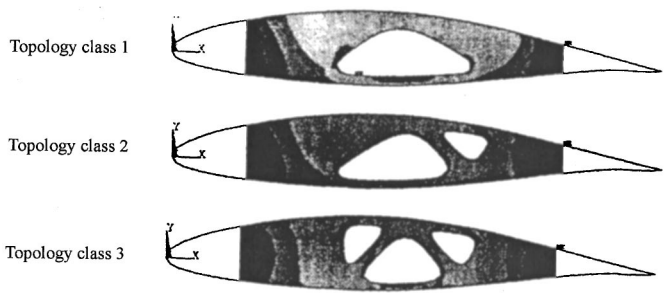

Fig. 41 Step-wise positioning and shape optimization of a wing rib in three topology classes; Load case 1: Pull-out after gliding flight

5.2.3 Optimization using topological sensitivity

Following the above concept a modified approach is under development, see Garreau *et al* [230]. Here, the optimal design problem is to minimize a cost function $f(\Omega) = F(\Omega, u_\Omega)$, where u_Ω is the solution to a partial differential equation defined on the domain Ω (Fig. 30*a*). Let γ be the domain penetrated by a small spherical hole of radius r_h and center $\boldsymbol{r} \in \Omega$. Then an asymptotic expansion of the function f can be obtained in the following form:

$$f(\Omega^{p+1}) - f(\Omega^p) = f(r_h) g(\boldsymbol{r}) + \varphi[f(r_h)], \tag{5.27}$$

where $\lim_{r_h \to 0} f(r_h) = 0$ and $f(r_h) > 0$.

The *topological sensitivity* provides an information for creating a small hole located at $\boldsymbol{r}$. Hence, the function $g(\boldsymbol{r})$ can be used in a similar way as a descent direction in an optimization process. This topological sensitivity was used by Eschenauer and Schumacher [212] and Schumacher [95] in the case of compliance minimization. Next, Sokolowski and Zochowski [99] gave some mathematical justifications to this topological sensitivity in the plane stress state with free boundary conditions on the hole, and generalized it to various cost functions (see also [65,100,277,315]). In the procedure by Garreau, the topological sensitivity is derived in linear elasticity for a large class of cost functions and boundary conditions on the hole, using an adaptation of the adjoint method and a domain truncation. Particularly, this method can handle a Dirichlet boundary condition and the optimization of a criterion like the von Mises stress hypothesis.

Principle of the procedure. The aim of topological sensitivity analysis is to obtain an asymptotic expansion of a criterion with respect to the creation of a small hole, a ball. The latter is introduced into a domain Ω, where $\boldsymbol{r} \in \Omega$ and $r_B > 0$ is sufficiently small for the ball $B(\boldsymbol{r}, r_B)$ to be included in $\Omega (r_B \to 0)$, see Fig. 43. The perforated domain then is

$$\Omega_{r_B} = \Omega / \overline{B(\boldsymbol{r}, r_B)}. \tag{5.28}$$

The physical behavior of the ball depends on the boundary condition. In an analogy with the above-mentioned concept, the homogeneous Neumann condition (free boundary

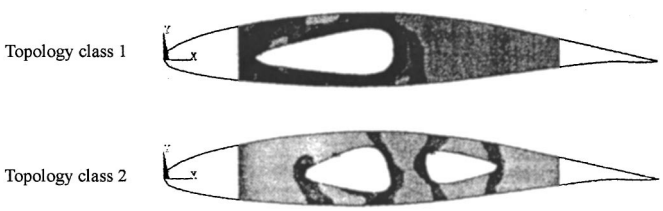

Fig. 42 Step-wise positioning and shape optimization of a wing rib in two topology classes; Load case 2: tank pressure

condition) is imposed on the boundary of the ball. This means that $B(\boldsymbol{r},r_B)$ represents a perforation, ie, a void.

If we denote the boundary of the ball by γ, then the homogeneous Dirichlet condition imposed on γ leads to a boundary condition like the one used for welds or rivets, but this kind of condition is difficult to handle by the classical homogenization method. In order to obtain an asymptotic expansion of a cost function $f(r_B)$ with respect to r_B, some tools and ideas of classical shape optimization like a generalized adjoint method (see Cea [171]) and the domain truncation technique are adapted to the topological case as described in Garreau *et al* [230].

According to (5.27), the topological sensitivity gives information on the opportunity to create a small hole around $\boldsymbol{r}$. By minimizing a cost function, a hole is created where $g(\boldsymbol{r})<0$ may decrease the function *f*. Following the paper by Cea *et al* [172], the previous expression leads to the following optimality condition:

$$g(\boldsymbol{r})\geqslant 0 \quad \forall r\in\Omega. \tag{5.29}$$

This condition is used to derive topological optimization algorithm described in Garreau *et al* [230].

The topological sensitivity $g(\boldsymbol{r})$ is computed on each element. Then, the elements are sorted with respect to this sensitivity. The lowest elements are removed. The number of elements removed at each step is given by the volume ratio (volume of elements removed)/volume of the previous structure). In the following examples, this volume ratio is taken to be between 5 and 10%. At each iteration, most of the computational time is required for solving the elasticity problem. As only a few iterations are needed, this method is not expensive in terms of computational cost.

Applications

Example: Cube under a single load [230]

The example is similar to one treated by Jacobsen *et al* [257]. In this example, the admissible design domain Ω_0 is a cube (see Fig. 44*a*). The four vertices of the bottom face can slide on the horizontal plane, ie, the vertical displacement is zero at those points. A load is applied on the center of the top face. Fifty iterations were performed with 9 percent of material being removed at each step. Figure 44*b* shows several intermediate designs obtained during the optimization process. The mesh was refined after 25 iterations. When the four bottom corners are fixed, (homogeneous Dirichlet condition), the horizontal bars between the four supports disappear, and the optimal design just consists of four rods joined in a pyramidal structure.

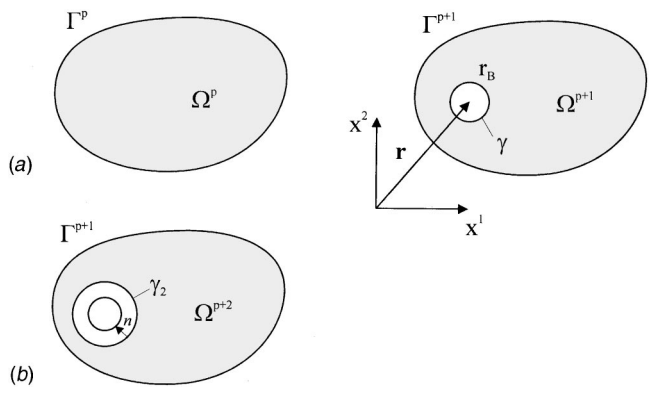

Fig. 43 *a*) Initial domain and domain after perforation; *b*) Truncated domain

6 FURTHER APPROACHES–NEW APPLICATIONS

While it has been the aim of the preceding sections to give an overview of the current state of knowledge in the field of topology optimization of continuum structures, Section 6.1 gives a brief survey of the literature that reflects recent developments, and in Section 6.2, some new avenues of application of topology optimization are presented. It should be mentioned in this context that the augmentations are based both on micro-structure and macro-structure techniques (see Section 5).

6.1 Recent developments

This section presents a brief survey of literature in sub-areas of topology optimization with rapid recent development, and most of the literature has appeared since the comprehensive reviews in Rozvany *et al* [90,369] and Bendsøe [9] of literature published up to 1995. The following literature survey is not claimed to be exhaustive, and for broad coverage the reader is referred to the proceedings of the world congresses on structural and multidisciplinary optimization held in Goslar in 1995, see Olhoff and Rozvany [75]; held in Zakopane in 1997, see Gutkowski and Morz [44]; and in Buffalo in 1999, see Bloebaum [16]. Moreover, in the NATO ARW Proceedings in Budapest in 2000, see Rozvany and Olhoff [91], from the Optimization in Industry-conference, see Belegundu and Mistree [8] and literature cited therein, as well as Bestle and Schiehlen [14] and Kull *et al* [59].

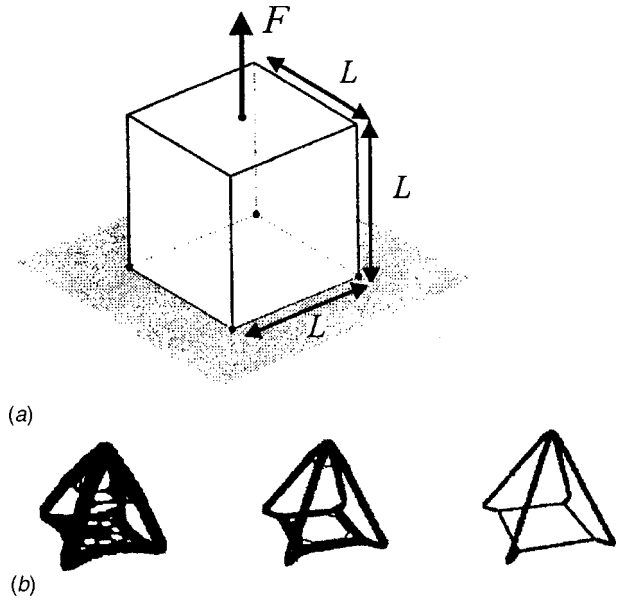

Fig. 44 *a*) Design domain and boundary conditions for the cube; *b*) Optimal layouts obtained after 28, 37, and 50 iterations. Volumes represent 7, 3, and 1%, respectively, of the initial volume.

Traditionally, most studies in topology optimization have been devoted to compliance minimization of linearly elastic 2D structures subject to a single case of in-plane loading, but much effort has been invested in extending the methodology. The reader is referred to Diaz and Bendsøe [194] and Bendsøe [9] for the extension to multiple cases of loading.

6.1.1 New types of structures and materials

Plate and shell structures. Topology and layout design problems have been extended to plate and shell bending problems by Suzuki and Kikuchi [397], Soto and Diaz [392–395], Diaz *et al* [196], Krog [58] and Krog and Olhoff [269–271]. In Olhoff *et al* [331] and Olhoff [326] plate-like structures are optimised using 3D theory of elasticity and optimum 3D microstructures.

3D Structures. In very recent years, topology optimization problems for 3D continuum structures have been solved by Cherkeav and Palais [185], Allaire *et al* [125], Diaz and Lipton [195], Jacobsen *et al* [257], Olhoff *et al* [330], Beckers [7,139], and Beckers and Fleury [140]. Solution of 3D problems using parallel computing is discussed by Borrwall and Petersson [18].

Advanced materials. Topology design of structures with multiple materials was first undertaken by Olhoff *et al* [333], and later by Krog [58], Krog and Olhoff [270,271], and Burns and Cherkaev [164]. All these studies were based on usage of microstructured material models. The problem has also recently been treated by Sigmund and Torquato [387], who use an adaptation of the SIMP model (see Section 2.3.4) to interpolate between multiple material properties, an issue that has very recently been studied very thoroughly by Bendsøe and Sigmund [151]. See also Eschenauer *et al* [213] for the use of brittle materials, and Rodrigues *et al* [361] for optimization of the distribution of a porous coating of a noncemented hip prothesis in biomechanics.

Nonlinearly elastic materials. Comparatively little work has been performed in the area of nonlinear elasticity, presumably due to the difficulty to model the nonlinear behavior of materials at intermediate density. For work in nonlinear elasticity with non-quadratic potentials, see Jog and Haber [258]; in plasticity see Yuge and Kikuchi [419], Maute *et al* [302], and Swan and Arora [398] and in damage and impact, see Bendsøe and Diaz [145] and Min *et al* [310].

Free material design. This problem category relates to a formulation for the optimum design of continuum structures, where the components of the elasticity tensor of the material appear in the role of design variables, see Bendsøe *et al* [147–149], and Alt *et al* [2]. In the first treatment of this problem, general analytical results were demonstrated for the case of minimum compliance design under a particular cost constraint, where unit cost is proportional to the trace or the second-order norm of the elasticity tensor. The following extensions and elaborations of this sort of model have been published: Guedes and Taylor [234] present an algorithm which provides a way to generate black-and-white topology designs through usage of a non-uniform unit relative cost factor; Taylor and Bendsøe [107], establish several generalized formulations with respect to design objective; Rodrigues *et al* [362] develop a technique for topology design applied to a two-material mixture; and Taylor [401,402] reformulates the free material design problem with the cost constraint expressed in a generalized form.

6.1.2 Design objectives and constraints

Eigenvalues. Topology optimization with respect to eigenfrequencies of structural vibration has been studied by Diaz and Kikuchi [198], Soto and Diaz [392], Diaz *et al* [196], Ma *et al* [291–293], Krog [58], Krog and Olhoff [269–271], and Pedersen [338–340]. Topology optimization with respect to dynamic loads is treated by Min *et al* [311]. Based on design sensitivities of buckling loads, see Haug *et al* [46], Wu and Arora [411], Sobieszczanski-Sobieski *et al* [391], buckling eigenvalue topology optimization has recently been undertaken by Folgado *et al* [224], Neves *et al* [318], and Folgado and Rodrigues [223].

Stress constraints. Topology optimization of continuum structures with consideration of stress constraints requires that one can devise a yield criterion for material at intermediate density. It is another complexity of the problem that a computational problem appears in the form of the so-called singularity phenomenon of topology design which is well understood for truss topology problems (see Cheng *et al* [177–179]) and references cited therein. For continuum structures, stress constraints are treated in Yang and Chen [415], Duysinx and Bendsøe [201], and Duysinx and Sigmund [202]. Topology optimization with different stress limits in tension and compression is considered by Duysinx [200].

Damage and impact. Recent work on topology design with respect to damage and impact has been recently reported in Bendsøe and Diaz [145] and Min *et al* [310]. Damage tolerant topology optimization is treated by Akgün [121].

Controlled structures. Constraints related to the simultaneous optimum design of structure and controls for a controlled structure has been recently studied by Yamakawa *et al* [413], Ou and Kikuchi [334,335], Yamakawa and Takagi [414] and Prasad [84].

Structures with design dependent loading. Topology optimization with respect to objectives pertaining to, eg, wind and snow loading, hydrostatic pressure or fluid flow, ie, loading that changes with the structural design, has very recently been considered in Hammer [244], Hammer and Olhoff [246,247], Eschenauer *et al* [27], Eschenauer and Schumacher [210–212], and Eschenauer [205,206].

Multiobjective formulations. Following the fundamentals of Multiobjective Optimization [30,102], topology optimization problems with multiple objectives have been considered in, among others, Diaz and Bendsøe [194], Diaz *et al* [196], Soto [101] for compliance problems, and in Soto and Diaz [196,392–395], Ma *et al* [291–293], for vibration problems, by treating the multiobjective criterion in the form of a weighted scalar function of the objectives, and in Lin and

Hajela [278] by applying genetic search strategies. In Krog [58], Krog and Olhoff [269–271], and Folgado *et al* [224], the multiple objectives of such problems are scalarized by using a weighted min-max formulation which is more relevant and of direct practical significance as it is a worst-case type of a design objective.

6.1.3 Computational issues

Optimization algorithms. Much work in topology design of continuum structures has relied on the applicability of optimality criteria methods for the mostly global design objectives which have been treated. To gain further versatility of the topology design methods there is now a tendency to move towards the use of more standardized mathematical programming methods. See, for example, Duysinx [25] for use of CONLIN, and Sigmund and Torquato [387], Krog and Olhoff [269–271] for use of SLP methods (see also [9]). A hierarchical method for optimization of material and structure is discussed in Rodrigues *et al* [360]. A 99 line topology optimization code written in Matlab is published by Sigmund [383–385]. See also Kutylowski [272] and Suryatama and Bernitsas [396] for new computational developments. Further methods are treated by Hörnlein and Schittkowski [50].

Emerging methods. The treatment of problems with a large number of degrees of freedom and/or design variables is a very time-consuming process. As an alternative to gradient based methods, a number of so-called *emerging methods* have been developed and applied in topology optimization. Among these, the following procedures shall be mentioned: Approach for multilevel design, see Haftka [240]; Evolutionary and genetic algorithms, see Goldberg [42], Hajela [241], Lin and Hajela [278], Hajela *et al* [242], Shonauer *et al* [375], Zhao *et al* [420], Kita and Tanie [265], Hajela and Vittal [243], Blachut and Eschenauer [15]. For local rules by means of cellular automata, see Wolfram [410] and Henschen [47]. An algorithm reported in Bulman and Hinton [162] combines ideas from the more intuitive evolutionary methods and the more rigorous homogenization methods.

Checkerboard control. In topology optimization of continuum structures, one often sees that the numerical results are *polluted* by so-called *checkerboard patterns*. This has been identified as a numerical problem related to the choice of interpolation spaces and physically speaking certain interpolation spaces make checkerboard patterns seem artificially stiff (see [79,197,258]). Various techniques have been proposed to circumvent this problem (see [9,386,425]). These techniques usually imply an increase in computer time, as the basic problem is that displacements are required to be approximated by higher order elements. The perimeter constraint (see Section 4.1 and [25]) and filter techniques (see Section 4.3 and [387]) are reported to be very efficient remedies for suppressing checkerboards. Application of wavelet approximations in topology optimization problems has also been found to suppress checkerboards very efficiently (see [192,193,347]).

Adaptive methods. As mentioned earlier, topology design of continuum structures has traditionally been implemented with reference to a fixed finite element mesh. However, the use of adaptive finite element methods does allow for an increased resolution of the structure. The idea is to start with a rough mesh and only refine where there is borders between material and void to be identified. Such an approach is described in Maute and Ramm [299–301], Kikuchi *et al* [262], Schwarz *et al* [374], Maute *et al* [302], and Ramm *et al* [354]. Other ways of integrating topology and shape design optimization are considered by Chang and Tang [175].

6.2 New Applications

This section presents some particularly interesting and rapidly developing new areas of application of methods of optimum topology design, namely in Subsection 6.2.1 the design of microstructures of materials with prescribed macroscopic material properties, in Subsection 6.2.2 the design of compliant mechanisms, and in Subsection 6.2.3 functional adaptation and topology optimization in biomechanics.

6.2.1 Design of materials for prescribed macroscopic properties

The problem of tailoring materials with specified elastic properties has attracted considerable interests over recent years (see, eg, [9,97,127,147,319,377,378]).

Milton and Cherkaev [309] developed a mathematical method for the design of materials which have an elasticity tensor matching an arbitrarily prescribed positive semidefinite fourth-order elasticity tensor compatible with thermodynamics. A material with Poisson's ratio close to 1 was constructed by Milton [308]. These developments were based on the use of layered material microstructures constructed from a rigid and an infinitely weak material. The materials obtained this way serve to substantiate that prescribed as well as extreme elastic properties can be achieved, but they are merely mathematical tools than practical composites due to their widely differing length scales, cf, Lakes [237].

Sigmund [97,377,378], on the other hand, treats the material design problem as a topology optimization problem of a periodic microstructure represented by a base cell that only involves a single length scale. The topology optimization problem is formulated as minimization of the density of material in the base cell, subject to equality constraints that express the prescription of the elastic properties. Some of the results will be presented in the sequel. In Sigmund [377,378], the microstructure is discretized by continuum-type finite elements where the material densities in the individual elements are taken as design variables. The effective elastic properties of the discretized microstructure are found by homogenization which leads to the definition of the material design problem as an inverse homogenization problem.

The optimization problem can be stated as

$$\begin{aligned} &\textit{Minimize} \quad \rho_{cell} = \int_{\Omega} \rho^{p} \, d\omega \\ &\textit{Subject to} \quad E^{H}_{ijkl} - E^{*}_{ijkl} = 0 \\ &\qquad\qquad 0 < \rho_{min} \leqslant \rho \leqslant \rho_{max}, \end{aligned} \tag{6.1}$$

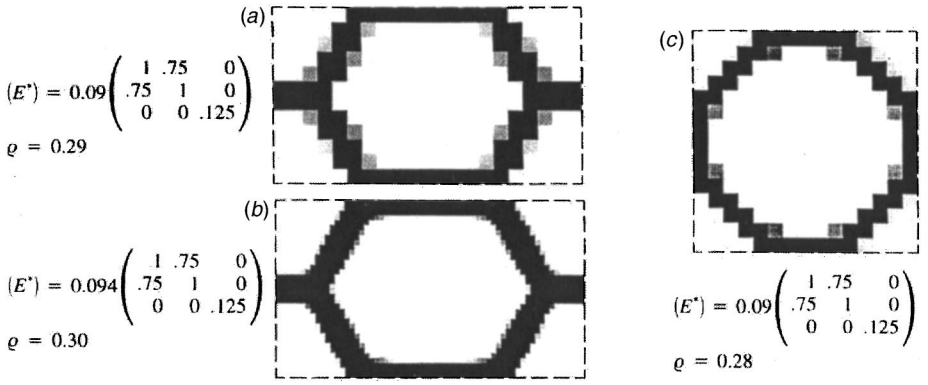

Fig. 45 Honeycomb microstructures with Poisson's ratio equal to 0.75. Three different base cells. with: *a*) 21×12 elements, *b*) 63 ×36 elements, and *c*) 15×15 elements, are used, Sigmund [378]

where ρ_{cell} is the density of material in the base cell, the local material densities ρ are the design variables constrained by ρ_{min} and ρ_{max}, Ω denotes the design domain (base cell), and p is a penalization power used to ensure that each element in the discretized cell will represent either solid or void. E^H_{ijkl} denotes the effective Cartesian elasticity tensor determined by the homogenization procedure briefly as described in Section 3.1, and E^*_{ijkl} is the prescribed elasticity tensor.

The microstructures presented in the following, see Sigmund [378], are all obtained from rectangular base cells discretized by four node bilinear finite elements, and the base material for all examples has *Young's* modulus 0.91 and *Poisson's* ratio 0.3 such that a purely solid base cell will have $E_{1111}=1.0$ (assuming plane stress).

As a *first example*, the optimization algorithm was used to *reinvent* the *perfect* honeycomb. Prescribing the elastic properties of a material with $E_{1111}=0.09$ and Poisson's ratio 0.75 in a rectangular and quadratic domain for the base cell, the results in Fig. 45 were obtained. The optimized microstructures in Figs. 45*a* and *b* are seen to display great similarity with the *perfect* honeycomb. If the rectangular base cell domain in Figs. 45*a* and *b* is changed to a quadratic one discretized by 15×15 elements, the optimization yields the *octagonal honeycomb* shown in Fig. 45*c*. As the density of the material is very nearly the same for the *perfect* and the *octagonal* honeycomb, preference may be made from manufacturability considerations.

As a *second example*, we consider the design of materials with negative Poisson's ratio, ie, materials that expand transversely when subjected to elongation. It is well known that Poisson's ratio is confined to the interval from 0 to 0.5 for solid isotropic materials, but for porous (eg, cellular) materials Poisson's ratio may approach the value −1 without violation of positive semi-definiteness of the elasticity tensor. Negative Poisson's ratio materials have attracted considerable interest in recent years, and use of such materials may, for example, be advantageous for hydrophones and mechanical fasteners (eg, *Rawlplugs*). However, numerical experiments in Sigmund [378] have shown that only low overall stiffness can be obtained if extreme elastic properties are prescribed. The reader is referred to Sigmund [97,377] and Theocaris and Stavroulakis [403] for potential applications and for a survey of recent research. Figure 46 (left) displays topologies of base cells obtained by Sigmund [378] subject to specification of elastic properties of materials with a negative Poisson's ratio. The illustrations on the right hand side of Fig. 46 are obtained by repeating the base cell periodically, and offer a clear picture of the aggregate microstructures; it is easily seen that horizontal elongation of the microstructures will give rise to expansion in the vertical direction, and thereby a negative value of the Poisson's ratio. An experimental project devoted to the manufacturing of the negative Poisson's ratio materials in real micro-scale (size of base cell: 30 μm) and subsequent testing of their elastic properties, has been successfully caried out at the Microelectronics Center in Lyngby, Denmark, see Larsen *et al* [63].

It will be finally illustrated via an example from Sigmund and Torquato [387] that the material topology optimization algorithm can be easily modified to be used for design of materials with prescribed thermoelastic properties. The de-

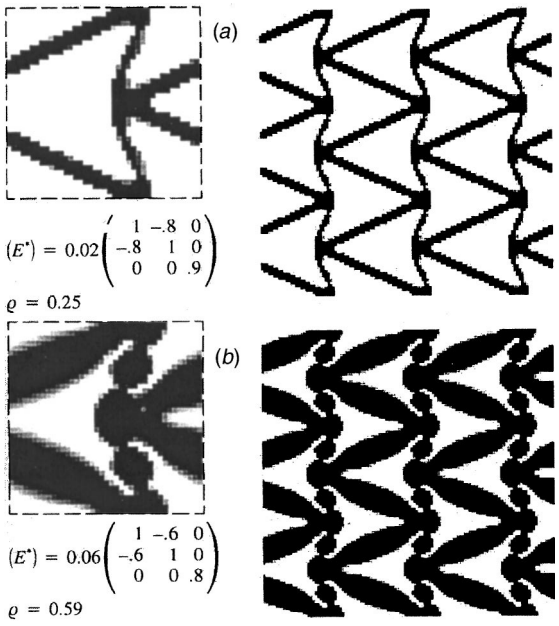

Fig. 46 Negative Poisson's ratio materials [*a*): −0.8; *b*): −0.6] obtained from base cells with 40×40 elements and enforcement of vertical symmetry [378]

sign of a material with a prescribed thermal expansion tensor α_{ij}^{*} cannot be performed alone by designing the microstructure based on one material; it is necessary to consider a mixture of at least two materials with different thermal expansion coefficients α_{ij}^{1} and α_{ij}^{2}.

Consider now a *third example* (see also Sigmund [382]), the problem of designing a material with a negative (isotropic) thermal expansion coefficient $\alpha^{*}<0$ by including two isotropic material phases 1 and 2 with different, but both positive thermal expansion coefficients $\alpha^{1}>\alpha^{2}>0$, in the base cell as shown in Fig. 47. The gray phase in Fig. 47 has the high thermal expansion coefficient α^{1} and the black phase has the low (but still positive) thermal expansion α^{2} coefficient. By performing the topology optimization on the base cell, one obtains the result shown in Fig. 47 (left). The resulting microstructure has a negative thermal expansion coefficient, cf, the deformation indicated in Fig. 47 (middle) of the microstructure when heated. Figure 47 (right) shows the periodic material composed of repeated base cells. Studying the optimal microstructure, one notices that it consists of several small bi-material beams that in an intricate way make the periodic structure contract when heated, even though the materials it is built from expand when heated.

6.2.2 Topology optimization of compliant mechanisms

The design (synthesis) of compliant mechanisms is a very important and rapidly increasing new field for the application of structural topology design methods. This subsection will present a few illustrative examples from the field.

A compliant mechanism gains its mobility from the flexibility of some or all of its members, as opposed to a conventional rigid-body mechanism. Advantages of compliant mechanisms are that they require fewer parts; are easy to fabricate; have less wear, friction, and backlash; have no need for lubrication; and have built-in restoring force. The concept of compliant or flexible mechanisms is not new (see, [163]) and is by no means restricted to small-scale mechanisms, but it has recently received increased attention because of the introduction of materials with superior properties and the rapidly expanding field of MicroElectro-Mechanical Systems (MEMS). The systems are built in submillimeter scale, are integrated with electronic circuits, and are manufactured using etching techniques from the semiconductor industry. Such systems are already widely used for integrated sensor applications, and have potential applications for in-body surgery, health monitoring, micromanipulation, and nano-fabrication (see [263]). Compliant mechanisms are well-suited for MEMS because of the problems with friction and wear that prohibit use of conventional rigid-body mechanisms.

The optimum design of a compliant mechanism depends on, eg, the manipulation task it should perform, the material of which it is to be made, the available design space, the locations of the input and output ports, and the available input force or actuator. Possible manipulation tasks can be crunching or clamping of workpieces, path generation, prescribed input/output force/deflection relationships, desired energy storage, and many others (see [84,166,226,227,322, 323,379,382]).

For some of the types of mechanisms just mentioned, the major design goal is maximization of the output force F_{out} (the force on the workpiece) for a given input force F_{in}. The ratio between the output and input forces $M=F_{out}/F_{in}$ is called the *Mechanical Advantage*. Three constraints are important in the synthesis of compliant mechanisms, see Sigmund [379]:

i) a constraint on the maximum stress in the mechanism (to hinder fatigue or failure),
ii) a constraint on deflection at the input port, and
iii) a constraint on volume to save material and cost. Here, the stress levels (*i*) in compliant mechanisms can be controlled indirectly by constraining the displacement at the input port.

Using the methodology of topology optimization [379,382], the above design problem can be defined as the problem of finding the optimum mechanism topology within a given design domain Ω that satisfies the above-mentioned goals and constraints, ie,

$$\begin{aligned} &\textit{Maximize:} && \text{Mechanical Advantage} && M \\ &\textit{Subject to:} && \text{Volume Constraint} && V\leqslant V^{*} \\ & && \text{Input displacement} && \Delta_{in}\leqslant\Delta_{in}^{*}. \end{aligned} \tag{6.2}$$

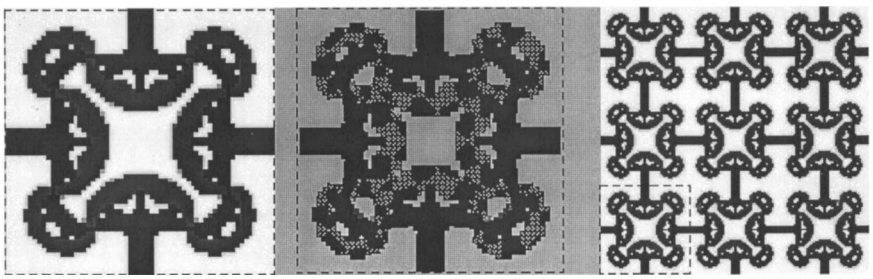

Fig. 47 Design of a material with negative thermal expansion coefficient. Left: base cell (design domain) with topology optimized bi-material microstructure that contracts when heated. The gray and the black material phases have a high and a low positive thermal coefficient, respectively, and the white sub-domains are void. Middle: thermal displacement of microstructure when heated. Right: Aggregate negative thermal expansion material [382]

Since a typical structure for micromanipulation purposes is a gripping device, let us consider the design example from Sigmund [379] shown in Fig. 48 (left). A horizontal input force at the mid-left side of the design domain should be converted to a closing of the jaws at the right-hand side of the design domain. The microgripper is constructed in Silicon, with $E=180$ GPa and yield strength $\sigma_Y=7$ GPa. For manufacturing reasons, the thickness is only $t=7\ \mu$m. To allow for underetching of the structure, it must be thin; ie have no wide elements. This can be controlled by allowing a low volume fraction of 20%. The input force is $F_{in}=1000\ \mu$N, and the workpiece (which should be a blood cell) has stiffness $K_s=1$ N/mm.

For an input displacement of $\Delta_{in}^*=2\ \mu$m, the optimum mechanism topology is shown in Fig. 49 (top left). The resulting output displacement is $\Delta_{out}^*=1.3\ \mu$m, and the mechanical advantage is $M=1.3$.

The output jaws of the gripping mechanism in Fig. 49 (top left) open and close in a crocodile-way, as seen in Fig. 49 (bottom left), ie, the jaws do not move in parallel. If interest is in a gripping mechanism with parallel moving jaws, two output ports must be considered. This is done by defining load conditions at the second output port (at the internal part of the jaws) and defining an extra mechanical advantage as the force relation between the extra output port and the input force. The objective function for the optimization problem in Eq. 6.2 then becomes

$$\phi=M_1+M_2-r(M_2-M_1)^2, \tag{6.3}$$

where r is a penalty parameter. Formulating the objective function in this way, the two mechanical advantages are constrained to be equal (by least square error), and they are at the same time maximized. Furthermore, an extra displacement constraint $\Delta_{in(2)}\leqslant\Delta_{in}^*$ is added to the optimization problem.

Repeating the optimization problem for two output ports and workpiece stiffness $K_S=0.5$ N/μm, the mechanism topology in Fig. 49 (top right) is obtained. From the displaced mechanism in Fig. 49 (bottom right), it can be see that the output jaws now move in parallel. The two resulting mechanical advantages are $M_1=M_2=0.9$ and $\Delta_{\text{out}}=1.8\ \mu$m.

This example shows that a mechanism with complex output behavior can be designed by the topology optimization technique.

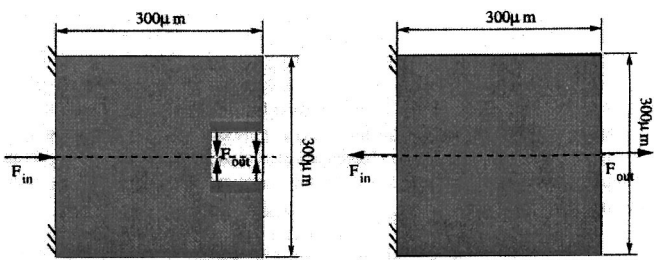

Fig. 48 Design domains for a micro gripper (left) and a micro displacement inverter and amplifier (right) [379]

The following examples from Sigmund [379] demonstrate the design of a simple force inverter and a displacement amplifier and discuss the energy conversion for such mechanisms.

The dimensions are the same as for the microgripper, and the design domain is sketched in Fig. 48 (right). We first consider the design of a displacement (and force inverter). The input force is $F_{in}=1000\ \mu$N, the workpiece stiffness is $K_S=0.2$ N/mm, and the allowed input displacement is $\Delta_{in}^*=5.0\ \mu$m. The resulting mechanism is shown in Fig. 50 (left). The resulting output displacement is $\Delta_{out}=4.8\ \mu$m, and the mechanical advantage is $M=0.97$. For this mechanism, the work done by the input force is calculated as $W_{in}=5$ nJ, and the work done by the output force is calculated as $W_{out}=4.7$ nJ, which means that 7% of the input work was stored as elastic energy in the mechanism. Note that if this had been a rigid-body mechanism, there would have been no *loss* of work between the input and the output ports.

Constraining the input displacement to be $\Delta_{in}^*=2.0\ \mu$m, and letting the stiffness of the workpiece be $K_S=0.03$ N/mm, the resulting output displacement is $\Delta_{out}=7.8\ \mu$m, and the mechanical advantage is $M=0.23$. The mechanism can be said to be a $1:-3.9$ displacement amplifier. The optimum topology for the mechanism is shown in Fig. 50 (right). For this mechanism, the input and output works can be found to be $W_{in}=2.0$ nJ and $W_{out}=1.8$ nJ, respectively, which means that 10% of the work was stored as elastic energy in the mechanism. If a high value of displacement amplification is needed, one could mount several of the $1:-3.9$ displacement amplifiers in series. However, this will result in poor work transmission, since 10% of the input work is lost for each amplifier.

The assumption of linear displacements is close to being violated for the last two design examples. If the displacement amplifier in Fig. 50 (right side) is studied, it is clear that the

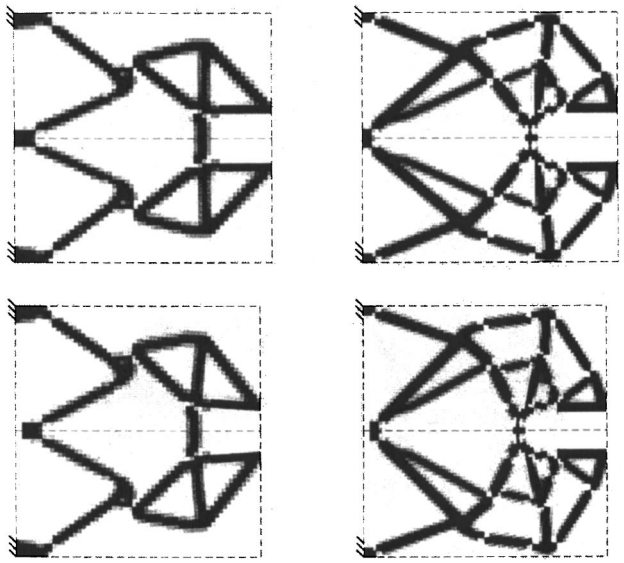

Fig. 49 Micro gripping mechanisms. Top left: optimum microgripper topology for one output port and its displacement pattern (bottom left). Top right: optimum microgripper topology for two output ports and its displacement pattern (bottom left). [379]

output displacement is limited by the point at which the two bars that lead to the output port become vertical. A linear displacement finite element model would not predict this locking. It is therefore clear that non-linear displacement theory must be considered, in order to generalize the design method to the design of large displacement mechanism, and this has been very recently done by Pedersen *et al* [336,337], Bruns and Tortorelli [159,160], Buhl *et al* [161], and Kemmler *et al* [261].

The reader is referred to Sigmund *et al* [388] and Sigmund [380–384] for topology optimization of single-and multimaterials structures with multiple objectives.

6.2.3 Functional adaptation and topology optimization in biomechanics

Biomechanics is a field of considerable current interest and research activity, cf, Reiter and Rammerstorfer [359], Pedersen and Bendsøe [78]. The concept of functional adaptation covers the fact that biological systems are generally able to adapt the shapes and topologies of their structures by sensing specific function-related stimuli and react according to the nature and magnitude of these stimuli in such a way that an optimized functionality of the system is obtained.

In particular, bone material is considered to adapt itself according to some functional stimulus which is directly related to the local mechanical loading pattern, ie, the local stresses and strains in the bone tissue. This adaptive reaction is considered to be governed by an optimization process making the bone a least weight structure with respect to its actual mechanical loading [87,119,274,358,359]. Topology design in the field of bone mechanics has recently been addressed by, eg, Reiter [87,357,358], Folgado and Rodrigues [222], Fernandes *et al* [217], and Bagge [5] and the use of special material models for topology design combined with bone remodeling schemes is, eg, discussed in Mullender *et al* [316], Tanaka *et al* [399], Pettermann *et al* [346], Bagge [5], and Pedersen and Bendsøe [78].

Appropriate algorithms for a systems description can only be obtained by drawing on phenomenological models with *black-box characteristics*. By using a potentially simple mathematical form, these models try to establish a relation between the cellular remodeling reactions with the mechanical characteristic quantities that determine the state of loading within the tissue; in the case of linear elastic material these quantities are the stress tensor σ^{ij}, the strain tensor ε_{ij}, or derived quantities, respectively. By adapting the mathematical coupling algorithms that are oriented at comparisons between empirically determined data and the growth reaction predicted by the model, one obtains a model which is capable of predicting stress-induced tissue reactions without having an accurate knowledge of the actual mechanisms. A number of models of this type have been developed over the previous years [167–170,187,188,255,296,297].

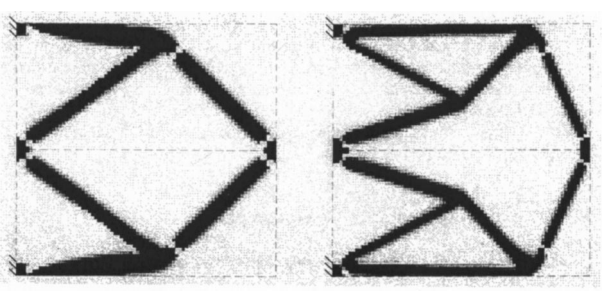

Fig. 50 Micro displacement inverters [379]

Carter *et al* [168] used a simple mathematical model to describe the stress-induced transformation processes that take place within bones. In order to measure the mechanical loading of the bone material, the model employs the local, effective density of the strain energy $\overline{U}_{eff}$ which is obtained by a suitably weighted time average over the local densities of strain energy determined from different load cases. $\overline{U}_{eff}$ is defined as

$$\overline{U}_{eff} = \left(\sum_i \frac{n_i}{\Sigma_j n_j} U_i^k \right)^{1/k}, \tag{6.4}$$

where n_i denotes the number of load cycles for the load case i, and k is the control parameter for the relative weighting of the influence of the number of cycles and of the load intensity. By applying different load conditions, it is intended to account for the mechanical loading to which a real bone is subjected over its daily load history.

The model of growth, which is presented in detail in Reiter and Rammerstorfer [359] and Reiter [357,358], is combined with a finite element analysis program for calculating the stress and strain distributions that are required to determine the density of the strain energy. By means of the thus augmented model, one can now perform an incremental simulation of the load-induced transformation processes that take place within the bone, where the actually continuous processes are discretized into suitably small time increments. Depending on the calculated distribution of $\overline{U}_{eff}$, the material densities and the resulting stiffnesses are varied in all finite elements of each increment, and the surface nodes are moved.

Although the presented algorithm dedicated to an adaptation of a structure to the given environmental conditions appears to be readily acceptable for the purpose, from an intuitive point of view, the results thus obtained still have to be subjected to a critical evaluation with respect to their optimality. Without attempting to give an exact definition of *optimality*, it shall only be stated that the term is used in the same way as it is employed in the fields of structural optimization and/or mathematical programing. Hence, if we talk about the optimization of biological or technical structures, we do not necessarily refer to the *absolute optimum* as such but rather to a minimization (or maximization) of an objective function by simultaneously fulfilling given constraints. In other words, the optimization aims at determining the *best-possible* solution for the given circumstances. However, the existence of such a best-possible solution appears plausible only if there exists an abstractly formalized problem; the practical determination of this solution may well be nontrivial, in particular for nonlinear and nonconvex mathematical optimizations. Generally, limitations are made to objec-

tive functions which can be formulated in a mathematically simple manner like the minimization of weight.

On the whole, there is a strong analogy between technical and natural construction and design optimizations. Technical structural optimization is entirely focused on the quality of the final configuration. Nature, on the other hand, has only a limited range of optimization strategies available, compared with mathematical programing.

If the mechanism of adaptation discussed above is assumed to be a sensible structural optimization strategy, its application in the scope of the optimization of technical designs seems a logical consequence. The methods of functional adaptation are particularly suitable in the field of topology optimization. Starting from an appropriately defined design domain with constant density that is discretized by means of finite elements, the density distribution due to the influence of different support and load conditions is iteratively varied by means of the growth algorithm. The following three examples present homogenized final designs obtained by application of this method. The structural topologies obtained in examples 2 and 3 can be subjected to further treatment in the form of shape optimization.

Applications

Example 1: Density distribution of a femoral head [87,358,361]

The applicability of the growth model mentioned above is shown at the example of a femor head. By means of a finite element model of a femor (2D, plane state of stress) as presented in Fig. 51*a* the density distribution of bone material as existing in a thighbone is simulated, proceeding from a constant σ_a-value. Figure 51 shows that the calculated distribution (Fig. 51*b*) is very similar to the real distribution derived from X-ray photographs (Fig. 51*c*).

Example 2: Cantilever disk under different loading [87,359]

The example in Fig. 52 presents the topologies obtained for two different loading conditions within a rectangular design domain which is clamped at the left-hand side. In the case of a vertical single load (Fig. 52*a*) one obtains the well-known optimum solution consisting of two bars, each under an angle of 45°. Figure 52*b* shows the optimal design obtained for a single load acting under an angle of 45°.

Example 3: Cube with two intersecting loads [358]

This example shows, see Fig. 53*a*, a cubic design domain which is fixed at its lower corner points and loaded by two intersecting uniformly distributed line loads on its top surface. Figure 53*b* presents the topology obtained by functional adaptation.

7 CONCLUSIONS

Basic concepts and knowledge concerning optimum topology design of continuum structures were discussed in this paper, and it has been attempted to give an overview of the current status of the field. Different solution procedures have

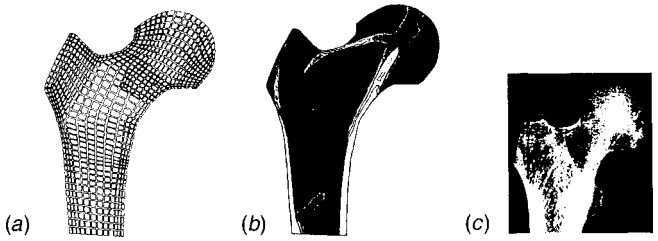

Fig. 51 Numerical simulation of the density distribution in a femoral head [87,358]: *a*) Finite element mesh, *b*) Calculated density distribution, and *c*) X-ray photograph

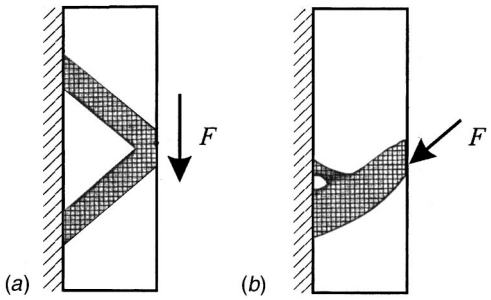

Fig. 52 Cantilever disk subjected to *a*) a vertical single load, and *b*) a single load acting under an angle of 45°

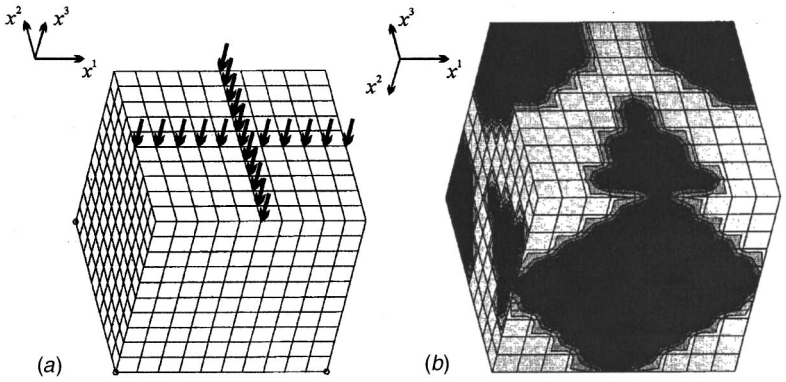

Fig. 53 *a*) Design domain of a cube and two intersecting loads (top view) and *b*) topology of the cube

been developed for these topology optimization problems, and in the present paper we have distinguished between two main classes of procedures, on one hand the Micro- or Material-approaches and on the other hand the Macro-or Geometrical-approaches.

Problem formulations based on solid, isotropic material models are generally not well-posed since the design space is not closed in an appropriate sense, and a regularization of the formulation is then required. The regularization can be achieved by either extending (relaxing) the design space such as to include solutions with microstructure in the problem formulation, or one can restrict the space of the admissible designs.

If it is desired to obtain or acquire knowledge of the global optimum solution associated with the highest possible value of the performance index (for example, in order to know the upper-bound benchmark for other designs), it is necessary to use the Material-or Micro-approach and extend the design space by including optimum microstructures in the problem formulation, after having determined their macroscopic material properties by a homogenization technique. The layered 2D and 3D microstructures considered in this article are optimum for integral stiffness (minimum compliance) design under a single case of loading, but optimum microstructures are as of yet unknown for most other design objectives.

Global optimum designs of the type just mentioned, generally consist of composite material in large sub-domains. This simply reflects the fact that composite materials are in general much more efficient than isotropic, solid materials. However, the large sub-domains with composite often make it difficult to visualize the overall structural topology, and are less attractive from the point of view of manufacture. In order to reduce the composite regions, one may apply a non-optimum microstructure like the *hole-in-cell* microstructure considered in the article, or introduce schemes for penalization of composite in the formulation or solution procedure for the problem.

A direct way to obtain distinct solid-void topologies within the realm of a well-posed problem, is to restrict the design space by including in the problem formulation an upper bound constraint on the perimeter or surface area of the structure, or, what is simpler and used more and more often, to apply an appropriate filtering technique, which will also have the effect of restricting rapid variations in the structural design. Approaches of this kind are advantageous because they admit application of simple material models like the SIMP model (which by itself penalizes intermediate material densities). This model is very popular in commercial topology optimization codes, and by now, it is also very often used in research directed toward extending the scope of topology design, since the simplicity of the model facilitates research into other aspects of the problems.

It is obvious that the creation of quite distinct solid-void topologies by the approaches just mentioned, greatly facilitates the manufacture of the designs obtained, but one should also bear in mind that there is a price to be paid for this, namely that the solution will be associated with a lower value of the performance index as compared to the corresponding global optimum solution obtained by usage of an optimum microstructure.

Geometrical- or Macrostructure approaches to topology optimization of continuum structures are all based on constitutive laws for usual solid, isotropic and anisotropic materials. These approaches encompass on one hand a number of heuristic methods like the *evolutionary* method, which have been proposed by different research groups, and on the other hand the *Bubble Method* which uses an iterative positioning and hierarchically structured shape optimization of new holes, so-called *bubbles*. Thus, here the boundaries of the structure are considered to be variable, and the shape optimization of new bubbles and of the other variable boundaries of the structure is carried out as a parameter optimization problem. Following this idea, an interesting similar approach of using so-called topological gradients to provide information on the possible advantage of the occurrence of a small hole in the structure, has just been proposed. In this context, further methods shall be mentioned like Genetic Algorithms, Design-of-Experiments-methods, Metamorphic Development, etc, that are being augmented to topology optimization.

On the basis of the account of the present state of knowledge presented in the main part of this article, the last section gives a supplementary survey of literature that reflects recent developments in topology optimization of continuum structures. Furthermore, new avenues of application of topology design are illustrated by way of very recent results in areas of tailoring materials for prescribed mechanical properties, design of compliant mechanisms with focus on Micro-ElectroMechanical Systems (MEMS), and topology optimization and functional adaptation in biomechanics.

ACKNOWLEDGMENT

The second author, Niels Olhoff, gratefully acknowledges the sponsorship from the Max Planck Research Award program and the collaboration with the first author, Hans A Eschenauer, funded by the German Federal Ministry for Education, Science, Research and Technology. Both authors are indebted to Michael Wengenroth of *Siegen:Kommunikation Communications Consultants* for his great initiative and devoted assistance in preparing the manuscript of this article.

REFERENCES

Books, reports, lecture notes, theses

[1] Alexandroff PS (1960), *Combinatorial Topology I-III*, Graylock Publ, Rochester NY.
[2] Alt W, Ben-Tal A, Kocvara M, Nemirovski A, and Zowe J (1997), Free Material Design via Semidefinite Programming: The Multiload Case with Contact Conditions, Report No 219, Institute for Applied Mathematics, Univ of Erlangen-Nuremberg, Germany.
[3] Anger G (ed) (1993), Inverse Problems: Principles and Applications in Geophysics, Technology and Medicine.
[4] Atrek E (1991), SHAPE User's Manual, Engineering Mechanics Research Corp, Troy, Michigan.
[5] Bagge M (1999), Remodeling of bone structure, DCAMM Report S 84, PhD-Thesis, Dept of Solid Mech, Technical Univ of Denmark.
[6] Beckers M (1996), Optimisation topologique de structure en variables Discrète, Tech Report, Université de Liège.
[7] Beckers M (1997), Optimisation de structures en variable discrete, These de Doctorat No 181, Universite de Liege, Belgium.

[8] Belegundu A, Mistree F (eds) (1998), Optimization in industry-1997, ASME, New York.
[9] Bendsøe MP (1995), *Optimization of Structural Topology, Shape and Material*, Springer, Heidelberg.
[10] Bendsøe MP and Mota Soares CA (eds) (1993), *Topology Design of Structures*, NATO ASI, Kluwer Academic Publishers, Dordrecht.
[11] Bennet JA, Botkin ME (eds) (1986), *The Optimum Shape: Automated Structural Design*, Plenum Press, New York.
[12] Bensoussan A, Lions J-L, and Papanicolaou G (1978), *Asymptotic Analysis for Periodic Structures*, North Holland, Amsterdam.
[13] Bergmann HW (ed) (1989), *Optimization: Methods and Applications, Possibilities and Limitations*, Springer, Berlin, Heiderlberg, New York.
[14] Bestle D and Schiehlen W (eds) (1995/1996), *Optimization of Mechanical Systems*, Stuttgart, Germany (1995), Kluwer Academic Publishers, Dordrecht, The Netherlands (1996).
[15] Blachut J and Eschenauer H (eds) (2001), *Emerging Methods for Multidisciplinary Optimization*, Lecture Notes CISM Course, Udine, Italy 2000, Springer, Wien/New York.
[16] Bloebaum CL (2000), *WCSMO 3—Third World Congress of Structural and Multidisciplinary Optimization, 1999*, Proceedings, Buffalo NY.
[17] Borrwall T and Petersson J (2000a), Topology optimization using regularized intermediate control, Report LiTH-IKP-R-1086, Division of Mechanics, Mechanical Engineering Systems, Linköping Univ, Sweden, 24 pp.
[18] Borrwall T and Petersson J (2000b), Large scale topology optimization in 3D using parallel computing, Report LiTH-IKP-R-1130, Division of Mechanics, Mechanical Engineering Systems, Linköping Univ, Sweden, 42 pp,
[19] Bourbaki N (1955), *Eléments des Mathématique*, Hermann, Paris.
[20] Bourdin B (1999), Filters in topology optimization, DCAMM Report No 627, Dept of Mathematics, Technical Univ of Denmark.
[21] Cherkaev A (2000), *Variational Methods for Structural Optimization*, Applied Mathematical Sciences 140, Springer-Verlag, New York.
[22] Cherkaev AV and Kohn RV (eds) (1997), *Topics in the Mathematical Modelling of Composite Materials*, Vol 31 of Progress in Nonlinear Differential Equations and Their Applications, Birkhäuser, Boston.
[23] Courant R and Hilbert D (1968), *Methods of Mathematical Physics I*, Interscience Pub, New York.
[24] Duysinx P (1995), Optimization topologique: Du milieu a la structure elastique, PhD Thesis, Faculty of Applied Sciences, Univ of Liege, Belgium.
[25] Duysinx P (1997), Layout optimization: A mathematical programming approach, DCAMM Report 540, Dept of Solid Mechanics, Technical Univ of Denmark.
[26] Eschenauer H (1968), Thermo-elastic plate equations: Buckling of a cantilever plate (in German), Doctoral Thesis, TH Darmstadt.
[27] Eschenauer H, Becker, W and Schumacher A (1998), Multidisciplinary structural optimization in aircraft design (in German), Final Report, BMBF-Bundesvorhaben DYNAFLEX.
[28] Eschenauer H and Olhoff N (eds) (1982), *Optimization Methods in Structural Design*, EUROMECH-Colloquium 164, B.I.-Wissenschaftsverlag, Wien.
[29] Eschenauer H, Olhoff N, and Schnell W (1996/97), *Applied Structural Mechanics: Fundamentals of Elasticity, Load-Bearing Structures, Structural Optimization*, Springer, Berlin, Heidelberg, New York, 398 p, 179 Figs.
[30] Eschenauer HA, Koski J, and Osyczka A (eds) (1990), *Multicriteria Design Optimization*, Springer, Berlin.
[31] Eschenauer HA, Mattheck C, and Olhoff N (1991), *Engineering Optimization in Design Processes*, Lecture Notes in Engineering, Springer, Berlin, Heidelberg, New York.
[32] Eschenauer HA and Schnell W (1993), Elastizitätstheorie-Grundlagen, Flächentragwerke, Strukturoptimierung, 3, Aufl, BI Wissenschaftsverlag, Mannheim.
[33] Evans LC and Gariepy RF (1992), *Measure Theory and Fine Properties of Functions*, CRC Press, Boca Ratan.
[34] Fernandes PR, Rodrigues H, Guedes JM (1996), Topology Optimization of 3d Linear Elastic Structures with a Constraint on ''Perimeter,'' IDMEC/CPM '96/004, Instituto Superior Technico, IDMEC, Lisboa/Portugal.
[35] Foldager J (1999), Design of composite structures, PhD Thesis, Institute of Mechanical Engineering, Aalborg Univ.
[36] Franz W (1960/64), *Topology I* (General Topology), *Topology II* (Algebraic Topology) (in German), De Gruyter (Samml, Göschen), Berlin.
[37] Galilei G (1638), Discorsi e Dimonstrazioni Mathematiche, a Due Nuove Scienze Attenenti alla Mecanica; Movimenti Locali, Leida.
[38] Gallagher RH and Zienkiewicz OC (eds) (1973), *Optimum Structural Design—Theory and Applications*, John Wiley and Sons, London.
[39] Gibianski LV and Cherkaev AV (1984), Design of Composite Plates of External Rigidity, Tech Report No 914, Ioffe Physico-Technical Institute, Acad. Sci. USSR, Leningrad, USSR (in Russian), English translation in: Cherkaev AV, Kohn RV (eds) (1997), *Topics in the Mathematical Modelling of Composite Materials*, Vol 31 of Progress in Nonlinear Differential Equations and Their Applications, Birkhäuser, Boston MA.
[40] Gibianski LV and Cherkaev AV (1987), Microstructures of composites of exremal rigidity and exact estimates of provided energy density (in Russian), Tech Report 1155, A. F. Ioffe Physical-Technical Institute, Academy of Sciences of the USSR, Leningrad, English Translation in: Cherkaev A. V and Kohn R. V. (eds) (1997), Topics in the Mathematical Modelling of Composite Materials, Birkhäuser: New York.
[41] Gilmore B, Hoeltzel DA, Azarm S, and Eschenauer HA (1993), Advances in design automation, *Proc of the 1993 ASME DETC*, Albuquerque, New Mexico/USA, Vol 1/2, ASME, New York.
[42] Goldberg DE (1989), *Genetic Algorithms in Search, Optimization and Machine Learning*, Addison Wesley.
[43] Green AE and Zerna W (1968), *Theoretical Elasticity*, Clarendon Press, Oxford, 2nd Ed.
[44] Gutkowski W and Mróz Z (eds) (1997), *Second World Congress of Structural and Multidisciplinary Optimization*, WCSMO-2, Institute of Fundamental Technological Research, Warsaw, Poland, Vol 182.
[45] Hammer VB (1994), Design of composite laminates with optimized stiffness, strength and damage properties, Ph.D.-thesis, DCAMM Report S 72, Dept for Solid Mechanics, Technical Univ of Denmark.
[46] Haug EJ, Choi KK, and Komkow V (1985), *Design Sensitivity Analysis of Structural Systems*, Academic Press, Orlando FL.
[47] Henschen S (2001), Topologieoptimierungen von Bauteilen mittels lokaler Verfahren unter Berücksichtigung der globalen Konfigurationsentropie, Doctoral Thesis, RWTH Aachen, Faculty of Applied Sciences.
[48] Hilton PJ and Wylie S (1960), *Homology Theory, an Introduction to Algebraic Topology*, Cambridge.
[49] Hocking JG and Young GS (1961), Topology, Addison-Wesley Publ. Co, Massachussetts.
[50] Hörnlein H and Schittkowski K (eds) (1993), *Software Systems for Structural Optimization*, Vol 110 International Series of Numerical Mathematics, Birkhäuser, Basel.
[51] Jäger J (1980), *Fundamental Topology* (in German), Schöninghe-Verlag, Paderborn.
[52] Jänich K (1996), *Topology* (in German), 3rd Ed, Springer-Verlag, Berlin, Heidelberg.
[53] Kelley JL (1955), *General Topology*, Van Nostrand, Toronto, New York, London.
[54] Kneppe G (1986), Direct solution strategies for the shape optimization of plate and shell structures (in German), Doctoral Thesis, Univ of Siegen, Fortschrittsberichte VDI-Reihe I, Nr. 135, Düsseldorf: VDI-Verlag.
[55] Koethe G (1960), *Topologically Linear Domains 1* (in German), Springer-Verlag, Berlin, Göttingen, Heidelberg.
[56] Krawietz A (1986), *Material Theory* (in German), Springer, Berlin, Heidelberg, New York, Tokyo.
[57] Krein MG and Nudelman AA (1977), *The Markov Moment Problem and Extrenal Problems*, Translation of Mathematical Monographs, 50, American Mathematical Society.
[58] Krog LA (1996), Layout optimization of disk, plate, and shell structures, Ph.D. thesis, Special Report No 27, Inst. of Mech. Eng., Aalborg Univ, Denmark.
[59] Kull, Ramm, Reiner (eds) (1995), *Evolution and Optimization* (in German), S Hirzel, Stuttgart.
[60] Lagrange JL (1770–1773), Sur la Figure des Colonnes, Miscellania Taurinensia.
[61] Langhaar HL (1962), *Energy Methods in Applied Mechanics*, John Wiley and Sons, New York.
[62] Lanzcos C (1962), *The Variational Principles of Mechanics*, Univ of Toronto Press, Toronto.
[63] Larsen UD, Sigmund O, and Bouwstra S (1995), Fabrication of compliant micromechanisms and materials with negative Poisson's ratio (manuscript).
[64] Lévy M (1873), *La Statique Graphique et ses Applications aux Constructiones*, Académie des Sciences, Paris.
[65] Lewinski T and Sokolowski J (1999), Topological derivative for nucleation of non-circircular voids, Research Report No 3798, INRIA Lorraine, Nancy, France, 37 pp.

[66] Lurie KA (1993), *Applied Optimal Control Theory of Distributed Systems*, Plenum Press, New York/USA.
[67] Lurie KA and Cherkaev AV (1982), Exact estimates of conductivity of mixtures composed of two isotropic media taken in prescribed proportion, Report No 783, Ioffe Physico-Technical Institute, Acad. Sci. USSR, Leningrad, USSR (in Russian), English translation in: Cherkaev AV, Kohn RV (eds) (1997), Topics in the Mathematical Modelling of Composite Materials, Vol 31 of Progress in Nonlinear Differential Equations and Their Applications, Birkhäuser, Boston, MA, USA.
[68] Mattheck C (1991), *Trees-the Mechanical Design*, Heidelberg.
[69] Mattheck C (1992), *Design in Nature* (in German), Freiburg.
[70] Maute K (1998), Topology and shape optimization of thin-walled structures (in German), Ph.D.-Thesis, Report No 25, Institut für Baustatik, Universität Stuttgart.
[71] Metzger K (1893), *Wind as a Decisive Factor for the Growth of Trees* (in German), Mündener Forstliche Hefte, Drittes Heft, Berlin.
[72] Michlin SG (1962), *Variational Methods in Mathematical Physics* (in German), Akademie-Verlag.
[73] Mota Soares CA (ed) (1986), Computer aided optimal design: Structural and mechanical systems, NATO/NASA/NSF/USAF Advanced Study Institute, Troia/PORTUGAL, June 29–July 11, 1986, Vol 2, Center for Mechanics and Materials of the Technical Univ of Lisbon.
[74] Neuber (1985), *Theory of Notch Stresses* (in German), Springer, Berlin, Heidelberg.
[75] Olhoff N and Rozvany GIN (eds) (1995), *Structural and Multidisciplinary Optimization*, Proc of WCSMO-1, Elsevier Science, Oxford/UK.
[76] Pedersen P (ed) (1993), *Optimal Design with Advanced Materials*, Proceedings IUTAM-Symposium Lyngby/DENMARK, Elsevier Science Publ, Amsterdam/The Netherlands.
[77] Pedersen P (1998), *Elasticity—Anisotropy—Laminates, Solid Mechanics*, Technical Univ of Denmark DTU.
[78] Pedersen P and Bendsøe MP (eds) (1999), *IUTAM Symposium Synthesis in Bio Solid Mechanics*, Copenhagen/Denmark, May 24–27, 1998, Kluwer, Dordrecht.
[79] Petersson J (1996), A finite element analysis of optimal variable thickness sheets, Mat. Report No 1996-44, Dept of Math., Technical Univ of Denmark.
[80] Petersson J (1998), Some convergence results in perimeter-controlled topology optimization, Tech Report LiTH-IKP-R-995, Institute of Technology, Dept of Mech Eng, Linköping Univ.
[81] Pontrjagin LS (1957/58), *Topological Classes I, II* (in German), Leipzig.
[82] Prager W (1961), *Introduction to Continuum Mechanics* (in German), Birkhäuser Verlag, Basel.
[83] Prager W (1969), Optimality criteria derived from classical extremum principles, SM Studies Series, Solid Mechanics Division, Univ of Waterloo, Ontario/CANADA.
[84] Prasad B (ed) (1989), *CAD/CAM Robotics and Factories of the Future*, Vol 2 (Proc of 3rd Int Conf CARS and FOF '88), Springer, Berlin.
[85] Querin OM (1997), Evolutionary structural optimization: Stress based formulation and implementation, PhD Dissertation, Dept of Aeronaut Eng, Univ of Sydney, Australia.
[86] Querin OM, Steven GP, and Xie YM (1996), *EVOLVE User Guide*, Dept of Aeronaut Eng, Univ of Sydney, Australia.
[87] Reiter TJ (1996), Functional adaption of bone and application in optimal structural design, Report, VDI Reihe 17, Nr. 145, VDI Verlag, Düsseldorf, Germany, 146 pp.
[88] Rozvany GIN (ed) (1991), Optimization of large structural systems, NATO-ASI Lecture Notes.
[89] Rozvany GIN (ed) (1997), Topology optimization in structural mechanics, Vol 374 of CISM Course and Lectures, Springer, Vienna/Austria.
[90] Rozvany GIN, Bendsøe MP, and Kirsch U, (1995), Layout optimization of structures, *Applied Mechanics Reviews*, **48**, 41–119.
[91] Rozvany GIN, Olhoff N (eds) (2001), *Topology Optimization of Structures and Composite Continua*, NATO ARW, Budapest, Hungary, May 8–12, 2000, Kluwer Academic Publishers, Dordrecht, The Netherlands.
[92] Rozvany GIN, Zhou M, and Sigmund O (1992), Topology optimization in structural design, Research Report in Civil Engineering, 59, Univ of Essen/Germany.
[93] Sanchez-Palencia E (1980), *Non-Homogeneous Media and Vibration Theory*, Lecture Notes in Physics 127, Springer, Berlin.
[94] Schubert H (1960), *Topology* (in German), Teubner, Stuttgart.
[95] Schumacher A (1996), Topology optimization of component structures using hole positioning criteria (in German), Doctoral Thesis, FOMAAS-Report Nr T09-01.96, Univ of Siegen.
[96] Sedov LI (1966), *Foundations of the Non-Linear Mechanics of Continua*, London: Pergamon Press.
[97] Sigmund O (1994a), Design of material structures using topology optimization, PhD thesis, DCAMM report S 69, Dept of Solid Mechanics, Technical Univ of Denmark.
[98] Sokolnikoff IS (1964), *Tensor-Analysis—Theory and Applications to Geometry and Mechanics of Continua*, New York: John Wiley & Sons, 2nd ed.
[99] Sokolowski J and Zochowski A (1997), On topological derivative in shape optimization, Research Report No 3170, INRIA Lorraine, Nancy, France.
[100] Sokolowski J and Zochowski A (2000), Topological derivatives of shape functionals for elasticity systems, Research Report, INRIA Lorraine, Nancy, France, 16 pp.
[101] Soto CA (1993), Shape optimization of plate structures using plate homogenization with applications in mechanical design, PhD thesis, Dept of Mechanical Engineering, Michigan State Univ.
[102] Stadler W (ed) (1988), *Multicriteria Optimization in Engineering and in the Sciences*, Plenum Press, New York.
[103] Steven GP, Querin OM, and Li Q (1999a), *Publications Collection Volume 2*, 1996–1997, Structural Optimization Research Group of Australasia (SORGA), Dept Aeronaut Eng, Univ of Sydney, Australia, 247 pp.
[104] Steven GP, Querin OM, and Li Q (1999b), *Publications Collection Volume 3*, 1998, Structural Optimization Research Group of Australasia (SORGA), Dept Aeronaut Eng, Univ of Sydney, Australia, 278 pp.
[105] Steven GP and Xie YM (1997), *Evolutionary Structural Optimization*, Springer-Verlag, London, 188 pp.
[106] Szabo I (1977), *History of Mechanical Principles* (in German), Birkhäuser-Verlag, Basel, Stuttgart.
[107] Taylor JE and Bendsøe MP (2000), A mutual energy formulation for optimal structural design, MAT-Report No 2000-20, Inst of Math, Technical Univ of Denmark.
[108] Thomsen J (1992), Optimization of properties of anisotropic materials and topologies of structures (in Danish), PhD-thesis, Inst of Mech Eng, Aalborg Univ, Denmark.
[109] Topping BHV and Papadrakis M (eds) (1994), *Advances in Structural Optimization*, CIVIL-COMP Ltd, Edinburgh/UK.
[110] Truesdell C (1965), *Continuum Mechanics IV-Problems of Nonlinear Elasticity*, Gordon and Breach, New York.
[111] Truesdell C (1965), *The Elements of Continuum Mechanics*, Springer, Berlin, Heidelberg, New York.
[112] Tsai SW, Halpin JC, and Pagano NJ (eds) (1968), *Composite Materials Workshop*, Technomic Pub, Stamford CT.
[113] Van Gemert RJ (1996), Additive evolutionary structural optimization, Undergraduate Honours Thesis, Dept of Aeronaut Eng, Univ of Sydney, Australia.
[114] Vinson JR and Sierakowski RL (1987), *The Behavior of Structures Composed of Composite Materials*, Martinus Nijhoff Publ, Dordrecht, The Netherlands.
[115] Washizu K (1982), *Variational Methods in Elasticity and Plasticity*, 3rd Ed, Pergamon Press, New York.
[116] Weinert M (1994), Sequential and parallel strategies for finding optimal layouts of complex shell structures (in German), PhD-Dissertation, Uni-GH Siegen, FOMAAS, TIM-Bericht Nr T05-05.94.
[117] Wheedon RL and Zygmund A (1977), *Measure and Integral: an Introduction to Real Analysis*, Monographs in Pure and Applied Math, 43, Marcel Dekker, New York.
[118] Wolfersdorf Lv (1994), *Inverse and Ill-posed Problems* (in German), Berlin: Akademie-Verlag.
[119] Wolff J. (1892): On the transformation of bones (in German) Berlin.
[120] Young V (1997), Bi-directional Evolutionary Structural Optimization (BESO), 2-D and 3-D, Undergraduate Honours Thesis, Dept of Aeronaut Eng, Univ of Sydney, Australia.

Papers

[121] Akgün MA (2001), Damage tolerant topology optimization under multiple damage configurations, In: Rozvany GIN, Olhoff N (eds): *Topology Optimization of Structures and Composite Continua*, NATO ARW, Budapest, Hungary, May 8–12, 2000, Kluwer Academic Publishers, Dordrecht, The Netherlands (to appear).
[122] Allaire G (1994), Explicit lamination parameters for three-dimensional shape optimization, *J Control and Cybernetics* **23**, 311–326.
[123] Allaire G (2001), Shape optimization with general objective functions using partial relaxation, In: Rozvany G I N, Olhoff N (eds): Topology *Optimization of Structures and Composite Continua*, NATO ARW,

Budapest, Hungary, May 8–12, 2000, Kluwer Academic Publishers, Dordrecht, The Netherlands (to appear).
[124] Allaire G and Aubry S (1999), On optimal microstructures for a plane shape optimization problem, *Struct. Optim.* **17**, 86–94.
[125] Allaire G, Bonnetier E, Francfort G, and Jouve F (1995), Shape optimization by the homogenization method, Report, Lab d'Analyze Numerique, Universite Paris 6.
[126] Allaire G and Kohn R V (1993), Optimal design for minimum weight and compliance in plane stress using extremal microstructures, *Eur. J. Mech, A/Solids* **12**(6), 839–878.
[127] Almgren, RF (1985), An isotropic three-dimensional structure with Poisson's ratio=−1, *J. Elasticity* **15**, 427–430.
[128] Ambrosio L and Buttazzo G (1993), An optimal design problem with perimeter penalization, *Calc. Var.* **1**, 55–69.
[129] Atkin RJ and Craine RE (1976), Continuum theory of mixtures: Applications, *J. Inst. Math. Applics* **17**(2), 153–207.
[130] Atrek E (1989), SHAPE: A program for shape optimization of continuum structures, *Proc First Int Conf.: Opti'89*, Comp. Mechanics Publications, Berlin: Springer Verlag, 135–144.
[131] Atrek E (1993), SHAPE: A structural shape optimization program, In: Hörnlein H, Schittkowski K (eds): *Software Systems for Structural Optimization*, Vol 110 International Series of Numerical Mathematics, Basel: Birkhäuser Verlag, 229–249.
[132] Atrek E and Agarwal B (1992), Shape optimization of structural design, In: Billingsley K R, Brown III, H U Derohanes E (eds): *Scientific Excellence in Supercomputing-The IBM 1990 Contest Prize Papers*, Univ of Georgia, Athens/GA: Baldwin Press.
[133] Atrek E and Kodali R (1989), Optimum design of continuum structures with SHAPE, In: Prasad B. (ed): *CAD/CAM Robotics and Factories of the Future, Vol 2* (*Proc of 3rd Int Conf CARS and FOF-'88*), Berlin: Springer, 11–15.
[134] Avellaneda M (1987), Optimal bounds and microgeometrics for elastic two-phase composites, *SIAM, J. Appl. Math.* **47**(6), 1216–1228.
[135] Avellaneda M, and Milton GW (1989), Bounds on the effective elasticity tensor composites based on two-point correlation, In: Hui D, Kozik T J (eds): *Composite Material Technology*, ASME, 89–93.
[136] Banichuk NV (1993), Shape design sensitivity analysis for optimization problems with local and global functionals, *Mech. Struct. and Mach.* **21**(3), 375–397.
[137] Banichuk NV, Barthold F-J, Falk A, and Stein E (1995), Mesh refinement for shape optimization, *Struct. Optim.* **9**, 46–51.
[138] Baumgartner A, Harzheim L, and Mattheck C (1992), SKO: Soft Kill Option: The biological way to find an optimum structure topology, *Int. J. Fatigue* **14**(6), 387–393.
[139] Beckers, M (1999), Topology optimization using a dual method with discrete variables, *Struct. Optim.* **17**, 14–24.
[140] Beckers M and Fleury C (1997), Topology optimization involving discrete variables, In: Gutkowski W, Mróz Z (eds): *Second World Congress of Structural and Multidisciplinary Optimization*, WCSMO-2, Institute of Fundamental Technological Research, Warsaw, Poland, Vol 2, 533–538.
[141] Bendsøe MP (1982), G-closure and homogenization problems arising in plate optimization, In: Eschenauer H, Olhoff N (eds): *Optimization Methods in Structural Design, EUROMECH-Colloquium 164*, Wien: B.1.-Wissenschaftsverlag, 270–275.
[142] Bendsøe MP (1989), Optimal shape design as a material distribution problem, *Struct. Optim.*, **1**, 193–202.
[143] Bendsøe MP (1997), Variable-topology optimization: Status and challenges, In: Wunderlich W (ed): *Proc ICTAM*, Kyoto, August 25–31, 1996, Elsevier Science BV, Amsterdam, The Netherlands.
[144] Bendsøe MP (1999), Variable-topology optimization: Status and challenges, In: Wunderlich W. (ed): *Proc European Conf on Computational Mechanics*—ECCM '99, Aug 31–Sept 3, 1999, Munich, Germany, CD-Rom, Tech Univ of Munich, Germany, 21 pp.
[145] Bendsøe MP and Diaz A (1998), A method for treating damage related criteria in optimal topology design of continuum structures, *Struct. Optim.* **16** (2/3), 108–115.
[146] Bendsøe MP, Diaz A, and Kikuchi N (1993), Topology and generalized layout optimization of elastic structures, In: Bendsøe MP, Mota Soares CA (eds): *Topology Design of Structures*, Dordrecht: Kluwer Academic Publishers, 159–205.
[147] Bendsøe MP, Diaz A, Lipton R, and Taylor JE (1994a), Optimal design of material properties and material distribution for multiple loading conditions, *Int. J. of Num. Meth. Engng* **38**, 1149–1170.
[148] Bendsøe MP, Guedes JM, Haber RB, Pedersen P, and Taylor JE (1994b), An analytical model to predict optimal material properties in the context of optimal structural design, *J. Appl. Mech.* **61**, 930–937.
[149] Bendsøe MP, Guedes JM, Plaxton S, and Taylor JE (1996), Optimization of structure and material properties for solids composed of softening material, *Int. J. Solids Struct* **33**, 1799–1813.
[150] Bendsøe MP and Kikuchi N (1988), Generating optimal topologies in structural design using a homogenization method, *Comp. Meths. Appl. Mech. Engrg* **71**, 197–224.
[151] Bendsøe MP and Sigmund O (1999), Material interpolations in topology optimization, *Arch. Appl. Mech.* **69**, 635–654.
[152] Bennet JA and Botkin ME (1983), Shape optimization of two-dimensional structures with geometric problem description and adaptive mesh refinement, *AIAA/ASME/ASCE/AHS 24th Structures, Sturctural Dynamics and Materials Conf* (Part I), Lake Tahoe, Nevada/USA, 422–431.
[153] Bennet JA, and Botkin ME (1985), Structural shape optimization with geometric description and adaptive mesh refinement, *AIAA J.* **23**, 458–464.
[154] Ben-Tal A and Taylor JE (1991), A unified model for elastoplatic structural analysis via dual variational principles, In: Komkov V (ed): *Proc SIAM-Dayton Conf on Design Theory*.
[155] Bletzinger K-U and Kimmich S, Ramm, E (1991), Effecient modeling in shape optimal design, *Computing Systems in Engineering* **2**, 483–495.
[156] Botkin ME (1981), Shape optimization of plate and shell structures, *AIAA/ASME/ASCE/AHS 22nd Structural Dynamics and Materials Conf (Part I)*, Atlanta, GA, 242–249.
[157] Bourgat JF (1977), Numerical experiments of the homogenization method for operators with periodic coefficients, *Lecture Notes in Mathematics 740*, Springer-Verlag, Berlin, 330–356.
[158] Bremicker M, Kikuchi N, Chirehdast M, and Papalambros PY (1991), Integrated topology and shape optimization in structural design, *Mech. Struct. and Mach* **19**(4), 551–587.
[159] Bruns TE and Tortorelli DA (2000a), Topology optimization of nonlinear elastic structures and compliant mechanisms, *Comp. Meth. Appl. Mech. Engrg.* (to appear).
[160] Bruns TE and Tortorelli DA (2000b), Topology optimization of geometrically nonlinear structures and complaint mechanisms, In: Bloebaum CL (ed): *WCSMO-3-Proc Third World Congress of Structural and Multidisciplinary Optimization*, May 17–21, 1999, Buffalo NY, CD-Rom, Univ of Buffalo.
[161] Buhl T, Pedersen CBW, and Sigmund O (2000), Stiffness design of geometrically nonlinear structures using topology optimization, *Struct. Multidisc. Optim* **19**, 93–104.
[162] Bulman S and Hinton E (2000), Constrained adaptive topology optimization of engineering structures, In: Bloebaum CL (ed): *WCSMO-3-Proc Third World Congress of Structural and Multidisciplinary Optimization*, May 17–21, 1999, Buffalo NY, CD-Rom, Univ of Buffalo.
[163] Burns RH and Crossley FRE (1964), Kinetostatic synthesis of flexible link mechanisms, ASME-Paper, 68(36).
[164] Burns T and Cherkaev A (1997), Optimal distribution of multimaterial composites for torsional beams, *Struct. Optim.* **13**, 4–11.
[165] Buttazzo G and Dal Maso G (1993), An existence result for a class of shape optimization problems, *Arch. Rational Mech. Anal.* **122**, 183–195.
[166] Canfield S and Frecker M (2000), Topology optimization of compliant mechanisms for displacement amplifcation, In: Bloebaum CL (ed): WCSMO-3-*Proc Third World Congress of Structural and Multidisciplinary Optimization*, May 17–21, 1999, Buffalo NY, CD-Rom, Univ of Buffalo.
[167] Carter DR and Fyhrie DP (1990), Femoral head apparent density distribution predicted from bone stresses, *J. Biomech.* **23**, 1–10.
[168] Carter DR, Fyhrie DP, and Whalen RT (1987), Trabecular bone density and loading history: Regulation of connective tissue biology by mechanical energy, *J. Biomech.* **20**, 785–794.
[169] Carter DR and Hayes WC (1977), The compressive behavior of bone as a two-phase porous structure, *J. Bone and Joint Surg.* **59-A**, 954–962.
[170] Carter DR, Orr TE, and Fyhrie DP (1989), Relationship between loading history and femoral cancellous bone architecture, *J. Biomech.* **22**, 231–244.
[171] Céa J (1986), Conception optimale ou identification de forme, calcule rapide de la dérivée directionelle de la fonction coût, *MAAN*, **30**(3), 371–402.
[172] Céa J, Gioan A, and Michel J (1973), Quelques résultats sur I'identification de domains, CALCOLO.
[173] Céa J and Malanowski K (1970), An example of a max-min problem in partial differential equations, *SIAM J. Control* **8**, 305–316.
[174] Chang K-H and Choi KK (1992), A geometry-based parameterization method for shape design of elastic solids, *Mech. Struct. Mach.* **20**(2), 215–252.
[175] Chang KH and Tang PS (2000), Integration of topology and shape design optimizations for structural components, In: Bloebaum CL

(ed): WCSMO-3-Proc Third World Congress of Structural and Multidisciplinary Optimization, May 17–21, 1999, Buffalo NY, CD-Rom, Univ of Buffalo.
[176] Cheng G (1981), On non-smoothness in optimal design of solid, elastic plates, *Int. J. Solids Struct.* **17**, 795–810.
[177] Cheng G (1997), Some development of structural topology optimization, In: Tatsumi T, Watanabe E, and Kambe T (eds): *Theoretical and Applied Mechanics 1996*, Elsevier Sciences BV, Amsterdam, 379–394.
[178] Cheng G and Guo X (1997), ε-related approach in structural topology optimization, *Struct. Optim.* **13**(4), 258–266.
[179] Cheng G and Jiang Z (1992), Study on topology optimization with stress constraints, *J. Eng. Optim.* **20**, 129–148.
[180] Cheng G and Olhoff N (1981), An investigation concerning optimal design of solid elastic plates, *Int. J. Solids Struct.* **17**, 305–323.
[181] Cheng G and Olhoff N (1982), Regularized formulation for optimal design of axisymmetric plates, *Int. J. Solids Struct.* **18**(2), 153–169.
[182] Cherkaev AV and Gibiansky LV (1993), Coupled estimates for the bulk and shear moduli of a two-dimensional isotropic elastic composite, *J. Mech. Phys. Solids* **41**(5), 937–980.
[183] Cherkaev AV and Gibiansky LV (1994), Variational principles for complex conductivity, viscoelasticity and similar problems with complex moduli, *J. Math. Physics* **35**(1), 127–145.
[184] Cherkaev AV and Gibiansky LV (1996), External structures of multiphase heat conducting composites, *Int. J. Solids Struct* **33**(18), 2609–2618.
[185] Cherkaev AV and Palais R (1996), Optimal design of three-dimensional axisymmetric elastic structures, *Struct. Optim.* **12**, 35–45.
[186] Clausen T (1851), Über die Form architektonischer Säulen, Bull. Phys-Math de l'Académy St. Petersburg, 9, 368.
[187] Cowin SC (1987), Bone remodeling of diaphyseal surfaces by torsional loads: Theoretical predictions, *J. Biomech.* **20**, 1111–1120.
[188] Cowin SC, Hart RT, Balser JR, and Kohn DH (1985), Functional adaptation in long bones: Establishing in vivo values for surface remodeling rate coefficients, *J. Biomech.* **18**, 665–684.
[189] Cristescu M and El-Yafi F (1986), Interactive shape optimization, In: Mota Soares CA (ed): *Computer Aided Optimal Design: Structural and Mechanical Systems*, NATO/NASA/NSF/USAF Advanced Study Institute, froia/PORTUGAL, June 29–July 11, 1986, Vol 2, Center for Mechanics and Materials, Tech Univ of Lisbon, 262–271.
[190] Dems K and Mroz Z (1983), Variational approach by means of adjoint systems to structural optimization and sensitivity analysis Part I, *Int. J. Solids Struct.* **19**, 677–692.
[191] Dems K and Mroz Z (1984), Variational approach by means of adjoint systems to structural optimization and sensitivity analysis Part II, *Int. J. Solids Struct.* **20**, 527–552.
[192] DeRose Jr GCA and Diaz AR (1999), Single scale wavelet approximations in layout optimization, *Struct. Optim.* **18**, 1–11.
[193] DeRose Jr GCA and Diaz AR (2000), Solving three-dimensional layout optimization problems using fixed scale wavelets, *Comput. Mech.* **25**(2), 274–285.
[194] Diaz A and Bendsøe MP (1992), Shape optimization of structures for multiple loading situations using a homogenization method, *Struct. Optim.* **4**, 17–22.
[195] Diaz A and Lipton R (1997), Optimal material layout for 3D elastic structures, *Struct. Optim.* **13**, 60–64.
[196] Diaz A, Lipton R, and Soto CA (1994), A new formulation of the problem of optimum reinforcement of Reissner-Midlin plates, *Comp. Meth. Appl. Mechs. Eng* **123**, 121–139.
[197] Diaz A, and Sigmund O (1995), Checkerboard patterns in layout optimization, *Struct. Optim.* **10**, 40–45.
[198] Diaz AR and Kikuchi N (1992), Solutions to shape and topology eigenvalue optimization problems using a homogenization method, *Int. J. Num. Math. Eng* **35**, 1487–1502.
[199] Diaz AR and Lipton R (2000), Optimal material layout in three-dimensional elastic structures subjected to multiple loads, *Mech. Struct. Mach.* **28**(2/3).
[200] Duysinx P (2000), Topology optimization with different stress limits in tension and compression, In: Bloebaum CL (ed): *WCSMO-3-Proc 3d World Congress of Structural and Multidisciplinary Optimization*, May 17–21, 1999, Buffalo NY, CD-Rom, Univ of Buffalo.
[201] Duysinx P and Bendsøe MP (1998), Topology optimization of continuum structures with local stress constraints, *Int. J. Num. Meths. Eng.* **43**(18), 1453–1478.
[202] Duysinx P and Sigmund O (1998), New developments in handling stress constraints in optimal material distribution, *Proc of the 7th AIAA/USAF/NASAISSMO Symp on Multidisciplinary Analysis and Optimization*, Vol 1, AIAA, 1501–1509.
[203] Eschenauer HA (1988), Multicriteria optimization techniques for highly accurate focussing systems, In: Stadler W (ed): *Multicriteria Optimization in Engineering and in the Sciences*, Plenum Press, New York, 309–354.
[204] Eschenauer HA (1992), Multidisciplinary modeling and optimization in design processes, *ZAMM* **72**, 6, T437–T447.
[205] Eschenauer HA (1998), Development of highly precise radio telescopes: A typical multidisciplinary problem, In: Belegundu A and Mistree F (eds): *Optimization in Industry-1997*, ASME, 13–30.
[206] Eschenauer HA (1999), Multidisciplinary engineering strategies for product and process development—modeling, simulation, optimization, applications, In: Toropov VV (ed): *Engineering Design Optimization, Product and Process Development, Proc 1st ASMO UK/ISSMO Conf on Engineering Design Optimization*, MCB Univ Press, Bradford, 1–17.
[207] Eschenauer HA, Gatzlaff H, and Kiedrowski HW (1980), Entwicklung und Optimierung hochgenauer Panelstrukturen, Technische Mitteilungen Krupp, Forsch-Berichte, 38, 43–57.
[208] Eschenauer HA, Geilen J, and Wahl H J (1993), SAPOP: An optimization procedure for multicriteria structural design, In: Hörnlein H and Schittkowski K (eds): *Software Systems for Structural Optimization, Vol 110* International Series of Numerical Mathematics, Basel: Birkhäuser Verlag, 207–227.
[209] Eschenauer HA, Kobelev VV, and Schumacher A (1994), Bubble method for topology and shape optimization of structures, *Struct. Optim.* **8**, 42–51.
[210] Eschenauer HA and Schumacher A (1993a), Bubble Method: A special strategy for finding best possible initial designs, *Proc of 1993 ASME Design Tech Conf-19th Design Automation Conf*, Albuquerque, New Mexico, Sept. 19–22, Vol 65-2, 437–443.
[211] Eschenauer HA and Schumacher A (1993b), Possibilities of applying various procedures of topology optimisation to components subject to mechanical loads, *ZAMM* **73**, T392–T394.
[212] Eschenauer HA and Schumacher A (1997), Topology and shape optimization procedures using hole positioning criteria-theory and applications, In: Rozvany GIN (ed): *Topology Optimization in Structural Mechanics*, Vol 374 of CISM Courses and Lectures, Wien: Springer, 135–196.
[213] Eschenauer HA, Schumacher A, and Vietor T (1993), Decision makings for initial designs made of advanced materials, In: Bendsøe MP and Mota Soares CA (eds): *Topology Design of Structures*, Dordrecht: Kluwer Academic Publ, 469–480.
[214] Eschenauer HA and Wahl HJ (1993), A decomposition strategy for optimization of structures using the FE-submodel-technique, *ZAMM* **73**, T395–T397.
[215] Farin G (1991), Splines in CAD/CAM, In: *Surveys on Mathematics for Industry*, Springer-Verlag, Austria, 1991, pp. 39–73.
[216] Fernandes P, Guedes JM, and Rodrigues H (1999a), Topology optimization of three-dimensional linear elastic structures with a constraint on "perimeter," *Comput. Struct.* **73**, 583–594.
[217] Fernandes P, Rodrigues H, and Jocobs C (1999b), A model of bone adaptation using a global optimization criterion based on the trajectorial theory of Wolff, *Comp. Meth. Biomech. Biomed. Eng.* **2**, 125–138.
[218] Fleury C (1986), Shape optimal design by the convex linearization method, In: Bennet JA and Botkin ME. (eds): *The Optimum Shape: Automated Structural Design*, New York: Plenum Press, 297–320.
[219] Foldager J (1997), Design optimization of laminated composite plates divided into rectangular patches with use of lamination parameters, In: Gutkowski W and Mroz Z (eds): *Proc WCSMO 2-Second World Congress of Structural and Multidisciplinary Optimization*, Inst of Fundamental Technological Research, Warsaw, Vol 2, 669–675.
[220] Foldager J, Olhoff N, and Hansen JS (1998), A general procedure forcing convexity in ply angle optimization in composite laminates, *Struct. Optim.* **16**(2/3), 201–211.
[221] Foldager JP, Hansen JS, and Olhoff N (2000), A convex formulation in ply-angle optimization, In: Bloebaum CL (ed): *WCSMO-3-Proc 3rd World Congress of Structural and Multidisciplinary Optimization*, May 17–21, 1999, Buffalo NY. CD-Rom, Univ of Buffalo.
[222] Folgado J and Rodrigues H (1997), Topology optimization methods applied to the design of orthopaedics implants, In: Gutkowski W and Mróz Z (eds): *WCSMO-2: Second World Congress of Structural and Multidisciplinary Optimization*, Inst of Fundamental Technological Research, Warsaw, Poland, Vol 2, 563–568.
[223] Folgado J and Rodrigues H (1998), Structural optimization with a nonsmooth buckling load criterion, *Control Cybernetics* **27**(2), 235–253.
[224] Folgado J, Rodrigues H, and Guedes JM (1995), Layout design of plate reinforcements with a buckling load criterion, In: Olhoff N and

Rozvany GIN (eds): *Structural and Multidisciplinary Optimization*, ISSMO, Goslar, Germany, Oxford: Pergamon, 659–666.
[225] Francfort GA and Murat F (1986), Homogenization and optimal bounds in linear elasticity, *Arch. Rat. Mech. Anal* **94**, 307–334.
[226] Frecker M, Kikuchi N, and Kota S (1997), Optimal design of compliant mechanisms, In: Gutkowski W and Mroz Z (eds): *Proc WCSMO 2-Second World Congress of Structural and Multidisciplinary Optimization*, Inst. of Fundamental Technological Research, Warsaw, Vol 1, 345–350.
[227] Frecker M, Kikuchi N, and Kota S (1999), Topology optimization of compliant mechanisms with multiple outputs, *Struct. Optim.* **17**, 269–278.
[228] Freudenthal AM and Geiringer H (1958), The mathematical theories of the inelastic continuum, In: Flügge S, *Handbuch der Physik VI*, Berlin, Göttingen, Heidelberg: Springer, 229–269.
[229] Fukunaga H and Vanderplaats GN (1991), Stiffness optimization of orthotropic laminates composites using lamination parameters, *AIAA J* **29**, 641–646.
[230] Garreau S, Masmoudi M, and Guillaume P (1999), The topological sensitivity for linear isotropic elasticity, *ECCM'99*, Munich/Germany.
[231] Grauer M and Boden H (1993), On the solution of nonlinear engineering optimization problems on parallel computers, FOMAAS Research Report, TIM01-03.94, 96–105.
[232] Grenestedt JL and Gudmundsson P (1993), Layup optimization of composite material structures, In: Pedersen P (ed): *Optimal Design with Advanced Materials*, Proc IUTAM Symp, 311–336.
[233] Guedes JM and Kikuchi N (1990), Pre- and postprocessing for materials based on the homogenization method with adaptive element methods, *Comput. Meth. Appl. Mech. Eng.* **83**, 143–198.
[234] Guedes JM and Taylor JE (1997), On the prediction of material properties and topology for optimal continuum structures, *Struct. Optim.* **14**, 193–199.
[235] Guillaume P and Masmoudi M (1994), Computation of high order derivatives in optimal shape design, *Numerische Mathematik.* **67**, 231–250.
[236] Haber RB and Bendsøe MP (1998), Problem formulation, solution procedures and geometric modeling: Key issues in variable-topology optimization, In: *Proc 7th AIAA/USAF/NASA/ISSMO Symp on Multidisciplinary Analysis and Optimization*, Vol I, AIAA, 1864–1837.
[237] Haber RB, Jog CS, and Bendsøe MP (1994), Variable-topology shape optimization with a control on perimeter, In: *Advances in Design Automation*, Vol 69, ASME, 261–272.
[238] Haber RB, Jog CS, and Bendsøe MP (1995), The perimeter method—a new approach to variable-topology shape optimization, In: Olhoff N, Rozvany GIN (eds): *Structural and Multidisciplinary Optimization, Proc of WCSMO-1*, Elsevier Science, Oxford/UK, 153–160.
[239] Haber RB, Jog CS, and Bendsøe MP (1996), A new approach to variable-topology design using a constraint on the perimeter, *Struct. Optim.* **11**, 1–12.
[240] Haftka RT (1984), An improved computational approach for multilevel optimum design, *J. Struct. Mech.* **12**, 245–261.
[241] Hajela P (1990), Genetic Search—An approach to the nonconvex optimization problem, *AIAA J* **28**, 1205–1210.
[242] Hajela P, Lee E, and Lin C-Y (1993), Genetic algorithms in structural topology optimization, In: Bendsøe MP, Mota Soares CA (eds): *Topology Design of Structures*, Kluwer Academic Publ, Dordrecht, 117–134.
[243] Hajela P and Vittal S (2000), Evolutionary computing and structural topology optimization-A state of the art assessment, In: Olhoff N and Rozvany G (eds): *Lecture Notes, NATO Advanced Research Workshop*, Kluwer Academic Publ (to appear).
[244] Hammer VB (1999), Optimal laminate design subject to single membrane loads, *Struct. Optim.* **17**, 65–74.
[245] Hammer VB, Bendsøe MP, Lipton R, and Pedersen P (1997), Parametrization in laminate design for optimal compliance, *Int. J. Solids Struct.* **34***(4)*, 415–434.
[246] Hammer VB and Olhoff N (2000a), Topology optimization of continuum structures subjected to pressure loading, *Struct. Multidisc. Optim* **19**, 85–92.
[247] Hammer VB and Olhoff N (2000b), Topology optimization with design dependent loads, In: Bloebaum CL (ed): *WCSMO 3-Third World Congress of Structural and Multidisciplinary Optimization*, Buffalo NY 1999.
[248] Hartzheim L and Graf G (1995), Optimization of engineering components with the SKO method, *Proc of 9th Int Conf on Vehicle Structural Mechanics and CAE*, April 4–6, 1995, Troy MI, 235–243.
[249] Hartzheim L and Graf G (1997), Shape and topology optimization in automotive industry, High Performance Computing in Automotive Design, Engineering and Manufacturing, *Proc of 3rd Int Conf on High Performance Computing in Automotive Industry*, Oct. 7–10, 1996, Paris, France, 167–182.
[250] Hartzheim L, Graf G, Klug S, and Liebers J (1999), Topology optimisation in practice, ATZ, *Automobiltechnische Zeitschrift* **101**, 7/8, 11–16.
[251] Hashin Z and Shtrikman, S (1963), A variational approach to the theory of the elastic behavior of multiphase materials, *J. Mech. Phys. Solids.* **11**, 127–140.
[252] Hassani B and Hinton E (1998), A review of homogenization and topology optimization, *Comput Struct* **71**(6), Part I: Homogenization theory for media with periodic structure 707–718, Part II: Analytical and numerical solution of homogenization equations 719–738, Part III: Topology optimization using optimality criteria 739–756.
[253] Henkel F-O, Schumann-Luck A, and Atrek E (1991), Formoptimierung mit NISA-SHAPE, XX, *Int Finite Element Congress* (FEM '91), Baden-Baden/Germany.
[254] Hinton E, Sienz J, Bulman S, and Hassani B (1997), Fully integrated design optimization of engineering structures using adaptive finite element models, In: Gutkowski W and Mroz Z (eds.): *Proceedings WCSMO 2-Second World Congress of Structural and Multidisciplinary Optimization*, Inst of Fundamental Technological Research, Warsaw, Vol 1, 73–78.
[255] Huiskes R, Weinans H, Grooteboer HJ, Dalstra M, Fudala B, and Slooff TJ (1987), Adaptive bone-remodeling theory applied to prosthetic-design analysis, *J. Biomech.* **22**, 1135–1150.
[256] Imam MH (1982), Three-dimensional shape optimization, *Int J Numer Methods Eng* **18**, 661–673.
[257] Jacobsen JB, Olhoff N, and Rønholt E (1997), Generalized shape optimization of three-dimensional structures using materials with optimum microstructures, *Mech. Mat.* **28**, 207–225.
[258] Jog C and Haber RB (1996), Stability of finite element models for distributed-parameter optimization and topology design, *Comp. Meth. Appl. Mech. Eng.* **130**, 203–226.
[259] Jog CS and Haber RB (1995), Checkerboard and other spurious modes in solutions to distributed-parameter and topology design problems, In, Olhoff N and Rozvany GIN (eds): *WCSMO-1-First World Congress of Structural and Multidisciplinary Optimization*, Pergamon Press, Oxford, UK, 237–242.
[260] Jog CS, Haber RB, and Bendsøe MP (1994), Topology design with optimized adaptive materials, *Int. J. Num. Meths. Eng.* **37**, 1323–1350.
[261] Kemmler R, Schwartz S, and Ramm E (2000), Topology optimization including geometrically nonlinear response, In: Bloebaum CL (ed): *WCSMO-3-Proc Third World Congress of Structural and Multidisciplinary Optimization*, May 17–21, 1999, Buffalo NY, CD-Rom, Univ of Buffalo.
[262] Kikuchi N, Chung KY, Torigaki T, and Taylor JE (1986), Adaptive finite element methods for shape optimization of linearly elastic structures, *Comp. Meth. Appl. Mech. Eng.* **57**, 67–89.
[263] Kim CJ, Pisano AP, and Muller RS (1992), Silicon-processed overhanging microgripper, *J. Microelectromech. Systems*, **1**, 31–36.
[264] Kirsch U (1990), On the relationship between optimum structural topologies and geometries, *Struct Optim* **2**, 39–45.
[265] Kita E and Tanie H (1999), Topology and shape optimization of continuum structures using GA and BEM, *Struct Optim* **17**, 130–139.
[266] Kohn RV and Strang G (1986a), Optimal design in elasticity and plasticity, *Num. Meths. Eng.* **22**, 183–188.
[267] Kohn RV and Strang G (1986b), Optimal design and relaxation of variational problems, *Comm. Pure Appl. Math.* **39**, Part I: 1–25, Part II: 139–182; Part III: 353–357.
[268] Korycki R, Eschenauer HA, and Schumacher A (1993), Incorporation of adjoint method sensitivity analysis within the optimization procedure SAPOP, In: *Proc of 11th Polish Conf. on Computer Methods in Mechanics*, May 11–15.
[269] Krog LA and Olhoff N (1995/96), Topology optimization of integral rib reinforcement of plate and shell structures with weighted-sum and max-min objectives, In: Bestle D and Schiehlen W (eds): *Optimization of Mechanical Systems, Stuttgart*, Germany (1995), Kluwer Academic Publ, Dordrecht, The Netherlands (1996), 171–179.
[270] Krog LA and Olhoff N (1997), Topology and Reinforcement layout optimization of disk, plate, and shell structures, In: Rozvany GIN (ed): *Topology Optimization in Structural Mechanics*, Vol 374 of CISM Course and Lectures, Springer, Vienna, Austria, 237–322.
[271] Krog LA and Olhoff N (1999), Optimum topology and reinforcement design of disk and plate structures with multiple stiffness and eigenfrequency objectives, *Comput Struct* **72**, 535–563.
[272] Kutylowski R (2000), On an effective topology procedure, *Struct. Multidisc. Optim* **20** 49–56.

[273] Lakes R (1993), Design considerations for materials with negative Poisson's ratio, *J. Mech. Design*, **115**, 696–700.
[274] Lekszycki T (2000), Application of optimally conditions in modeling of the adaptation phenomenon of bones, In: Bloebaus C. L. (ed), *WCSMO-3-Proc Third World Congress of Structural and Multidisciplinary Optimzation*, May 17–21, 1999, Buffalo NY, CD-Rom, Univ of Buffalo.
[275] Leon (1908), Über die Störungen der Spannungsverteilung, die in elastischen Körpern durch Bohrungen und Bläschen entstehen, Österr, Wochenzeitschrift für den öffentlichen Baudienst, Nr 9, 163–168.
[276] Levinson M (1965), The complementary energy theorem in finite elasticity, *J. Appl. Mech* **32**, Dec, 826–828.
[277] Lewinski T, Sokolowski J, and Zochowski A (2000), Justification of the bubble method for the compliance minimization problems of plates and spherical shells, In: Bloebaum CL (ed): *WCSMO-3-Proc Third World Congress of Structural and Multidisciplinary Optimization*, May 17–21, 1999, Buffalo NY, CD-Rom, Univ of Buffalo.
[278] Lin C-Y and Hajela P (1992), Genetic search strategies in multicriterion optimal design, *Struct Optim* **4**, 144–156.
[279] Lipton R (1994), Optimal bounds on effective elastic tensors for orthotropic composites, *Proc R. Soc. Lond. A*, 443, 399–410.
[280] Lipton R (1994a), On optimal reinforcement of plates and choice of design parameters, *J. Control Cybernetics* **23**(3), 481–493.
[281] Lipton R (1994b), Optimal design and relaxation for reinforced plates subject to random transverse loads, *J. Probabilistic Eng. Mech.* **9**, 167–177.
[282] Lipton R and Diaz A (1995), Moment formulations for optimum layout in 3D elasticity, In: Olhoff N and Rozvany GIN (eds): *Structural and Multidisciplinary Optimization*, Pergamon Press, Oxford, UK, 161–168.
[283] Lipton R and Diaz A (1997a), Optimal material layout for 3-D elastic structures, *Struct Optim* **13**, 60–64.
[284] Lipton R and Diaz A (1997b), Reinforced Mindlin plates with extremal stiffness, *Int. J. Solids Struct* **34**(28), 3691–3704.
[285] Liu J-S, Parks GT, and Clarkson PJ (1999a), Topology optimization of both trusses and continuum structures using a unified metamorphic development method, *Proc of 1st ASMO UK/ISSMO Conf on Engineering Design Optimization*, llkley, West Yorkshire, UK, 257–264.
[286] Liu J-S, Parks GT, and Clarkson PJ (1999b), Metamorphic Development: A new topology optimization method for truss structures, *Proc of 40th AIAA/ASME/ASCE/AHS/ASC Structures, Structural Dynamics and Materials Conf*, St Louis MO, April 12–15, 1999, AIAA-99-1387, 1578–1588.
[287] Liu J-S, Parks GT, and Clarkson PJ (1999c), Can a structure grow towards an optimum topology layout?-Metamorphic Development: a new topology optimization method, *Proc 3rd World Congress of Structural and Multidisciplinary Optimization* (WCSMO-3), Buffalo NY, May 17–21, 1999.
[288] Liu JS, Parks GT, and Clarkson PJ (2000), Metamorphic development: A new topology optimization method for continuum structures, *Struct. Multidisc. Optim* **20**, 288–300.
[289] Lurie KA and Cherkaev AV (1986), Effective characteristics of composite materials and the optimal design of structural elements, *Uspekhi Mekhaniki* **9**, 3–81, English translation in : Cherkaev AV, Kohn RV (eds): *Topics in the Mathematical Modelling of Composite Materials*, Vol 31 of Progress in Nonlinear Differential Equations and Their Applications, Birkhäuser, Boston MA, 1997, 175–258.
[290] Lurie KA, Cherkaev AV, and Fedorov A (1982), Regularization of optimal design problems for bars and plates, Part I: *JOTA* **37**, 499–522, Part II: *JOTA* **37**, 523–543; Part III: *JOTA* **42**, 247–284.
[291] Ma ZD, Cheng HC, and Kikuchi N (1994), Structural design for obtaining desired eigenfrequencies by using the topology and shape optimization method, *Comput. Syst. Eng.* **5**, 77–89.
[292] Ma ZD, Kikuchi N, and Cheng HC (1995a), Topological design for vibrating structures, *Comp. Meth. Appl. Mech. Eng.* **121**, 259–280.
[293] Ma ZD, Kikuchi N, Cheng HC, and Hagiwara I (1995b), Topological optimization technique for free vibration problems, *J. Appl. Mech.* (March '95).
[294] Magister R and Post PU (1995), Use of structural optimization in the development of pneumatic components, In: Olhoff N and Rozvany GIN (eds): *Proc WCSMO 1-First World Congress of Structural and Multidisciplinary Optimization*, Goslar, Pergamon Press, Oxford, 445–452.
[295] Maier G (1973), Limit design in the absence of a given layout: A finite element zero-one programming problem, In: Gallagher RH and Zienkiewicz OC (eds): *Optimum Structural Design-Theory and Applications*, London: John Wiley and Sons, 223–239.
[296] Martin RB (1972), The effects of geometric feedback in the development of osteoporosis, *J. Biomech* **5**, 447–455.
[297] Martin RB and Burr DB (1982), A hypothetical mechanism for the stimulation of Osteonal remodeling by fatigue damage, *J. Biomech* **15**, 137–139.
[298] Mattheck C, Baumgartner A, and Walther F (1995), Bauteiloptimierung durch die Simulation biologischen Wachstums, In: Kull, Ramm, Reiner (eds): *Evolution und Optimierung*, Stuttgart: S. Hirzel, 107–120.
[299] Maute K and Ramm E (1994a), Adaptive techniques in topology optimization, *5th AIAA/USAF/NASA/ISSMO Symp on Multidisciplinary Analysis and Optimization*, Vol 1, AIAA, 121–131.
[300] Maute K and Ramm E (1994b), Adaptive topology optimization, *Struct Optim* **10**, 100–112.
[301] Maute K and Ramm E (1995), General shape optimization—an integrated model for topology and shape optimization, In: Olhoff N and Rozvany GIN (eds): *WCSMO-1-First World Congress of Structural and Multidisciplinary Optimization*, Pergamon Press, Oxford, UK, 299–306.
[302] Maute K, Schwarz S, and Ramm E (1998), Adaptive topology optimization of elastoplastic structures, *Struct. Optim.* **15**, 81–91.
[303] Maute K, Schwarz S, and Ramm E (1999), Structural optimization, The interaction between form and mechanics, *ZAMM* **79**(10), 651–673.
[304] Maxwell JC (1989), On Reciprocal Figures, frames and diagrams of forces, *Scientific Papers* **2**, 160–207.
[305] Michell AGM (1904), The limits of economy of materials in frame structures, Philosophical Magazine, Series 6, Vol 8(47), 589–597.
[306] Miki M (1982), Material design of composite laminates with required in-plane elastic properties, In: Hayashi T, Kawata K, Umekawa M (eds): *Proc Progress in Science and Engineering of Composites*, ICCM IV, Tokyo.
[307] Miki M and Sugiama Y (1991), Optimal design of laminated composite plates using lamination parameters, *AIAA J* **29**, 275–283.
[308] Milton GV (1992), Composite material with Poisson's ration close to-I, *J. Mech. Phys. Solids* **40**(5), 1105–1137.
[309] Milton GV and Cherkaev AV (1993), Materials with elastic tensors that range over the entire set compatible with thermodynamics, Paper presented at the joint *ASCE-ASME-SES MettN*, Univ of Virginia, Charlottesville VA.
[310] Min S, Kikuchi N, Park YC, Kim S, and Chang S (1997), Optimal reinforcement design of structures under impact loads, In: Gutkowski W and Mróz Z (eds): *ECSMO-2: Second World Congress of Structural and Multidisciplinary Optimization*, Inst of Fundamental Technological Research, Warsaw, Poland, Vol 2, 583–588.
[311] Min S, Kikuchi N, Park YC, Kim S, and Chang, S (1999), Optimal topology design of structures under dynamic loads, *Struct. Optim.* **17**, 208–218.
[312] Mlejnek HP (1991), Some aspects in the genesis of structures, In: Rozvany GIN (ed): *Optimization of Large Structural Systems*, NATO-ASI Lecture Notes.
[313] Mlejnek HP (1995), Some recent extensions in the distribution of isotropic material, In: Olhoff N and Rozvany GIN (eds): *WCSMO-1-First World Congress of Structural and Multidisciplinary Optimization*, Pergamon Press, Oxford/UK, 225–230.
[314] Mlejnek HP and Schirrmacher R (1993), An engineers approach to optimal material distribution and shape finding, *Comp. Meth. Appl. Mech. Eng* **106**, 1–26.
[315] Mroz Z and Bojczuk D (2000), Topological derivative concept in optimal design of structures, In: Bloebaum CL (ed): *WCSMO-3-Proc Third World Congress of Structural and Multidisciplinary Optimization*, May 17–21, 1999, Buffalo NY, CD-Rom, Univ of Buffalo.
[316] Mullender MG, Huiskes R, and Weihnans H (1994), A physiological approach to the simulation of bone remodelling as a self-organizational control process, *J. Biomech* **11**, 1389–1394.
[317] Naghdi P M (1964), Non-linear thermoplastic theory of shells, In: Olszak W and Sawczuk A, *Non Classical Shell Problems*, Amsterdam: North-Holland Publ, 1–268.
[318] Neves MM, Rodrigues H, and Guedes JM (1995), Generalized topology design of structures with a buckling load criterion, *Struct. Optim.* **10**, 71–78.
[319] Neves MM, Rodrigues H, and Guedes JM (2000), Optimal design of periodic linear elastic microstructures, *Comput. Struct.* **76**, 421–429.
[320] Niordson F (1982), Some new results regarding optimal design of elastic plates, In: Eschenauer H and Olhoff N. (eds): *Optimization Methods in Structural Design*, EUROMECH-Colloquium 164, Wien: B. I.-Wissenchaftsverlag, 380–386.
[321] Niordson FI (1983), Optimal design of plates with a constraint on the slope of the thickness function, *Int. J. Solids Struct* **19**, 141–151.
[322] Nishiwaski S, Saitou K, Min S, and Kikuchi, N (2000a), Topological

design considering flexibility under periodic loads, *Struct. Multidisc. Optim.* **19**, 4–16.
[323] Nishiwaki S, Silva ECN, Saitou K, and Kikuchi N (2000b), Topology optimization of actuators using structural flexibility, In: Bloebaum CL (ed): *WCSMO-3—Proc Third World Congress of Structural and Multidisciplinary Optimization*, May 17–21, 1999, Buffalo NY, CD-Rom, Univ of Buffalo.
[324] Noll W (1958), A mathematical theory of the mechanical behavior of continuous media, *Arch. Rational Mech. Anal.* **2**, 197–226.
[325] Olhoff N (1996), On optimum design of structures and materials, *Meccanica* **31**, 143–161.
[326] Olhoff N (2001), Comparative study of optimizing the topology of plate-like structures via plate theory and 3-D theory of elasticity, In: Rozvany GIN and Olhoff N (eds): *Topology Optimization of Structures and Composite Continua*, NATO ARW, Budapest, Hungary, May 8–12, 2000, Kluwer Academic Publ, Dordrecht, The Netherlands (to appear).
[327] Olhoff N, Bendsøe MP, and Rasmussen J (1991), On CAD-integrated structural topology and design optimization, *Comp. Meths. Appl. Mech. Eng.* **89**, 259–279.
[328] Olhoff N and Eschenauer H (1999), On optimal topology design in mechanics, In: Wunderlich W. (ed): *Proc European Conf on Computational Mechanics-ECCM '99*, August 31–September 3, 1999, Munich, Germany, CD-Rom, Technical Univ of Munich, Germany, 71 pp.
[329] Olhoff N, Lurie KA, Cherkaev AV, and Fedorov A (1981), Sliding regimes of anisotropy in optimal design of vibrating plates, *Int. J. Solids Struct.* **17**(10), 931–948.
[330] Olhoff N, Røholt, E, and Scheel J (1998a), Topology optimization of three-dimensional structures using optimum microstructures, *Struct. Optim.* **16**, 1–18.
[331] Olhoff N, Rønholt E, and Scheel, J (1998b), Topology optimization of plate-like structures using 3-D elasticity and optimum 3-D microstructures, In: *Proc 7th AIAA/USAF/NASA/ISSMO Symp on Multidisciplinary Analysis and Optimization*, Vol 1, AIAA, 1853–1863.
[332] Olhoff N and Taylor J (1983), On structural optimization, *J. Appl. Mech.* **50**, 1134–1151.
[333] Olhoff N, Thomsen J, and Rasmussen J (1993), Topology optimization of bi-material structures, In: Pedersen P (ed): *Optimal Design with Advanced Materials*, Lyngby, Denmark, Amsterdam: Elsevier, 191–206.
[334] Ou JS and Kikuchi N (1996a), Optimal design of controlled structures, *Struct Optim* **11**, 19–28.
[335] Ou JS and Kikuchi N (1996b), Integrated optimal structural and vibration control design, *Struct. Optim.* **12**, 209–216.
[336] Pedersen CBW, Buhl T, and Sigmund O (2000), Topology synthesis of large-displacement complaint mechanisms, *Int. J. Num. Meth. Engrg*. (to appear).
[337] Pedersen CWB, Buhl T, and Sigmund O (1999), Topology synthesis of large-displacement compliant mechanisms, *1999 ASME Design Engineering Tech Conf*, Paper No DETC/DAC-8554, Las Vegas, Nov.'99 (to appear).
[338] Pedersen NL (2000a), Maximization of eigenvalues using topology optimization, *Struct. Multidisc. Optim.* **20**, 2–11.
[339] Pedersen NL (2000b), Topology optimization of AFM probes with constraints on eigenvalues, In: Bloebaum CL (ed): *WCSMO-3-Proc Third World Congress of Structural and Multidisciplinary Optimization*, May 17–21, 1999, Buffalo NY, CD-Rom, Univ of Buffalo.
[340] Pedersen NL (2001), On topology optimization of plates with prestress, *Int. J. Num. Meth. Engrg*. (to appear).
[341] Pedersen P (1989), On optimal orientation of orthotropic materials, *Struct. Optim.* **1**, 101–106.
[342] Pedersen P (1990), Bounds on elastic energy in solids of orthotropic materials, *Struct. Optim.* **2**, 55–63.
[343] Pedersen P (1991), On thickness and orientational design with orthotropic materials, *Struct Optim*, **3**, 69–78.
[344] Petersson J, Beckers M, and Duysinx P (2000), Almost isotropic perimeters in topology optimization: Theoretical and numerical aspects, In: Bloebaum CL (ed): *WCSMO-3-Proc Third World Congress of Structural and Multidisciplinary Optimization*, May 17–21, 1999, Buffalo NY, CD-Rom, Univ of Buffalo, NY.
[345] Petersson J, and Sigmund O (1998), Slope constrained topology optimization, *Int. J. Num. Meths. Eng.* **41**, 1417–1434.
[346] Pettermann H E, Reiter T J, and Rammerstorfer F G (1997), Computational simulation of Internal bone remodeling, *Arch. Computat. Methods Eng.* **4**, 4, 295–323.
[347] Poulsen TA (2000), Multi-scale representations in design optimization, In: Bloebaum CL (ed): *WCSMO-3—Proc Third World Congress of Structural and Multidisciplinary Optimization*, May 17–21, 1999, Buffalo NY, CD-Rom, Univ of Buffalo.
[348] Prager W (1974), A note on discretized Michell structures, *Comput. Meth. Appl. Mech. Eng.* **3**, 349–355.
[349] Prager W (1976), Transmission optimale des charges par flexion, *Anales de l'Institute Technique du Batiment et de Travaux Publics*, Serie: Theories et Methodes de Calcul, No 193, 82–91.
[350] Querin OM, Steven, GP, and Xie YM (1997a), Improved computational efficiency using bi-directional evolutionary structural optimization (BESO), Abstract for *4th World Congress on Computational Mechanics* (held in Argentina).
[351] Querin OM, Steven GP, and Xie YM (1997b), Evolutionary structural optimization in 3D elasticity, *Proc WCSMO-2, 2nd World Congress on Structural and Multidisciplinary Optimization*, Zakopane, Poland, Vol 1, 143–148.
[352] Querin OM, Steven GP, and Xie YM (1998), Evolutionary structural optimization (ESO) using a bidirectional algorithm, *J. Eng. Comput.* **15**(8), 1031–1048.
[353] Querin OM, Steven GP, and Xie YM (2001), Advances in evolutionary structural optimization: 1992–2000, In: Rozvany GIN, Olhoff N (eds): *Topology Optimization of Structures and Composite Continua*, NATO ARW, Budapest, Hungary, May 8–12, 2000, Kluwer Academic Publishers, Dordrecht, The Netherlands (to appear).
[354] Ramm E, Bletzinger K-U, Reitinger R, and Maute K (1994), The challenge of structural optimization, In: Topping, BHV, Papadrakis M (eds): *Advances in Structural Optimization*, CIVIL-COMP Ltd, Edinburgh/UK, 27–57.
[355] Reinhardt HJ, Seiffarth F, and Háo DN (1993), Approximate solutions of III-posed Cauchy problems for parabolic differential equations, In: Anger G (ed): *Inverse Problems: Principles and Applications in Geophysics, Technology and Medicine*, 284–298.
[356] Reissner E (1965), On a variational theorem for finite elastic deformations, In: Truesdell C, *Continuum Mechanics IV-Problems of Non-Linear Elasticity*, New York: Gordon and Breach, 103–109.
[357] Reiter TJ (1993), Topologieoptimierung mittels eines bilogischen Wachstumsalgorithmus, *ZAMM* **73**(7/8).
[358] Reiter TJ (1995), Knochen-eine selbstoptimierende Struktur? In: Kull U, Ramm E, and Reiner R, *Evolution und Optimierung*, Stuttgart, S Hirzel, 121–135.
[359] Reiter TJ and Rammerstorfer FG (1993), Simulation of natural adaptation of bone material and application in optimum composite design, In: Pedersen P. (ed): *Optimal Design with Advanced Materials*, Amsterdam, London: Elesevier, 25–36.
[360] Rodrigues H, Guedes JM, and Bendsøe MP (2000), Hierarchical optimization of material and structure, In: Bloebaum CL (ed), *WCSMO-3—Proc Third World Congress of Structural and Multidisciplinary Optimization*, May 17–21, 1999, Buffalo NY, CD-Rom, Univ of Buffalo.
[361] Rodrigues H, Miranda PS, and Guedes JM (2001), Optimization of porous coating distribution of noncemented hip prothesis, In: Rozvany GIN and Olhoff N (eds.), *Topology Optimization of Structures and Composite Continua*, NATO ARW, Budapest, Hungary, May 8–12, 2000, Kluwer Academic Publ, Dordrecht, The Netherlands (to appear).
[362] Rodrigues H, Soto CA, and Taylor JE (1999), A design model to predict optimal two-material composite structures, *Struct Optim* **177**, 186–198.
[363] Rodriguez(-Velasquez) J and Seireg A (1988), A geometric rule-based methodology for shape synthesis: 2-D cases, In: *Proc 1988 ASME Int Computers in Engineering Conf and Exposition*, San Francisco, CA, Vol 2, 35–41.
[364] Rosen DW and Grosse IR (1992), A feature based shape optimization technique for the configuration and parametric design of flat plates, *Eng. Comp.* **8**, 81–91.
[365] Rossow HP and Taylor JE (1973), A finite element method for the optimal design of variable thickness sheets, *AIAA J*, **11**, 1566–1569.
[366] Rovati M and Taliercio A (1991), Optimal orientation of the symmetry axes of orthotropic 3D-materials, In: Eschenauer HA, Mattheck C, and Olhoff N (eds): *Engineering Optimization in Design Processes*, Berlin, Heidelberg, New York: Springer, 127–134.
[367] Rozvany GIN, Bendsøe MP, and Kirsch U (1995), Layout Optimization of Structures, *Appl. Mech. Rev.* **48**, 41–119.
[368] Rozvany GIN and Prager W (1976), Optimal design of partially discretized grillages, *J. Mech. Phys. Solids* **24**, 125–136.
[369] Rozvany GIN, Zhou M, and Birker T (1992), Generalized shpae optimization without homogenization, *Struct. Optim.* **4**, 250–252.
[370] Rozvany GIN, Zhou M, Birker T, and Sigmund O (1993), Topology optimization using interactive continuum-type optimality criteria (COC) methods for discretized systems, In: Bendsøe MP and Mota

Soares CA (eds): *Topology Design of Structures*, Dordrecht: Kluwer Academic Publishers.
[371] Rozvany GIN, Zhou M, Rotthaus M, Gollub W, and Spengemann F (1989), Continuum-type optimality criteria methods for large finite element systems with displacement constraints, Parts I and II, *Struct. Optim.* **1**, 47–72.
[372] Sankaranaryanan S, Haftka RT, and Kampania RK (1993), Truss topology optimization with stress and displacement constraints, In: Bendsøe MP, and Mota Soares CA (eds): *Topology Design of Structures*, Dordrecht: Kluwer Academic Publ, 71–78.
[373] Schmit LA and Mallet RH (1963), Structural syntheses and design parameters, In: Hierarchy Journal of the Structural Division, *Proc of ASCE*, Vol 89, No 4, 269–299.
[374] Schwarz S, Maute K, Menrath H, and Ramm E (1997), Adaptive topology optimization including elastoplasticity. In: Gutkowski W, Mroz Z (eds): *Proc WCSMO 2—Second World Congress of Structural and Multidisciplinary Optimization*, Inst of Fundamental Technological Research, Warsaw, Vol 2, 569–576.
[375] Shonauer M, Kallel L, and Jouve F (1996), Mechanical inclusions identification by evolutionary computation, *Revue européenne des élément finis* **5**(5–6), 619–648.
[376] Sienz J and Hinton E (1997), Reliable structural optimization with error estimation, adaptivity and robust sensitivity analysis, *J. Comp. Struct.* **64**, 31–63.
[377] Sigmund O (1994b), Materials with prescribed constitutive parameters: An inverse homogenization problem, *Int. J. Solids Struct.* **31**, 2313–2329.
[378] Sigmund O (1995), Design of material structures using topology optimization, In: Olhoff N and Rozvany GIN (eds): *WCSMO-1—First World Congress of Structural and Multidisciplinary Optimization*, Pergamon Press, Oxford/UK.
[379] Sigmund O (1997), On the design of compliant mechanisms using topology optimization, *J. Mech. Struct. Mach.* **25**, 493–524.
[380] Sigmund O (1998a), Systematic design of electrothermomechanical microactuators using topology optimization, In: *Modelling and Simulation of Microsystems, Semiconductors, Sensors and Actuators*, MSM98, Santa Clara, CA/USA, 1492–1500.
[381] Sigmund O (1998b), Topology optimization in multiphysics problems, In: *Proc of 7th AIAA/USAF/NASA/ISSMO Symp on Multidisciplinary Analysis and Optimization*, Vol 1, AIAA, 1492–1500.
[382] Sigmund O (1999), Topology optimization: A tool for the tailoring of structures and materials, *Philosophical Transactions of the Royal Society: Science into the Next Millennium* (Issue 2, Mathematics, Physics and Engineering), 211–228.
[383] Sigmund O (2000a), Topology optimization of multi-material, multiphysics structures, In: structures using topology optimization, In: Bloebaum CL (ed): *WCSMO-3-Proc. Third World Congress of Structural and Multidisciplinary Optimization*, May 17–21, 1999, Buffalo NY, CD-Rom, Univ of Buffalo.
[384] Sigmund O (2000b), Design of multiphysics actuators using topology optimization, Part I: One-material structures, Part II: Two-material structures, *In. J. Num. Meth. Engrg.* (to appear).
[385] Sigmund O (2000c), A 99 line topology optimization code written in, *Matlab. Struct. Multidisc. Optim.* (to appear).
[386] Sigmund O and Petersson J (1998), Numerical instabilities in topology optimization: A survey on procedures dealing with checkerboards, mesh-dependencies and local minima, *Struct. Optim.*, **16**(1), 68–75.
[387] Sigmund O and Torquato S (1997), Design of materials with extreme thermal expansion using a three-phase topology optimization method, *J. Mech. Phys. Solids* **45**, 1037–1067.
[388] Sigmund O, Torquato S, and Aksay IA (1998), On the design of 1–3 piezocomposites using topology optimization, *J. Mat. Res*, **13**, 1038–1048.
[389] Sobieszczanski-Sobieski J (1988), Optimization by decomposition: a step from hierarchic to non-hierarchic systems, *Proc 2nd NASA/Air Force Symp on Recent Advances in Multidisciplinary Analysis and Optimization*, Hampton VA, Sept. 28–30, 1988.
[390] Sobieszczanski-Sobieski J (1989), Multidisciplinary optimization for engineering systems, In: Bergmann HW (ed): *Optimization: Methods and Applications, Possibilities and Limitations*, Springer, Berlin, Heidelberg, New York, 42–62.
[391] Sobieszczanski-Sobieski J, Bloebaum CL, and Hajela P (1988), Sensitivity of control-augmented structure obtained by a system decomposition method, *Proc of the IAA/ASME/ASCE/AHS 29th Structures, Structural Dynamics, and Materials Conf*, Williamsburg VA, April 18–20, 1988, Paper-No 88–2205.
[392] Soto CA and Diaz A (1993a), Layout of plate structures for improved dynamic response using a homogenization method, In: Gilmore B, *et al* (eds): Advances in Design Automation, *Proc of the 1993 ASME DETC*, Albuquerque NM, 667–674.
[393] Soto CA and Diaz A (1993b), On the modelling of ribbed plates for shape optimization, *Struct. Optim.* **6**, 175–188.
[394] Soto CA and Diaz AR (1993c), A model for layout optimization of plate structures. In: Pedersen P (ed): *Optimal Design with Advanced Materials*, Lyngby, Denmark, Amsterdam: Elsevier, 337–350.
[395] Soto CA and Diaz AR (1993d), Optimum layout of plate structures using homogenization, In: Bendsøe MP, Mota Soares CA (eds): *Topology Design of Structures*, Sesimbra/PORTUGAL, Nato-ASI, Dordrecht: Kluwer Academic Publ, 407–420.
[396] Suryatama D and Bernitsas MM (2000), Topology and performance redesign of complex structures by large admissible perturbations, *Struct. Multidisc. Optim* **20**, 138–153.
[397] Suzuki K and Kikuchi N (1991), Optimization using the homogenization method: Generalized layout design of three-dimensional shells for car bodies, In: Rozvany GIN (ed): *Optimization of Large Structural Systems*, NATO-ASI Lecture Notes, 110–126.
[398] Swan CC, and Arora JS (1997), Topology design of material layout in structured composites of high stiffness and strength, *Struct. Optim.* **13**, 45–59.
[399] Tanaka M, Adachi T, and Tomita Y (1995), Optimum design of lattice continuum material suggested by mechanical adaptation of cancellous bone, In: Olhoff N and Rozvany GIN (eds): *WCSMO- I—First World Congress of Structural and Multidisciplinary Optimization*, Pergamon Press, Oxford, UK, 185–192.
[400] Taylor JE (1993), A global extremum principle for the analysis of solids composed of softening material, *Int. J. Solids. Struct* **30**(15), 2057–2069.
[401] Taylor JE (1998), An energy model for the optimal design of linear continuum structures, *Struct. Optim.* **16**, 116–127.
[402] Taylor JE (2000), Addendum to: An energy model for the optimal design of linear continuum structures, *Struct. Multidisc. Optim* **19**, 317–320.
[403] Theocaris PS and Stavroulakis GE (1998), Multilevel optimal design of composite structures including materials with negative Poisson's ratio, *Struct. Optim.* **15**, 8–15.
[404] Thierauf G (1996), Optimal topologies of structures: homogenization, pseudo-elastic approximation and the bubble-method, *Engineering Computations*, Vol 13, No 1, MCB Univ Press, Bradford/UK.
[405] Topping BHV and Khan AI (1991), Parallel computations for structural analysis, re-analysis and optimization, *Proc of NATO: DFG Advances Study Institute* "Optimization of Large Structural Systems," Berchtesgaden, Germany, Sept. 23-Oct. 4, 1991.
[406] Truesdell C and Noll W (1965), The non-linear field theories of mechanics, In: Fluegge W (ed): *Handbuch der Physik III/3*, Berlin, Heidelberg, New York: Springer.
[407] Truesdell C and Toupin R (1960), The classical field theories, In: Flügge S, *Handbuch der Phasik III/I*, Berlin-Göttingen-Heidelberg: Springer.
[408] Tsai SW and Pagano NJ (1968), Invariant properties of composite materials, In: Tsai SW, Halpin JC, and Pagano MJ (eds.), *Composite Materials Workshop*, Technomic Publ Stamford CT, 233–255.
[409] Wolff J (1870), Über eine innere Architektur der Knochen und ihre Bedeutung für die Frage vom Knochenwachstum, *Archiv für die pathologische Anatomie und Physiologie und für klinische Medizin (Virchovs Archiv)* **50**, 389–453.
[410] Wolfram S (1983), Statistical mechanics of cellular automata, *Rev. Modern Phys.* **55**, 601–644.
[411] Wu CC and Arora JS (1988), Design sensitivity analysis of nonlinear buckling load, *J. Computational Mech.* **3**, 129–140.
[412] Xie YM and Steven GP (1993), A simple evolutionary procedure for structural optimization, *J. Comput Struct* **49**(5), 885–896.
[413] Yamakawa H, Asakawa Y, and Ukida K (1995), Simultaneous optimization of topology of structural system and control system by using genetic algorithms, In: Olhoff N and Rozvany GIN (eds): *WCSMO-1-First World Congress of Structural and Multidisciplinary Optimization*, Pergamon Press, Oxford, UK, 623–628.
[414] Yamakawa H and Takagi Y (2000), Some examinations of optimization for topology, shape of structural systems and design of control systems using genetic algorithms, In, Bloebaum CL (ed), *WCSMO-3—Proc Third World Congress of Structural and Multidisciplinary Optimization*, May 17–21, 1999, Buffalo NY, CD-Rom, Univ of Buffalo.
[415] Yang RJ and Chen CJ (1998), Stress-based topology optimization, *Struct. Optim.* **12**, 98–105.
[416] Yang RJ and Chuang CH (1994), Optimal topology design using linear programming, *J. Comput Struct.* **52**(2), 265–275.
[417] Young V (1998), 3-D bi-directional evolutionary structural optimiza-

tion (BESO), *Proc Australasian Conf on Structural Optimization* (held in Sydney), 275–282.
[418] Young V, Querin OM, Steven GP, and Xie YM (1999), 3D and multiple load case bi-directional evolutionary structural optimization (BESO), *Struct. Optim.* **18**, 183–192.
[419] Yuge K and Kikuchi N (1995), Optimization of a frame structure subjected to a plastic deformation, *Struct. Optim.* **10**, 197–208.
[420] Zhao C, Hornby P, Steven GP, and Xie YM (1998), A generalized evolutionary method for numerical topology optimization of structures under static loading conditions, *Struct. Optim.* **15**(3–4), 251–260.
[421] Zhao CB, Steven GP, and Xie YM (1996), Evolutionary natural frequency optimization of thin plate bending vibration problems, *Struct. Optim.* **11**, 244–251.
[422] Zhao CB, Steven GP, and Xie YM (1997), Evolutionary optimization of maximizing the difference between two natural frequencies of a vibrating structure, *Struct. Optim.* **13**, 148–154.
[423] Zhou M and Rozvany GIN (1991), The COC algorithm, Part II: Topological, geometrical and generalized shape optimization, *Comput. Meth. Appl. Mechs. Eng.* **89**, 309–336.
[424] Zhou M and Rozvany GIN (2001), On the validity of ESO type methods in topology optimization, *Struct. Multidisc. Optim.* (to appear).
[425] Zhou M, Shyy YK, and Thomas HL (2000), Checkerboard and minimum member size control in topology optimization, In: Bloebaum CL (ed): *WCSMO-3—Proc Third World Congress of Structural and Multidisciplinary Optimization,* May 17–21, 1999, Buffalo NY, CD-Rom, Univ of Buffalo.

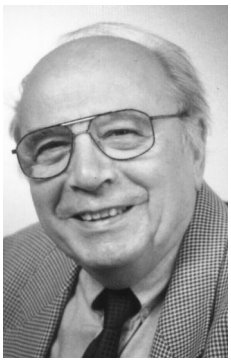

Hans A. Eschenauer *studied Theoretical Mechanical Engineering at the Technical Univ of Berlin. After graduating as "Dipl.-Ing." (MSc) in 1957 he worked in different development departments of industrial companies. In 1963 he became scientific assistant at the Institute of Mechanics of the Faculty of Mathematics and Physics at Technical Univ of Darmstadt, where he received his Doctor of Engineering (Dr-Ing) degree in the field of Mechanics in 1968. After further industrial employment with Krupp Industries as Head of the Antenna Structures and Advanced Technologies department in Duisburg, he was appointed Full Professor for mechanics at the Univ of Siegen in 1975, where he gave courses on Mechanics and Applied Mechanics with special emphasis on fundamentals, plates, shells, and structural optimization. His main research activities were in the fields of Multiobjective, Multilevel, Topology, and Multidisciplinary Structural and System Optimization. In addition, he held various positions in the Dept of Mechanical Engineering and in the autonomous university administration (eg, Senate, research committees). In 1984 he established the Research Laboratory for Applied Structural Optimization, and in 1992 he became founder and Head of the Board of the Research Center for Multidisciplinary Analyses and Applied Structural Optimization FOMAAS, a central university institute. After his retirement in 1995 he remained Head of the FOMAAS-Board until 1999. He is still Member of the Board and responsible for some research projects in cooperation with industry. During his industrial employment and university service times, Hans Eschenauer received several awards, among other the European Steel Design Award in 1974, the 1995 ASME Design Automation Award, the 1996 ASME Machine Design Award and the URP Award of Ford Motor Company, Detroit, USA in 2000. He is member of several national and international professional societies and executive and award committees, and acts as referee for various research councils and scientific journals. He is the author, co-author and editor of various monographs and textbooks, and has contributed more than 230 papers in scientific journals. He chaired and co-chaired numerous international conferences and seminars.*

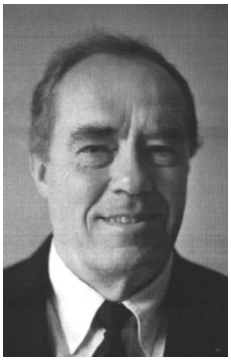

Niels Olhoff *received his MSc in Mechanical Engineering (1965), PhD in Solid Mechanics (1969), and Dr Techn degree in Optimum Structural Design (1979) from the Technical Univ of Denmark (DTU). He was Assistant Professor (1969–70) and Associate Professor (1970–85) in Strength of Materials at the Dept of Solid Mechanics of DTU. Since 1985 he is Professor of Computer Aided Mechanical Engineering Design at the Institute of Mechanical Engineering of Aalborg Univ, Denmark. During 1989–98 he served as Director of the Danish Technical Research Council's Program of Research on Computer Aided Engineering Design. Professor Olhoff is the author of more than 140 papers published in reviewed international scientific journals and proceedings, and he is the editor or co-editor of ten proceedings of international scientific conferences, symposia and advanced research courses chaired or co-chaired by him. He is Senior Advisor for the international journal "Structural and Multidisciplinary Optimization" and Associate Editor of "Mechanics of Structures and Machines" and "Computer Methods in Applied Mechanics and Engineering." He is President and member of the Executive Committee of the International Society for Structural and Multidisciplinary Optimization (ISSMO), and he is a member of the Executive Committee of the Nordic Association for Computational Mechanics (NoACM). Since 1988, Professor Olhoff has been a member and since 1992 the Secretary of the Congress Committee and the Executive Committee of the International Union of Theoretical and Applied Mechanics (IUTAM). Currently, he serves as Chairman of the Danish National Committee for IUTAM. He received the Esso Prize for Excellence in Technical Research in 1980, Tuborg's Travel Grant in 1982, was appointed Honorary Professor of Dalian Univ of Technology, Dalian, PR China in 1996, and received the Max Planck Research Award in 1997. He is an elected member of the Danish Academy of Technical Sciences, and an elected foreign member of the Royal Society of Arts and Sciences in Gothenburg, Sweden.*